ELUCIDATION OF THE REACTION MECHANISMS INVOLVED IN THE CATALYSIS MEDIATED BY GLUTAMINE SYNTHETASE IN *Escherichia coli*

by

LYNDON CAREY OLDFIELD

A dissertation submitted in fulfillment of the requirement for the degree

Master of Science

Department of Molecular and Cell Biology

University of Cape Town

Supervisors : Professor Sharon Reid

Dr Colin Kenyon (CSIR Bio/Chemtek)

Table of Contents

Abstract

Structural and molecular dynamics analysis of the glutamine synthetase from *E.coli* indicates that a possible mechanism by which the adenylylation/deadenylylation of the enzyme affects the enzyme specificity for either MgATP or Mn_2ATP and NH_4^+ or NH_3, is by switching between two putative serine protease-like catalytic triads. Site-directed mutagenesis of a number of residues identified as playing a role in these catalytic triads, led to the following observations. Both Ser52 and Ser53 were important for the catalytic activity of the enzyme. It was determined that the Ser52 residue appeared to have adenylylated functionality and the Ser53 residue, deadenylylated functionality. Evaluating these serine mutant enzymes in the presence of the serine protease inhibitors, AEBSF and PMSF, led to the conclusion that Ser52 and Ser53, did, indeed, appear to form part of a catalytic triad, as the activity of the enzymes were inhibited in the presence of the inhibitors. When both serine residues were removed in a single mutant, activity was not significantly inhibited by either inhibitor. His210 and His211 were found to be equally important to the functionality of the enzyme, and the results, in consultation with the enzyme model, led to the conclusion that the His210 residue had deadenylylated activity and the His211 residue had adenylylated activity. All the potential acid residues, when removed, had an effect on activity, but this was to be expected as all had previously been identified in the literature as important in the active site of the glutamine synthetase from *E.coli*. Again, consultation of the model led to the conclusion that the two acid residues that filled the function of the acid residue in each catalytic triad, were Glu129 for the adenylylated from of the enzyme, and Glu357 for the deadenylylated from of the enzyme. These catalytic triads are believed to be comprised of Ser52', His211 and Glu129 for the adenylylated form of the enzyme, and Ser53', His210 and Glu357 for the deadenylylated form of the enzyme. Possible model mechanisms for the both the adenylylated and deadenylylated forms of the enzyme are proposed.

Acknowledgements

I wish to express my gratitude to the following people :

- **Dr Colin Kenyon.** For his time, guidance and support.
- **Professor Sharon Reid.** For her guidance and support.
- **Ilze Spies and Bernelle Verster.** For help with the assays.
- **Nthati Toko.** For the HPLC analyses.
- **Reshnee Baboolall.** For the biomass from the continuous culture experiments.
- **Dr Caswell Hlongwane.** For the MALDI-TOF analysis.
- **My fellow co-workers in the Structural Biology Laboratory.** For their valuable advice, interest and friendship.
- **My husband and children.** For their love, support and encouragement.
- **CSIR.** For financial support.

List of Abbreviations

Amp	Ampicillin
ADP	Adenosine 5'-diphosphate
AEBSF	4-(2-Aminoethyl)benzenesulphonyl fluoride
AMP	Adenosine 5'-monophosphate
ATP	Adenosine 5'-triphosphate
Bp	Base pairs
dNTP	Dinucleotide triphosphates
IPTG	Isopropyl-1-thio-glactoside
kb	Kilobase
mins	minutes
PCR	Polymerase Chain Reaction
PMSF	Phenylmethanesulphonyl fluoride
SDS-PAGE	Sodium dodecyl sulphate polyacrylamide gel electrophoresis
TAE	Tris-Acetate-EDTA Buffer
TCA	Trichloroacetic acid
Tet	Tetracycline
µl	microlitres
X-Gal	5-Bromo-4-chloro-3-indolyl-β-D-galactoside

Chapter 1

Introduction

Glutamine and glutamate are central molecules in the metabolism of nitrogen. Glutamine synthetase is essential for the formation of glutamine, for the synthesis of a number of nitrogen-containing metabolites, such as purines and pyrimidines as well as for the assimilation of ammonia under nitrogen-limited conditions.

The reactions responsible for the assimilation of ammonia and the synthesis of glutamate and glutamine are shown below:

$$NH_4^+ + \text{L-glutamate} + ATP \xrightarrow{Mn^{2+}/Mg^{2+}} \text{L-glutamine} + ADP + P_i \quad (1)$$

$$\text{Glutamine} + \text{2-ketoglutarate} + NADPH \longrightarrow \text{2-glutamate} + NADP^+ \quad (2)$$

$$NH_3 + \text{2-ketoglutarate} + NADPH \longrightarrow \text{glutamate} + NADP^+ \quad (3)$$

These three reactions are catalysed by glutamine synthetase, glutamate synthase and glutamate dehydrogenase, respectively.

Glutamine synthetase is the only known biosynthetic reaction leading to the formation of glutamine and along with glutamate synthetase, is responsible for ammonia assimilation under nitrogen-limited growth conditions (Tullius *et al*, 2003). Mutations in *glnA*, the structural gene for glutamine synthetase, result in an absolute requirement for glutamine (Magasanik, 1982).

Ammonium is an excellent source of nitrogen for enterobacteria. In the presence of high concentrations of this solute in the environment, diffusion of uncharged ammonia (NH_3) across the cytoplasmic membrane into the cytoplasm is sufficient to promote cell growth. When diffusion into the cell becomes limiting for metabolism, a special ammonium transporter, designated AmtB, is synthesized (Burkovski, 2003).

Once in the cytoplasm of *E.coli*, ammonium can be assimilated by two different pathways, depending on its concentration. When present in high concentrations, glutamine synthetase is repressed and ammonium is primarily fixed by glutamate dehydrogenase, which oxidises one mol of NADPH per mol of ammonium assimilated. At ammonium concentrations below 1mM, the affinity of glutamate dehydrogenase for ammonium is too low, resulting in the high affinity glutamine synthetase/ glutamate synthase system taking over (Merrick, 1995; Burkovski, 2003). Therefore, in cells grown in a nitrogen-limited growth medium, glutamine synthetase is the only active ammonia-assimilating enzyme, and glutamate synthase assumes the only glutamate-forming role. Under nitrogen-limited conditions, glutamine synthetase has two functions: the synthesis of glutamine and the assimilation of ammonia when the growth of the cell is limited by the availability of ammonia.

The reactions catalysed by glutamine synthetase and glutamate synthase form an ammonia assimilatory cycle (Figure 1.1) which allows the net assimilation of ammonia into glutamine via glutamine synthetase and the replenishment and maintenance of an adequate intracellular level of glutamate.

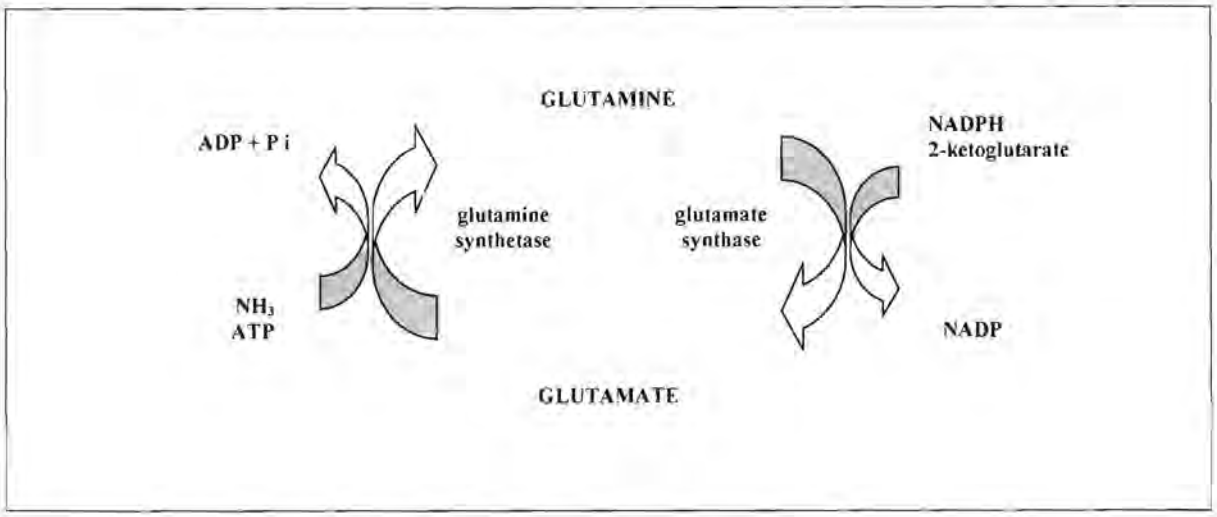

Figure 1.1. Ammonia assimilatory cycle (Reitzer and Magasanik, 1996)

Glutamine Synthetase – Biochemistry

Glutamine synthetase catalyses the ATP-dependent synthesis of L-glutamine from ammonia and L-glutamate, and requires two divalent metal ions, designated n1 and n2, for catalysis. The enzyme from *Escherichia coli* is a large, highly regulated metalloenzyme (~600 000 Mr) with 12 identical subunits arranged in two face-to-face hexagonal rings (Nosworthy and Ginsburg, 1997).

It exists in both unmodified and covalently modified forms with the modification being enzymatic adenylylation of a single tyrosine residue per subunit. Of the several reactions that it catalyses, the physiologically important one is the biosynthesis of glutamine from glutamate which requires two divalent cations per subunit (eq 1):

$$\text{Glutamate} + NH_4^+ + \text{ATP} \xrightarrow{Me^{2+}} \text{Glutamine} + \text{ADP} + P_i + H^+ \quad (1)$$

where Me^{2+} can be either magnesium or manganese. This reaction is often referred to as the 'biosynthetic' or 'forward' reaction, and is considered the most physiologically relevant reaction the glutamine synthetase catalyses (Eisenberg, 2000).

Saturation of the high-affinity site, n1, in each subunit by Mn^{2+} or Mg^{2+} induces a conformational change converting the enzyme from a catalytically inactive or 'relaxed' form to a catalytically active or 'tense' conformation. The metal ion at the n1 site also plays a catalytic role in the binding of glutamate, whereas the second divalent metal ion, n2, is thought to only play a role in the binding of ATP (Shapiro and Stadtman, 1970; Alibhai and Villafranca, 1994).

Initial formation of a γ-glutamyl phosphate forms during catalysis by the transfer of the γ-phosphate of ATP to the γ-carboxylate group of glutamate (eq 2). Efficient phosphoryl transfer between these two negatively charged groups, is co-ordinated by the n2 metal (eq 2). This is followed by phosphate displacement by ammonia to give inorganic phosphate and glutamine (eq 3) :

$$\text{ATP} + \text{Glutamate} \longrightarrow \text{ADP}\cdot\gamma\text{-Glutamate-P} \quad (2)$$

$$\text{ADP}\cdot\gamma\text{-Glutamate-P} + NH_4 \longrightarrow \text{ADP} + \text{Glutamine} + P_i \quad (3)$$

These intermediate structures have been modelled from the binding of methionine sulfoximine (MetSox) to glutamine synthetase. Metsox competes with glutamate for binding in the active site. In the presence of ATP, MetSox is phosphorylated by glutamine synthetase resulting in an essentially irreversible, non-covalent inhibition of the enzyme (Eisenberg, 2000).

Both the catalytic activity and the synthesis of glutamine synthetase are highly regulated (Magasanik, 1982). The activity of glutamine synthetase found in extracts of *E.coli* varies, depending on the nitrogen source used for growth. In media containing yeast extract or in the presence of high quantities (70mM) of ammonia, there is a low level of enzyme found. When cells are grown on glutamate or on limited quantities of ammonia (4mM) the specific activity of the enzyme is much higher (Shapiro and Stadtman, 1970).

Glutamine synthetase can be regulated by at least four different mechanisms : (a) adenylylation and deadenylylation of a tyrosine residue, (b) conversion between a relaxed (inactive) and tense (active) enzyme in response to variations in divalent cation, (c) cumulative feedback inhibition by multiple end products of glutamine metabolism and (d) repression and derepression of its biosynthesis in response to the nitrogen availability (Shapiro and Stadtman, 1970).

The catalytic activity of glutamine synthetase is regulated by the covalent addition of an AMP group to a tyrosine residue in each of the 12 subunits. This adenylylation reaction is catalysed by a specific glutamine synthetase adenyltransferase (ATase) (Shapiro and Stadtman, 1970). The ATase reaction is highly specific for glutamine synthetase; no other substrates have been identified or suggested (Mehta *et al*, 2004). In this reaction, the 5'-adenylyl moiety of ATP is linked to the phenolic hydroxyl group of one tyrosine residue in each subunit. The adenylyl

group is removed from glutamine synthetase in an associated deadenylylation reaction (Shapiro and Stadtman, 1970). In microbial culture, the adenylylation/deadenylylation of glutamine synthetase is carried out in response to the availability of ammonia in the culture medium (Senior, 1975).

Cells respond to an excess or deficiency of nitrogen through the intracellular ratio of glutamine to 2-ketoglutarate. If nitrogen is readily available, the rate of synthesis of glutamine by glutamine synthetase and the conversion of 2-ketoglutarate to glutamate by glutamate synthase and glutamate dehydrogenase increases. When there is a deficiency of nitrogen in the cell, the rate of glutamine synthesis and the rate of 2-ketoglutarate utilization decreases.

The regulation of glutamine synthetase activity through adenylylation and deadenylylation is accomplished by the interaction of three proteins: uridylyltransferase/uridylyl-removing enzyme, the signal transduction protein P_{II} and adenylytransferase (shown in Figure 1.2). The enzymes catalysing the adenylylation and deadenylylation reactions are also subject to fine metabolic control. A high intracellular concentration of glutamine activates the uridylyl-removing enzyme, which causes the deuridylylation of the regulatory protein P_{II}. This unmodified P_{II} interacts with adenylytransferase, which in turn catalyzes the adenylylation of glutamine synthetase, thus resulting in an inactive form of glutamine synthetase.

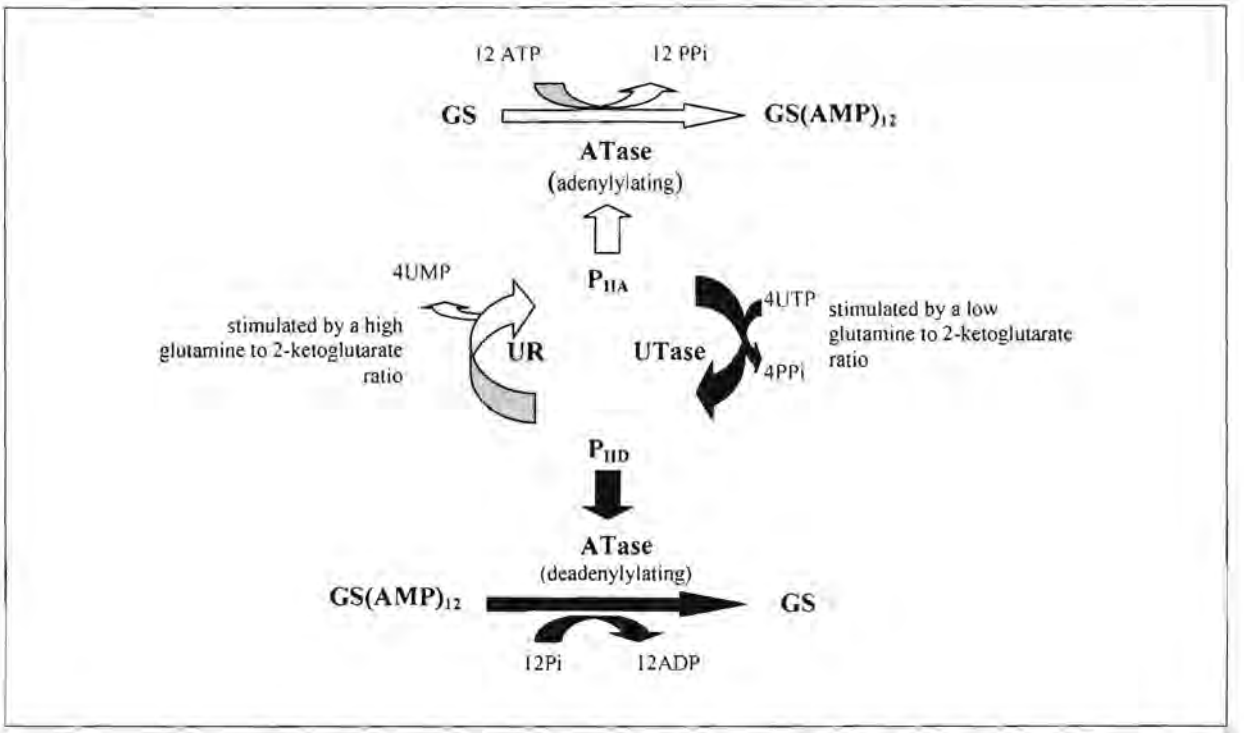

Figure 1.2. Schematic diagram showing the regulation of glutamine synthetase through adenylylation and deadenylylation (Reitzer and Magasanik, 1996).

Conversely, a high intracellular concentration of 2-ketoglutarate activates uridylyltransferase, which transfers a UMP group to each subunit of the regulatory protein P_{II} to form P_{II}-UMP. P_{II}-UMP interacts with adenylyltransferase, which then catalyses the removal of AMP from glutamine synthetase resulting in an active form of glutamine synthetase (Merrick and Edwards, 1995; Reitzer and Magasanik, 1996; Ninfa and Atkinson, 2000).

Divalent cations, specifically Mn^{2+} and Mg^{2+}, play an important role in the structure and function of glutamine synthetase. The enzyme requires two divalent metal ions for catalysis which are distinguished from one another by their dissociation constants. The more tightly bound n_1 metal ion is required to keep the enzyme in its catalytically active conformation while the less tightly bound n_2 metal ion is thought to facilitate nucleotide binding (Abell *et*

al; 1995). Literature has shown that the divalent cation required for the catalytic process varies with the extent of adenylylation. Deadenylylated enzyme is specific for Mg^{2+} and adenylylated enzyme is specific for Mn^{2+} (Shapiro and Stadtman, 1970). The presumed physiological form of the enzyme has two Mg^{2+} ions bound to each of the 12 active sites, although Mn^{2+} ions also support glutamine synthetase activity *in vitro*. Adenylylation of GS is accompanied by a change in the metal ion specificity of the reactions that it catalyzes and by changes in the internal reaction thermodynamics of phosphoryl transfer from ATP to glutamate (Ginsburg *et al*, 1970; Abel and Villafranca, 1991).

Glutamine synthetase activity is subject to cumulative feedback inhibition by the products of glutamine metabolism. The adenylylated form of glutamine synthetase is inhibited by L-alanine, glycine, histidine, tryptophan, CTP, AMP, carbamyl phosphate and glucosamine-6-phosphate (Reitzer and Magasanik, 1996). Each inhibitor was found to decrease glutamine synthetase activity partially such that the residual activity in the presence of several inhibitors, equalled the product of the individual residual activities. This was interpreted as the result of each inhibitor acting at a different site on the enzyme. Acting together, therefore, the feedback products were found to abolish activity. This is probably not the case, but can rather be attributed to the mixed adenylylation state of the glutamine synthetase. Crystal structures of glutamine synthetase in complex with alanine, serine and glycine have revealed that these inhibitors bind to the glutamate substrate site (Liaw *et al*, 1993; Liaw *et al*, 1994). Similarly, GDP, ADP and AMP bind to the ATP site, thereby suggesting a simpler mechanism for feedback control than that of cumulative inhibition from separate sites (Eisenberg, 2000).

Glutamine Synthetase – The Genes

The structural gene for glutamine synthetase is the *glnA* gene. Mutations in this gene result in an inability to produce enzymatically active glutamine synthetase, and consequently, in a requirement for glutamine for growth. The *glnA* gene forms part of an operon, together with the *ntrB* and *ntrC* genes which code for NR_I and NR_{II} respectively. The genes involved in the regulation of glutamine synthetase are shown in Table 1.1, and the structure of the operon in shown in Figure 1.3.

Table 1.1 Genes and proteins involved in the regulation of glutamine formation

Gene	Product
glnA	glutamine synthetase
glnB	P_{II}
glnD	Uridylyltransferase/uridylyl-removing enzyme
glnE	Adenylyltransferase
rpoN (*glnF, ntrA*)	σ^{60}
ntrB	Nitrogen Regulator I (NR_I)
ntrC	Nitrogen Regulator II (NR_{II})

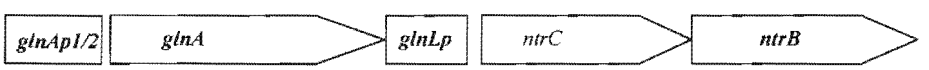

Figure 1.3. The structure of the operon containing the genes involved in glutamine synthesis.

The operon has three promoters: *glnAp1*, *glnAp2* and *glnLp*. The three promoters enable the cell to maintain a low level of glutamine synthetase and NR_I during growth with an excess of nitrogen and to increase the level of glutamine synthetase and NR_I rapidly in response to a low level of nitrogen (Reitzer and Magasanik, 1986).

The regulation of the transcription of *glnA* in response to the availability of nitrogen is achieved through the action of uridylyltransferase/uridylyl-removing enzyme, P_{II}, nitrogen regulator I (NR_I), and nitrogen regulator II (NR_{II}). This requires core RNA polymerase and σ^{60}, as opposed to σ^{70}. When the intracellular concentration of 2-ketoglutarate is high, uridylyltransferase converts P_{II} to P_{II}-UMP. In the absence of P_{II}, NR_{II} catalyses the conversion of NR_I to NR_I-phosphate, and this phosphorylated protein then activates the initiation of transcription at the σ^{60}-dependent promoter *glnAp2*. When the intracellular concentration of glutamine is high, however, uridylyl-removing enzyme converts P_{II}-UMP to P_{II}. P_{II} then causes NR_{II} to remove the phosphate group from NR_I-phosphate which then halts the initiation of transcription from *glnAp2*.

In cells growing under carbon limitation, but with an excess of nitrogen, *glnA* is transcribed from *glnAp1*, which is partially repressed by NR_I, resulting in a low level of glutamine synthetase (Reitzer and Magasanik, 1996). The cells also maintain a low level of NR_I through transcription initiated at *glnLp*. Cells maintained in a nitrogen-deprived medium results in the activation of uridylyltransferase by the increase in intracellular 2-ketoglutarate. The uridylyltransferase then converts P_{II} to P_{II}-UMP and allows NR_{II} to convert NR_I to its active form, NR_I-phosphate. NR_I-phosphate can, in turn, fully activate the initiation of transcription at *glnAp2* by σ^{60}-RNA polymerase. The level of intracellular NR_I is increased through the transcription of *glnG* initiated at *glnAp2*. The increase in the level of NR_I results in complete repression at *glnAp1* and *glnLp*. A shift of the cells from nitrogen starvation to nitrogen excess causes the activation of uridylyl-removing enzyme through the increased intracellular glutamine and the removal of UMP from P_{II}-UMP by uridylyl-removing enzyme. The resulting P_{II} causes NR_{II} to remove the phosphate from NR_I-phosphate, thereby stopping the initiation of transcription from *glnAp2*. Maintaining growth in this medium results in the

decrease of the levels of glutamine synthetase and NR_I by dilution, which eventually leads to sufficient lifting of the repression at *glnAp1* and *glnLp* , to allow both glutamine synthetase and NR_I to be maintained at low levels (Reitzer and Magasanik, 1996).

Glutamine Synthetase – The Structure

Bacterial glutamine synthetase molecules are dodecamers formed from two face-to-face hexameric rings of subunits, with two active sites formed between two monomers, twelve active sites in total. The structure of the glutamine synthetase molecule has recently been extensively reviewed by Eisenberg (2000), and in this review each active site can be described as a `bifunnel' in which ATP and glutamate bind at opposite ends. The ATP binding site is referred to as the top of the bifunnel, because it opens to the external six-fold surface of the glutamine synthetase molecule. The two divalent cation binding sites, n1 and n2, where either magnesium or manganese bind, are found at the joint of the bifunnel. The n2 ion is involved in phosphoryl transfer, while the n1 ion stabilises glutamine synthetase in its active form, as well as plays a role in the binding of glutamate. The affinity for metal ions at the n1 site is 50 times greater than at the n2 site, which is caused by the greater negative charge toward the bottom half of the bifunnel in the vicinity of n1. The n1 metal ion has three glutamate side chains – 131, 212 and 220 – as ligands, while the n2 metal ion has two glutamate ligands, 129 and 357, as well as histidine 269 (Abell *et al*, 1995). All of the amino acids that serve as metal ion ligands are highly conserved in glutamine synthetases from various sources (Pesole *et al*, 1991).

The glutamine synthetase molecule is held together mainly by hydrophobic and hydrogen binding interactions between the two hexameric rings (Almassey *et al*, 1986). The stacking surface of the dodecamer is notably nonpolar, with aspartate, glutamate, histidine, serine, cysteine, arginine, lysine, glutamine or asparagine comprising 65% of the solvent-accessible surface (Atkins, 1994). Both the N-terminus and C-terminus of each site are helical. The N-terminal helix sits above the hexameric ring and is exposed to solvent, whilst the C-terminal helix is inserted into a hydrophobic hole in the eclipsed subunit on the opposite hexameric ring. The central channel of the dodecamer is lined by six four-stranded β-sheets, each built from an antiparallel loop contributed by subunits in opposite rings. This gives the dodecamer additional adhesion (Eisenberg, 2000).

Conformational changes and side-chain movements have been described for glutamine synthetase crystals soaked in solutions with various ligands (Liaw *et al*, 1993; Liaw and Eisenberg, 1994; Liaw *et al*, 1994). These residues are absolutely conserved among glutamine synthetase in both lower and higher organisms, and appear to play key roles in the mechanism of the biosynthetic reaction (Eisenberg, 2000).

The structure of the glutamine synthetase dodecamer, as described by Eisenberg (2000) is believed to contain several loops of functional importance. These loops are as follows:

- A loop consisting of the hydrophilic residues 156-173, which protrudes into the central channel of the dodecamer and is a site for proteolysis and ADP-ribosylation.
- A second loop, known as the adenylylation loop, contains tyrosine 397, which is covalently modified by the addition of AMP. This loop lies just outside the bottom entrance to the bifunnel.

- The glutamate 327 flap, consisting of residues 323 to 330, which guards the glutamate entrance to the active site. This 'flap' closes the active site, shielding the γ-glutamyl phosphate intermediate from hydrolysis. When the flap is closed, the glutamate 327 carboxylate forms part of the ammonium site. Aspartate 50' deprotonates the ammonium ion, forming ammonia. Ammonia then attacks the γ-glutamyl phosphate intermediate thereby forming a tetrahedral intermediate at the transition state. The glutamate 327 flap accepts a proton from the δ–amino group of the tetrahedral intermediate, yielding glutamine.
- A loop containing aspartate 50' is located on the N-terminal domain (residues 1-100). Each active site is formed at the interface between the C-terminal domain of one subunit and the N-terminal domain of an adjacent subunit within a dodecameric ring, resulting in most of the active site being formed by residues of the C-terminal domain. Aspartate 50' is in the N-terminal portion of the active site, and is believed to bind the ammonium substrate and then to accept a proton from ammonium, resulting in the formation of ammonia which can then attack the phosphorylated-glutamyl intermediate. The position of aspartate 50' is controlled by nucleotide binding. Both ADP and ATP enter the active site from the top of the bifunnel, with the phosphate chain pointing into the bifunnel. ADP induces arginine 359 interaction with aspartate 50' and stimulates arginine 344 interaction with aspartate 64', providing additional contacts for inter-subunit stabilisation within a ring. The movement of aspartate 50' helps in the formation of the ammonium binding site, and the movement of arginine 339 possibly assists phosphoryl transfer and phosphate binding. It is thought that ADP binding also increases the affinity for glutamate by inducing the movement of arginine 359 toward one of the γ-carboxylate oxygens of glutamate. Finally, the β-phosphate of ADP shifts glutamate 129 toward the n2 ion, histidine 269 and histidine 271.

Studies in which the metal ion ligand, histidine 269, was replaced by other amino acid residues, namely aspartate, asparagine, glutamate and glutamine, by site-directed mutagenesis have been carried out. All of the mutant enzymes showed little conformational change, and were still capable of binding two metal ions. The replacement of histidine 269 with neutral ligands such as asparagine and glutamine slightly altered the dissociation constants (3- to 4-fold), while substitution with glutamate decreased the dissociation constant slightly. The mutations had little effect on the substrate K_m's except in the case of H269E, whose k_m exhibited a 1000-fold increase over that of the wild type (Abell *et al*, 1995).

- Asparagine 264 is found on a flexible loop (residues 255-266) near the glutamate entrance at the lower end of the bifunnel and is adjacent to the glutamate 327 flap. When glutamate binds, the side chain swings away toward the ε-amino group of lysine 176, and was found to also be true when alanine, glycine and glutamine complex with glutamine synthetase.

As a result of the elucidation of these loops described above, it is possible to describe the enzymatic reaction mechanism of glutamine synthetase as a series of loop and side-chain movements. In the reaction mechanism, ATP binds at the top of the bifunnel, so that its terminal phosphate group binds adjacent to the n2 ion. This binding of ATP results in the movement of the aspartate 50' loop toward the site to which an ammonium ion will subsequently bind. Arginine 359 then moves toward the site to which the γ-carboxylate group of glutamate will subsequently bind. Both these movements increase the affinity for glutamate and ammonium binding. Following this, glutamate enters from the bottom of the bifunnel and binds above the glutamate 327 flap, with its γ-carboxylate group binding adjacent to the n1 ion. The amino group of glutamate shifts the asparagine 264 loop, aiding

serine 52' on the aspartate 50' loop, to stabilise the flap. The active site is now closed and is shielded from water, and ammonium binding is complete. The γ-phosphate of ATP is transferred to the γ-carboxylate of glutamate, thereby forming the intermediate. The two positive charged metal ions and arginine 359 participate in phosphoryl transfer by polarising the γ-phosphate group of ATP making the γ-phosphorous more positive. An ammonium ion enters the bifunnel and binds in the negatively charged pocket created by glutamate 327, aspartate 50', tyrosine 19, glutamate 212 and serine 53'. The side chain of aspartate 50' deprotonates the ammonium ion, forming ammonia, which then attacks the δ–carbon of the γ-glutamyl phosphate intermediate, which results in the release of a phosphate group. A salt-bridge is now formed between the tetrahedral adduct and glutamate 327, which then accepts a proton from the adduct, thereby neutralising the salt-bridge and forming glutamine. Finally, the glutamate 327 flap opens and glutamine is released.

Glutamine Synthetase in Other Organisms

Glutamine synthetase has been studied extensively in a number of organisms, resulting in the discovery of a number of similarities, as well as differences, to the enteric organisms.

Assimilation of ammonia by *Bacillus subtilis* requires the activity of glutamine synthetase. The enzyme is crucial as it provides most of the nitrogen for synthesis of the organism's nitrogen-containing compounds. Glutamine synthetase levels are highest when growth occurs in the presence of limiting ammonia compared to growth in an excess of nitrogen. Regulation by the nitrogen source is principally mediated at the level of transcription and by feedback inhibition and no evidence of an adenylylation/deadenylylation mechanism has been found (Schreier and Rostkowski, 1995; Burkovski, 2003). At least three regulatory proteins

independently control the expression of the gene products involved in nitrogen metabolism in response to nitrogen availability. The three genes are the *tnrA*, *glnR* and *codY*. The genes expressed at high levels during N-limited growth are controlled by two- related proteins, *glnR* and *tnrA* which bind to similar DNA sequences under different nutritional conditions. In general, *tnrA* is active during nitrogen limitation, and *glnR*-dependent repression occurs in cells that are grown in nitrogen-rich medium (Fisher, 1999). A third regulatory gene, *codY*, controls the expression of several genes involved in nitrogen metabolism, competence and acetate metabolism, in response to the growth rate of *B.subtilis*. The highest levels *codY*-dependent repression occur in cells growing rapidly in a medium rich in amino acids, and this regulation is relieved during the transition to nutrient-limited growth.

Corynebacterium glutamicum, like *E.coli*, has two anabolic pathways for the synthesis of glutamate - glutamate dehydrogenase and the glutamine synthetase/GOGAT system, which also represent the two main pathways for ammonium assimilation. The glutamine synthetase from *C.glutamicum* is regulated by post-translational modification, namely adenylylation (Jakoby *et al*, 1997; Nolden *et al*, 2001; Schultz *et al*, 2002).

The *ntrB/ntrC* two-component signal transduction system, responsible for activating the genes involved in ammonia assimilation in *E.coli*, appears to be absent in *C.glutamicum*. This absence, together with the presence of a repressor protein (*amtR*), resembles the situation in *B.subtilis* (Burkovski, 2003).

Glutamine synthetase activity in *Mycobacterium tuberculosis* is affected by the supply of ammonium and regulation appears to be similar to that of *E.coli*. The glutamine synthetase of *M. tuberculosis* plays a central role in nitrogen metabolism, and is one of ten proteins released

into the bacterium's extracellular environment when the organism is growing in human mononuclear phagocytes, the primary host cells. The regulation involves post-translational modification, and high nitrogen conditions result in the adenylylation of the glutamine synthetase. The presence of an adenylyl transferase (encoded by a *glnE* gene) has been demonstrated. It has also been shown, by disruption of the *glnA* gene, that it is essential for growth in *M. tuberculosis* (Parish and Stoker, 2000; Harth and Horwitz, 1999, 2003). In addition, glutamine synthetase has been identified as a potentially important determinant of *M. tuberculosis* pathogenesis. It has been found that glutamine synthetase mediates the extracellular catalysis of glutamine and this, therefore, suggests a direct involvement of the enzyme in the synthesis of the cell wall structure, poly-L-glutamate, found in pathogenic, but not non-pathogenic mycobacteria (Harth *et al*, 1994; Harth *et al*, 1999).

Glutamine synthetase enzymes amongst prokaryotic organisms are, on the whole, very well conserved at the protein level, as shown in Figure 1.4. In all of the organisms examined, a number of important residues are conserved in the glutamine synthetase amino acid sequences examined, most notably, the tyrosine residue (Y397 in *E.coli*) that is the site of adenylylation. In addition, there are a number of other regions that are highly conserved across all the organisms examined. These areas are, in *E.coli*, from residues 48 to 52, 210 to 213, 256 to 274 and 318 to 347.

Initially, it was thought that prokaryotes and eukaryotes expressed different forms of glutamine synthetase. Prokaryotes expressed GS I, while eukaryotes expressed GS II. GS II has, however also been found in various prokaryotic organisms, although GS I has not been found in eukaryotes. Within the GSI group, two significant prokaryotic subdivisions are known to occur: GSI-α and GSI-β (Brown *et al*, 1994). The GSI-α genes were found to occur

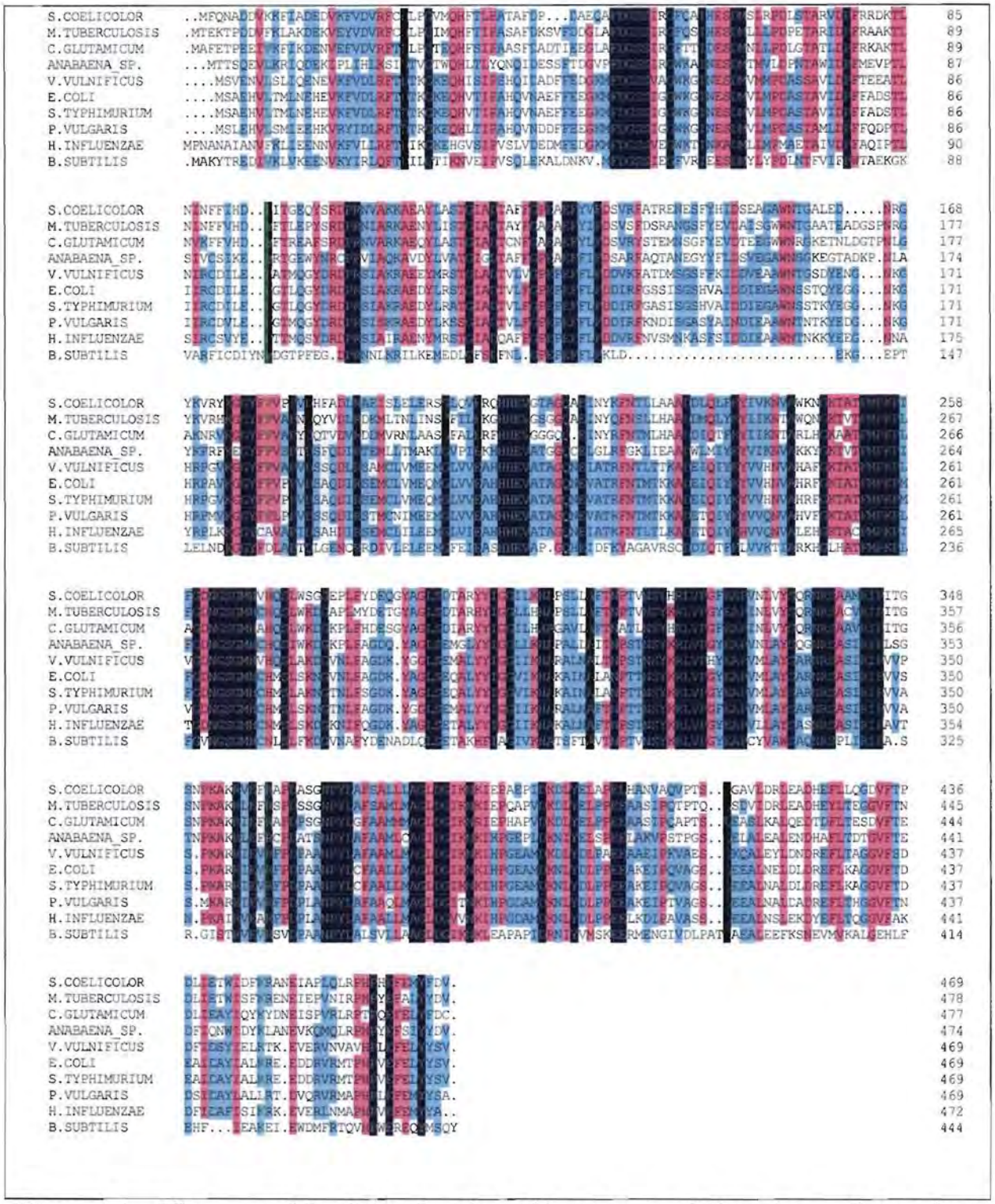

Figure 1.4. Alignment of the deduced amino acid sequences of glutamine synthetase from various organisms viz, *Streptomyces coelicolor*, *Mycobacterium tuberculosis*, *Corynebacterium glutamicum*, *Anabaena* sp., *Vibrio vulnificus*, *E.coli*, *Salmonella typhimurium*, *Proteus vulgaris*, *Haemophilus influenzae* and *Bacillus subtilis*.

■ 100% conserved; ■ 75-100% conserved; ■ 50-75% conserved.

in the thermophilic bacteria, the low G+C gram-positive bacteria, and the Euryarchaeota (including the methanogens, halophiles and some thermophiles), while the GSI-β genes occur in all other bacteria. The GSI-β genes also contain a 25 amino acid insertion sequence that does not occur in the GSI-α gene. Brown *et al* (1994) also proposed that the adenylylation control cascade does not occur in the GSI-α genes but is present in the GSI-β genes, and therefore, the regulation of GS via the adenylylation cascade occurs in the bacteria that have the GSI-β glutamine synthetase gene. The 25 amino acid insertion-sequence was also found not to occur in the GSII genes of eukaryotes and a number of soil dwelling bacteria.

Introduction to this Investigation

Current literature outlining the role of key amino acid side chains in the catalysis carried out by glutamine synthetase does not explain the difference in reaction mechanism that occurs as a result of the enzyme functioning in the adenylylated or deadenylylated forms. The high degree of conservation in the protein sequences of prokaryotic microorganisms facilitated a molecular modelling exercise of the glutamine synthetase of *E.coli.* The crystal structure model used in this study was 1f52.pdb (Gill and Eisenberg, 2001), which was obtained from the Brookhaven Protein Database. This is the crystal structure of the glutamine synthetase from *Salmonella typhimurium,* as the glutamine synthetase from *E.coli* has not yet been crystallised. The overall structure of the glutamine synthetase molecule, showing the dodecamer arranged in two face-to-face hexagonal rings, projected down the six-fold axis of symmetry is shown in Figure 1.5.

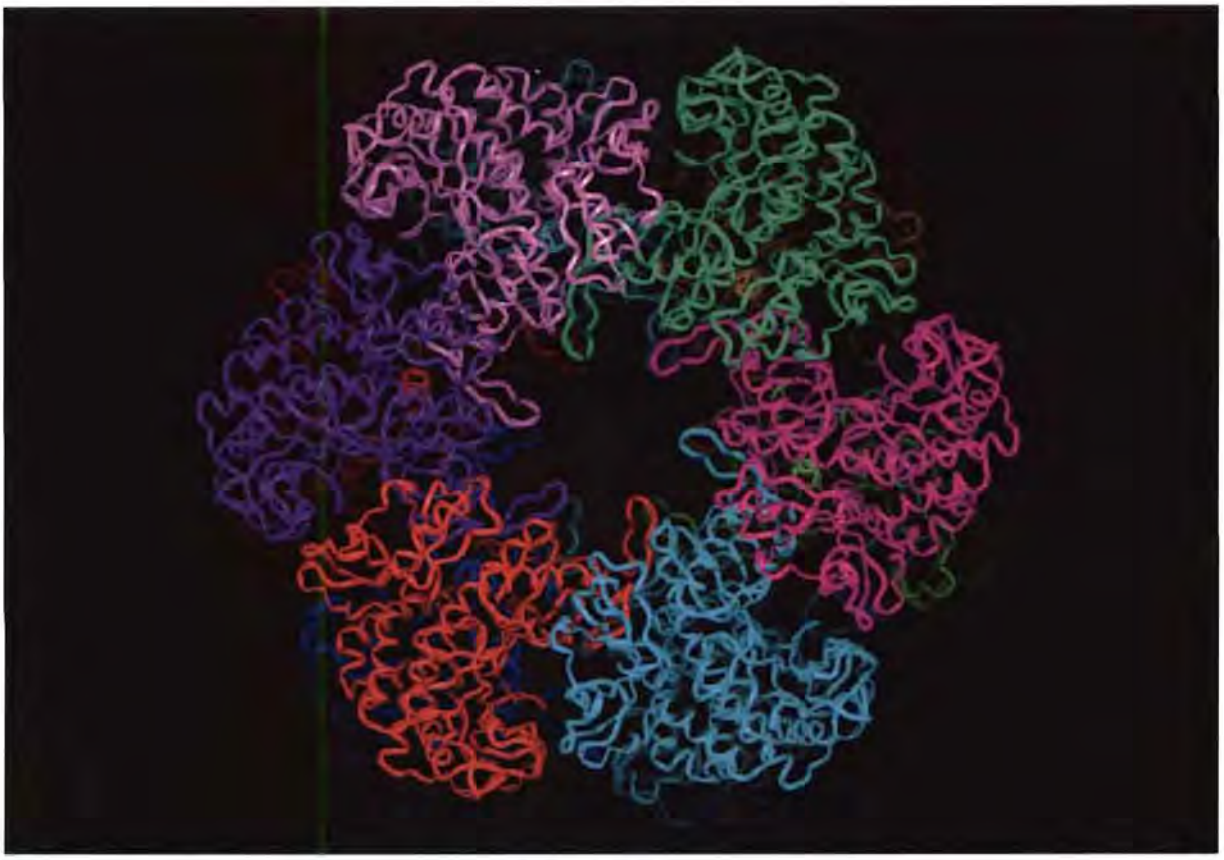

Figure 1.5. Structure of the *E.coli* glutamine synthetase molecule, showing the dodecamer arranged in two face-to-face hexagonal rings.

A second view of the molecule, viewed from the side, down one of the 2-fold axes, is shown in Figure 1.6.

Structural and molecular dynamics analysis of the glutamine synthetase indicate that a possible mechanism by which the adenylylation and deadenylylation of the enzyme affects the enzyme specificity for either MgATP or Mn_2ATP and NH_4^+ or NH_3, is by switching between two putative catalytic triads (Kenyon, personal communication). It has been postulated that these triads are involved in the nucleophilic attack by the activated serine on the carboxylic-phosphoric acid anhydride intermediate, glutamyl phosphate, to form an acyl

enzyme intermediate. The glutamyl acyl intermediate then undergoes nucleophilic attack by NH_3, releasing the glutamine from the surface of the enzyme.

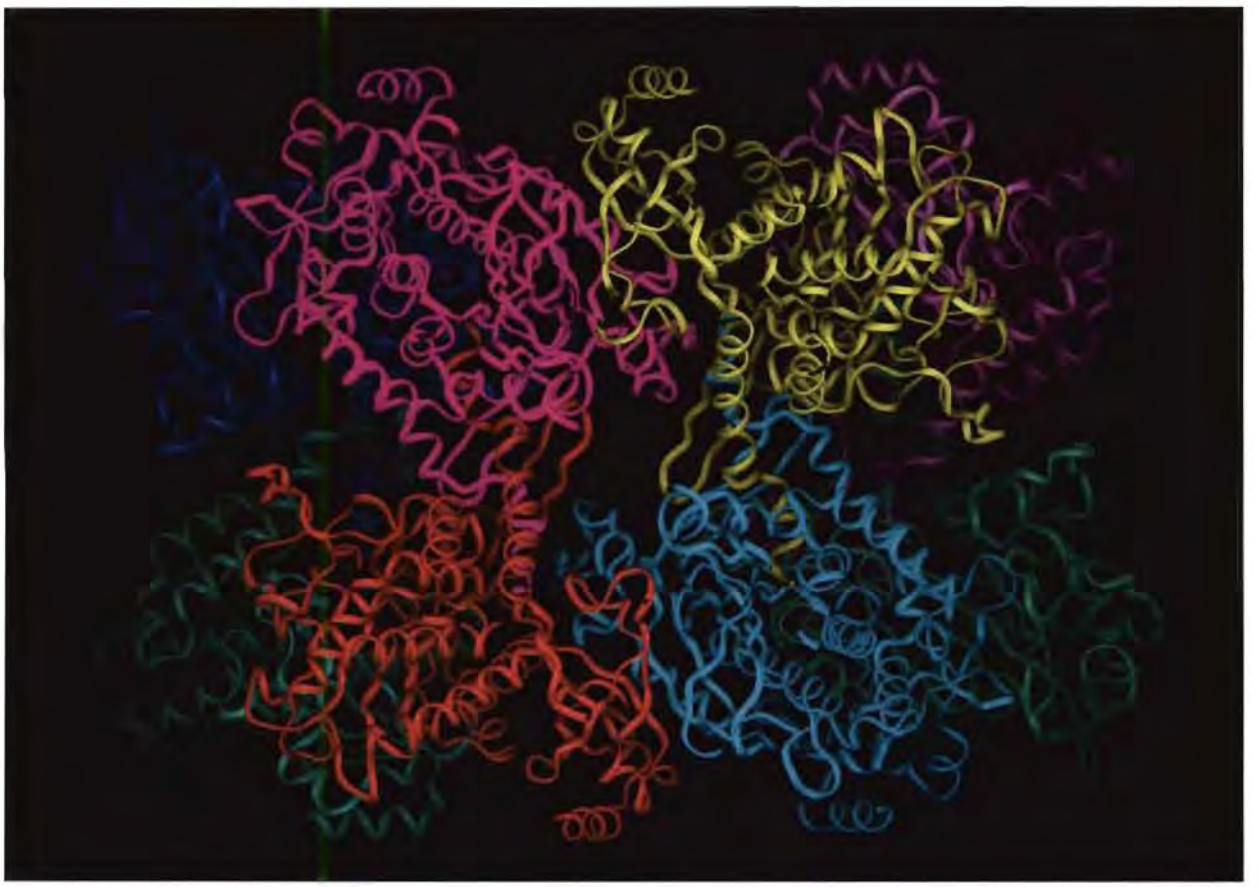

Figure 1.6. The *E.coli* glutamine synthetase molecule (front half) viewed from the side, down one of the 2-fold axes.

Figure 1.7 shows the model reduced to four subunits for explanation purposes, allowing the demonstration of the interaction of the subunits in the putative catalytic triad-based reaction mechanism.

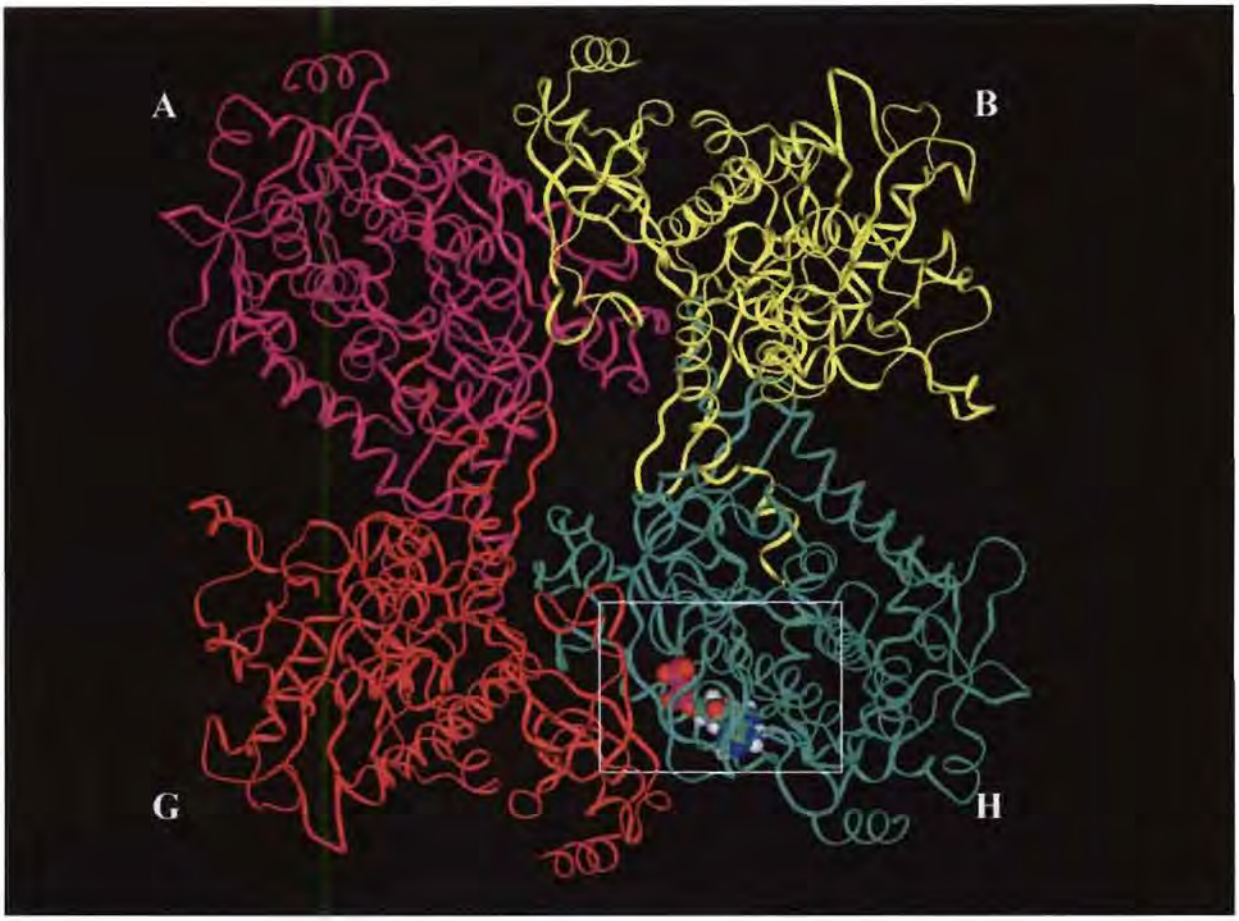

Figure 1.7. Structure of the glutamine synthetase molecule reduced to four subunits : A, B, G and H. The active site, with ADP bound, is boxed.

The presence of two catalytic triads would account for the fact that the glutamine synthetase from *E.coli* has two affinity constants for ammonia (Meek and Villafranca, 1980). The solution chemistry of the NH_4^+/NH_3 also dictates the regulation of GS, with adenylylated enzyme being produced under conditions of nitrogen excess and carbon limitation, and deadenylylated enzyme under conditions of nitrogen limitation and carbon excess (Senior, 1975). At low ammonium salt concentrations, the NH_4^+ dissociates to $NH_3 + H^+$ (Kenyon, 1992). The NH_3 is a strong nucleophile and capable of carrying out the nucleophilic attack on the proposed γ-glutamyl acyl enzyme intermediate.

Within the active site of glutamine synthetase, which occurs at the interface of two subunits (for example subunit A and subunit B in Figure 1.7), a cluster of serine and histidine residues are found. These residues are Ser52, Ser53, His210 and His211. A number of acid residues, Asp50, Glu129, Glu327 and Glu357, required to complete the putative catalytic triads, are also located in the active site (shown in Figure 1.8).

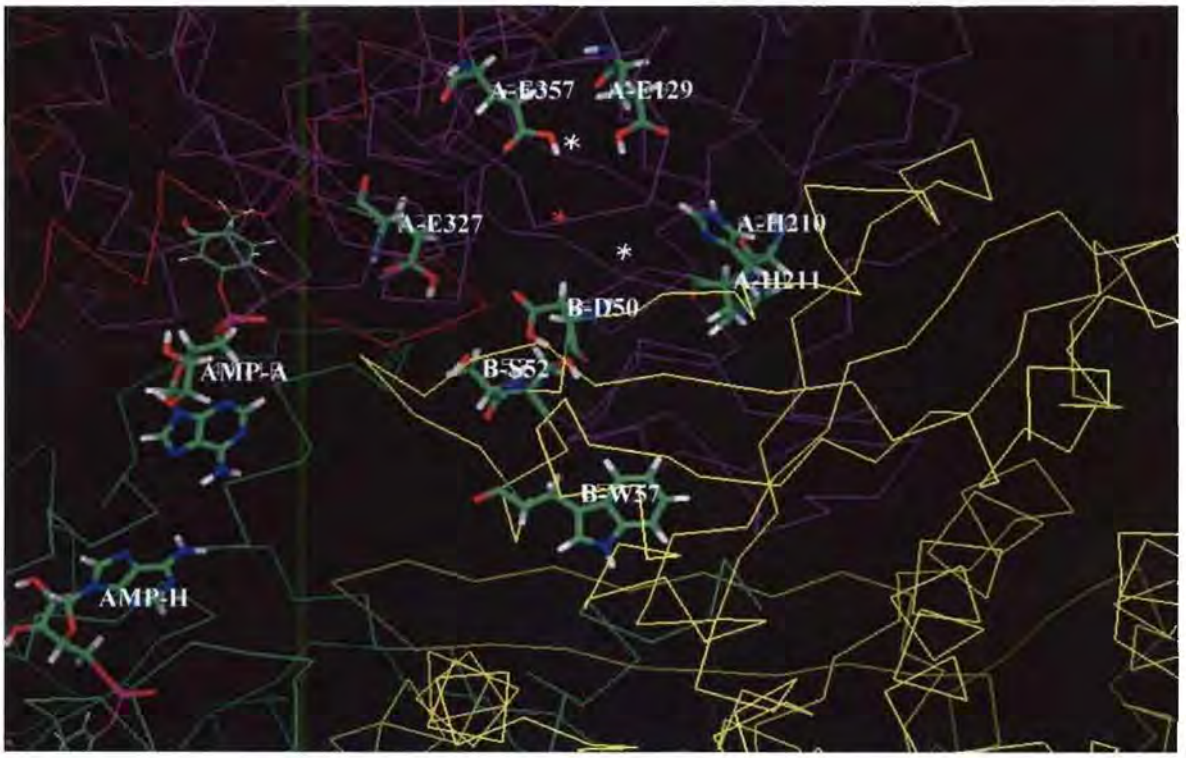

Figure 1.8. Structure of the active site of the glutamine synthetase molecule, showing some of the residues identified as forming part of the catalytic triad. The subunits shown are A and B.

The position of these residues in the protein sequence of the glutamine synthetase is shown in Figure 1.9.

```
1       MSAEHVLTML NEHEVKFVDL RFTDTKGKEQ HVTIPAHQVN AEFFEEGKMF DGSSIGGWKG
61      INESDMVLMP DASTAVIDPF FADSTLIIRC DILEPGTLQG YDRDPRSIAK RAEDYLRSTG
121     IADTVLFGPE PEFFLFDDIR FGSSISGSHV AIDDIEGAWN SSTQYEGGNK GHRPAVKGGY
181     FPVPPVDSAQ DIRSEMCLVM EQMGLVVEAH HHEVATAGQN EVATRFNTMT KKADEIQIYK
241     YVVHNVAHRF GKTATFMPKP MFGDNGSGMH CHMSLSKNGV NLFAGDKYAG LSEQALYYIG
301     GVIKHAKAIN ALANPTTNSY KRLVPGYEAP VMLAYSARNR SASIRIPVVS SPKARRIEVR
361     FPDPAANPYL CFAALLMAGL DGIKNKIHPG EAMDKNLYDL PPEEAKEIPQ VAGSLEEALN
421     ELDLDREFLK AGGVFTDEAI DAYIALRREE DDRVRMTPHP VEFELYYSV
```

Figure 1.9. Protein sequence of the *E.coli* glutamine synthetase, showing the residues identified as potentially being involved in the proposed catalytic triads (highlighted in yellow and purple). The tyrosine 397 residue involved in the covalent modification of glutamine synthetase is highlighted in green.

On the basis of this structural information, this investigation was undertaken to demonstrate that the role of adenylylation and deadenylylation of the enzyme, is as a possible switching mechanism between two serine protease-like catalytic triads, as well as demonstrating the detailed chemistry of this switching mechanism. This is a new reaction mechanism which has not previously been reported in the literature, although a number of the designated amino acid residues have been identified as being important for the catalytic activity of the enzyme.

Chapter 2

Plasmid Constructs, Site-Directed Mutagenesis and Mutant Gene Expression

2.1 Introduction

Structural and molecular dynamics analysis of the active site of the glutamine synthetase from *E.coli* led to the identification of two protease-like catalytic triads. In order to investigate the role that these residues played with respect to the functionality and regulation of the glutamine synthetase from *E.coli*, it was proposed to use site-directed mutagenesis (SDM) to specifically target these residues and then to assess the effect that altering these residues had on the active site of glutamine synthetase.

Two different systems were used for the SDM. The first was the Altered Sites® II *in vitro* Mutagenesis System from Promega, and the second was the QuikChange XL Site-Directed Mutagenesis System from Stratagene.

The majority of mutations were carried out using the Altered Sites System, as it provides a high-efficiency procedure for the generation and selection of oligonucleotide-directed mutants (procedure outlined in Figure 2.1). The system allows for the mutagenesis of double-stranded template DNA, as well as for sequential rounds of mutagenesis without any need for subcloning. The procedure uses antibiotic selection as a means to obtain a high frequency of mutants. The vector contains two

antibiotic resistance markers: a tetracycline resistance marker, which is active and an ampicillin resistance marker, which is inactive. Oligonucleotides which restore and knockout the two markers are provided in the kit. During the first round of mutagenesis, the tetracycline resistance gene is inactivated and the ampicillin resistance is restored. Should a second round of mutagenesis need be carried out on the mutant generated in the first round of mutagenesis, then the ampicillin resistance gene is again inactivated and the tetracycline resistance restored. Thus, multiple rounds of mutagenesis are very easily carried out, and the yield of mutants is increased.

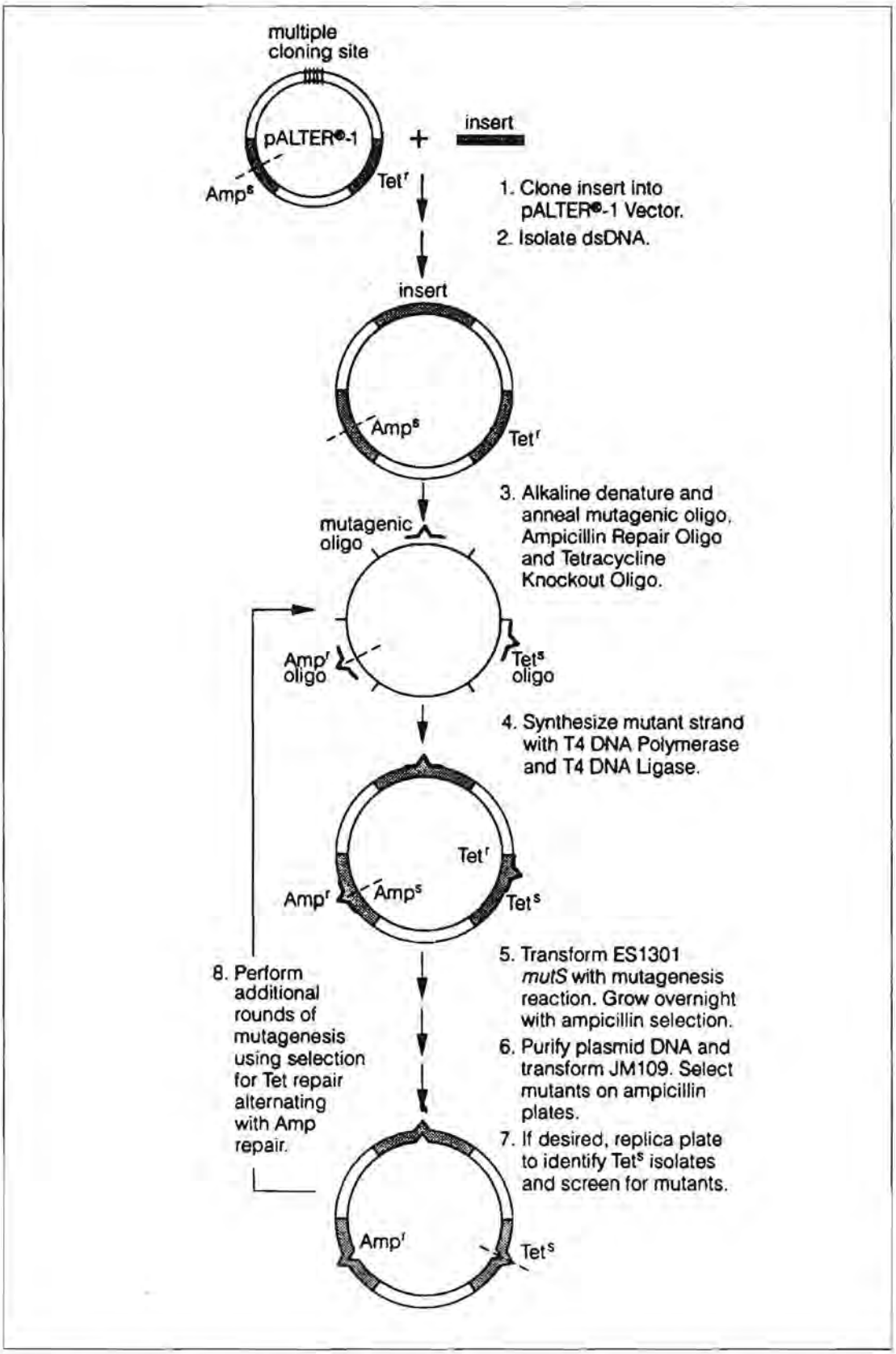

Figure 2.1. Schematic diagram of the Altered Sites *in vitro* mutagenesis procedure (Promega Corporation).

A few mutations could not be achieved using this system and another system was therefore sought. The QuikChange System from Stratagene is a polymerase chain reaction-based procedure that can be used to introduce mutations into virtually any vector. The basic procedure (as outlined in Figure 2.2) utilises a supercoiled double-stranded vector containing the insert of interest and two synthetic complementary oligonucleotide primers containing the desired mutation. The primers, each complementary to opposite strands of the vector, are extended during temperature cycling using *PfuTurbo* DNA polymerase. Incorporation of the oligonucleotide primers generates a mutated plasmid containing staggered nicks. Following temperature cycling, the product is treated with *Dpn* I. This restriction endonuclease is specific for methylated and hemi-methylated DNA and digests the parental DNA template, thereby selecting for mutation-containing synthesised DNA. The nicked vector DNA incorporating the desired mutations is then transformed into an *E.coli* host strain, following which individual colonies can be screened for the mutation.

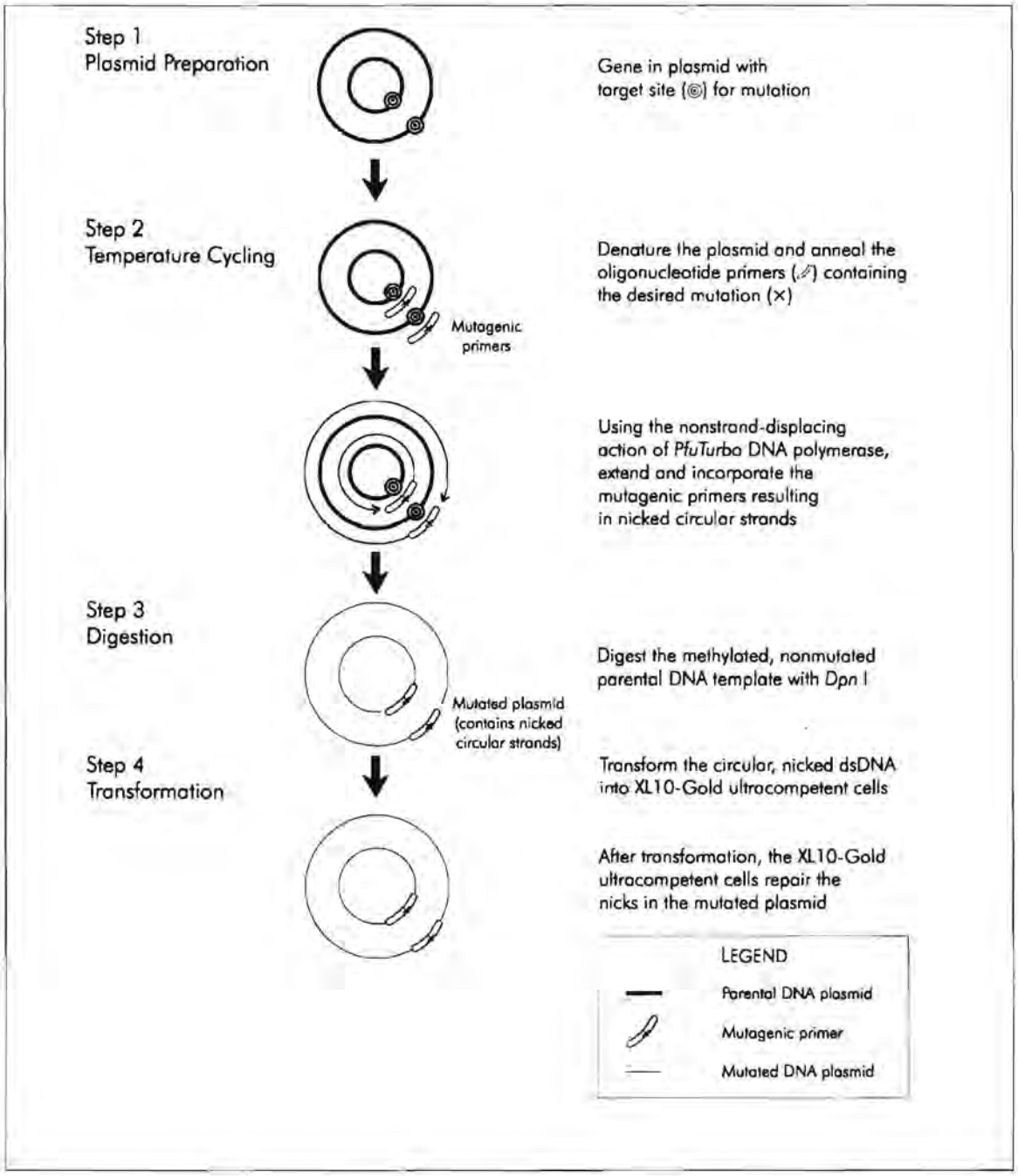

Figure 2.2. Overview of the QuikChange XL site-directed mutagenesis method (Stratagene).

Silent mutations were created in all of the oligonucleotide primers designed, allowing for the incorporation of a restriction endonuclease site to facilitate screening for mutant genes. This enabled simple, quick screening of a number of the colonies obtained for each mutagenesis reaction without the need for sequencing each one.

Once the mutagenesis was complete, each mutant gene was expressed in an *E.coli* glutamine synthetase auxotroph.

As the catalytic activity of glutamine synthetase is regulated by the covalent addition of an AMP group to the tyrosine residue in each subunit of the enzyme, it was proposed to first alter the tyrosine 397 residue (the site of adenylylation) to valine 397 in order to create a deadenylylated form of the enzyme. Each mutation could then be examined in both the adenylylated and deadenylylated forms of the enzyme. A summary of the other targeted residues, with the proposed changes, is shown in Table 2.1.

Table 2.1. Summary of the proposed amino acid changes with the intended targeted site

Key Residue	Proposed mutation
Ser 52	Ala 52
Ser 53	Ala 53
His 210	Val 210
His 211	Val 211
Asp 50	Ala 50
Glu 129	Ala 129
Glu 327	Val 327
Glu 357	Ala 357

2.2 Materials and Methods

2.2.1. Strains and Plasmids Used

All *E.coli* cultures were maintained on LM medium (5 g/l NaCl, 10 g/l yeast extract, 10 g/l tryptone; pH 7.2) unless otherwise stated. Agar was added at a concentration of 15 g/l when required. The medium was supplemented with 50 μg/ml ampicillin or 12.5 μg/ml tetracycline for pAlter-1, and with 100 μg/ml ampicillin for pBluescript II SK^+.

The strains and plasmids used in this study are listed in Table 2.2.

Table 2.2. Bacterial Strains and Plasmids Used

Plasmids/ Strains	Description	Properties
Plasmids:		
pAlter-1	Site-directed mutagenesis vector – Tet^R; Amp^S (Promega)	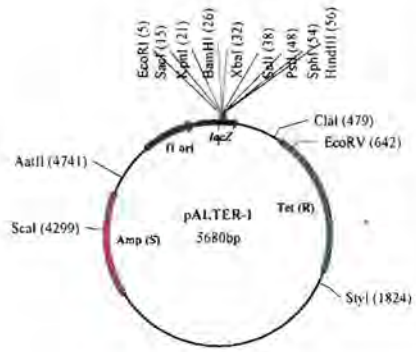
pBluescipt II SK$^+$	High copy number vector for general cloning and expression (Stratagene)	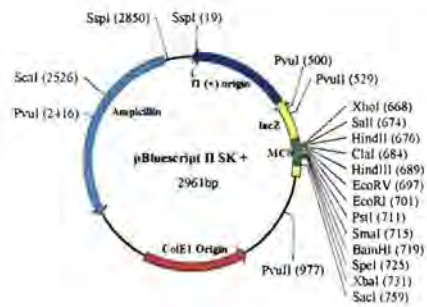
pGln6	Construct containing the *E.coli* wild type *glnA* gene	Backman et al (1981). PNAS 78 : 3743-3747.
Strains:		
***E.coli* JM109**	Host strain	*end*A1 *rec*A1 *gyr*A96 *thi hsd*R17 (r_k-,m_{k+}) *rel*A1 *sup*E44 λ- Δ(*lac-proAB*) [F',*traD*36 *proA+B+ lacl*qZΔM15]
***E.coli* XL1-Blue MR**	Host strain	*(mcrA)18 (mcrCB-hsdSMR-mrr)173 endA1 supE44 thi-1 recA1 gyrA96 relA1 lac*
***E.coli* YMC 11**	Glutamine synthetase auxotrophic strain	*endA thi-1 hsdR17 supE44 ΔlacU169 hutC$_{Klebs}$ Δ(glnA-glnG)2000*

2.2.2 General Techniques

DNA was isolated on a small scale using either the QiaPrep Spin Miniprep Kit (Qiagen) or by alkaline lysis (Sambrook *et al*, 1989). Large-scale DNA isolations were performed using the Qiagen Midi DNA Isolation Kit (Qiagen). Digestion of DNA was carried out using restriction enzymes purchased from Amersham Biosciences and used according to the manufacturer's instructions. Alkaline phosphatase was obtained from Amersham Biosciences. T4 DNA Ligase was obtained from Promega and used as per the protocol supplied with the enzyme. Agarose used for electrophoresis of DNA was of molecular biology grade.

Taq polymerase (rTaq) was obtained from TaKaRa Bio Inc. and was used for general screening purposes. High fidelity *Taq* polymerase (ExTaq) was also obtained from TaKaRa Bio and was used for amplifying genes for cloning.

Restriction digestion and agarose gel elecrophoresis were carried out using standard procedures (Sambrook *et al*, 1989). A 1 kb DNA ladder (Promega Corporation) was used for all electrophoresis.

Site-directed mutagenesis was carried out using the Altered Sites *in vitro* Mutagenesis Kit from Promega Corporation, or the QuikChange XL Site-Directed Mutagenesis Kit from Stratagene, as per the protocols supplied with each kit.

All chemicals were of analytical or molecular biology grade and were used without further purification. All chemicals were obtained from Merck or Sigma unless otherwise stated.

2.2.3 Cloning of the *E.coli* glutamine synthetase gene

Primers were designed to the sequence of the *E.coli glnA* gene obtained from Genbank (Accession Number X05173). The primers were designed with *Nsi*I restriction sites (shown in bold) at the 5' ends. The primers are shown below:

5' primer: 5' – GAT**ATGCAT**CCGTCAAATGCG -3'

3' primer: 5' – GCG**ATGCAT**AAAGTTTCCACGG - 3'

PCR was performed using DNA of pGLn6 as the template and the above primers. The PCR mixture contained 1µl of plasmid DNA (50 ng), 5 µl of each primer (2.5 pmol/µl), 4 µl of 2.5 mM dNTP's, 5 µl 10X buffer containing 20 mM $MgCl_2$ and 0.5 µl of High Fidelity Taq polymerase (2.5 units).

PCR was conducted with the initial denaturation of the template DNA at 95°C for 5 minutes, followed by 30 cycles of denaturation at 95°C for 5 minutes, annealing at 55°C for 1 minute and elongation at 72°C for 2 minutes. A final elongation step of 72°C for 10 minutes was also incorporated into the profile. Agarose gel electrophoresis was carried out to verify the fragment size produced by PCR. The

PCR product was purified using the HighPure PCR Purification Kit (Roche Diagnostics), and subjected to digestion with *Nsi*I.

To construct the template for SDM with the Altered Sites System, pAlter-1 was linearised with *Pst*I and dephosphorylated prior to ligation. Insert and vector were ligated at an insert:vector ratio of 3:1.

The ligation reaction was transformed into *E.coli* JM109 by electroporation using a Bio-Rad Gene Pulser, as per the manufacturer's instructions. Transformants were selected on LM Agar supplemented with 12.5 μg/ml tetracycline, 80 μg/ml X-Gal and 1 mM IPTG.

Several white colonies obtained on the transformation plates were then screened by isolating DNA using alkaline lysis, followed by digestion and agarose gel electrophoresis. Sequencing was carried out to confirm the presence and sequence of the *E.coli glnA* gene. In addition to the use of the M13/F and M13/R universal primers, gene-specific internal primers were designed from the known sequence of the gene. These are shown in Table 2.3.

Table 2.3. Sequence-specific primers used for sequencing of the cloned *E.coli glnA* gene

Primer	**Primer Sequence**
GlnSeq 1	5'-GCTGAACACGTACTGACGATG-3'
GlnSeq 2	5'-GTGGGAACCGGAGATAGATGATC-3'
GlnSeq 3	5'-CGATGTTCGGTGATAACGGCTC-3'
GlnSeq 4	5'-CGTACTTCGATACGACGTGCTTTC-3'

To construct the template for SDM with the QuikChange System, the glutamine synthetase gene was subcloned from the pAlter construct as a *Sac*I - *Hind*III fragment. The band containing the *glnA* gene was excised from the gel using a scalpel blade, and pushed through a 2 ml syringe into an Eppendorf tube, to crush the agarose, following which, 1 ml of phenol (equilibrated to pH 8.0) was added to the tube and the suspension vortexed for 1 minute. The sample was frozen at –70°C for at least 30 minutes. Once the sample had thawed, it was centrifuged at 13 000 rpm in an Eppendorf microfuge for 15 minutes. The aqueous phase was removed to a clean tube and then extracted once with phenol:chloroform:isoamyl alcohol (25:24:1), and then once with chloroform:isoamyl alcohol (24:1). The DNA was ethanol precipitated and resuspended in TE Buffer. This fragment was then ligated into pBluescript II SK^+, also digested with *Sac*I and *Hind*III, at an insert to vector ratio of 3:1. The ligation reaction was transformed into *E.coli* XL1-Blue by electroporation, and plated on LM agar plates containing 100 μg/ml ampicillin. Single transformant colonies were screened by isolating plasmid DNA using alkaline lysis, digesting the DNA with *Bam*HI and subsequently analysing the fragments by agarose gel electrophoresis.

2.2.4 Site- Directed Mutagenesis (SDM)

Altered Sites Mutagenesis

DNA of the wild type *glnA* gene in pAlter-1 was isolated from *E.coli* JM109 using the Qiagen Midi Prep Kit. The oligonucleotides designed to carry out the mutagenesis of the *glnA* gene using this system are listed in Table 2.4. Silent mutations incorporating a restriction site to facilitate primary screening for the mutation were built in to the SDM oligonucleotides. These are also shown in the table.

Table 2.4. Mutations carried out on the *E.coli glnA* gene using the Altered Sites System. Mutations to change amino acid residues are shown in bold and restriction sites are underlined

Mutation	Oligonucleotide Sequence	Restriction Site
Y397V	5'-TGGACAAAAACCTG**GTC**GACCTGCCGCCAG-3'	*Sal*I
S52A	5'-AAATGTTTGACGGC**GC**ATCGATTGGCGGCTG-3'	*Cla*I
S53A	5'-GTTTGACGGATCC**GCT**ATTGGCGGCTGG-3'	*Bam*HI
S52A S53A	5'-GTTTGACGGC**GCAGC**GATCGGCGGCTG-3'	*Pvu*I
H210V	5'-GGTTGAAGCCCAT**GTC**CACGAAGTCGCGACTG-3'	*Nru*I
H211V	5'-GAAGCCCATCAC**GTC**GAAGTAGCGACAGCTGG-3'	*Pvu*II
E327V	5'-GGTCCCGGGCTAT**GTA**GCATCGATAATGCTG-3'	*Cla*I

Following mutagenesis, single colonies were screened for the mutation of choice by isolating DNA from an overnight culture, and performing restriction analysis with the enzyme for the particular mutation being screened for.

Mutant genes were isolated from the pAlter-1 clones by digestion with *Sac*I and *Hind*III. The digests were then subjected to agarose gel electrophoresis to separate the vector and insert bands. The band containing the genes was excised from the gel and the DNA extracted using phenol as described in Section 2.2.3.

pBluescript II SK^+ was digested with *Sac*I and *Hind*III, and each mutant gene was then ligated into this vector at an insert:vector ratio of 3:1. The ligation reaction was transformed into the glutamine synthetase auxotrophic strain *E.coli* YMC11 by electroporation and transformants were selected on LM Agar supplemented with 50 µg/ml ampicillin.

Single colonies obtained on the transformation plates were subjected to a screening procedure using PCR using the M13/F and M13/R universal primers. In this procedure, single colonies were resuspended in 20 µl of distilled water. An aliquot (1 µl) of this colony suspension was added to a PCR reaction containing 2.5 µl of each primer (2.5 pmol/µl), 2 µl of 2.5 mM dNTP's, 2.5 µl 10X buffer, 2 µl of 25 mM $MgCl_2$ and 0.1 µl of *Taq* polymerase (0.5u). PCR cycles were carried out as described in Section 2.2.3. The PCR products were subsequently separated by agarose gel electrophoresis, and positive transformants selected on the basis of the correct band size. A positive control and a negative control were incorporated into the process to verify the results obtained.

Sequencing to confirm each mutation was outsourced. Forward and reverse gene-specific primers were designed from the known sequence of the gene for this purpose. These are shown in Table 2.5.

Table 2.5. Sequence-specific primers used for confirming the presence of the various mutations in the *E.coli glnA* gene

Primer	Mutation	Primer Sequence
Forward Primers		
GlnSeq 5	• S52A • S53A • S52A S53A	5'-GCTGAACACGTACTGACGATG-3'
GlnSeq 7	• E327V • Y397V	5'-GTCTGTCTGAGCAGGCGCTG-3'
GlnSeq 9	• H210V • H211V	5'-GCTATCGACGATATCGAAGG-3'
Reverse Primers		
GlnSeq 6	• S52A • S53A • S52A S53A	5'-GTGGGAACCGGAGATAGATGATC-3'
GlnSeq 8	• E327V • Y397V	5'-GCATAAAGTTTCCACGGCAA-3'
GlnSeq 9	• H210V • H211V	5'-GTTCTTGATACCATCAAGACCG-3'

QuikChange Mutagenesis

DNA of the selected templates (pBluescript constructs) was isolated from *E.coli* XL1-Blue using the Qiagen MidiPrep Kit. The oligonucleotides designed to carry out the SDM using this system are listed in Table 2.6. As this is a PCR-based system, two oligonucleotides (sense and antisense) are required for each reaction.

Following mutagenesis, single colonies were screened for the mutation of choice by isolating DNA from an overnight culture, and performing restriction analysis with the enzyme for the particular mutation being screened for.

Positive mutants obtained with the QuikChange System were transformed into *E.coli* YMC11 for expression purposes.

Sequencing to confirm each mutation was outsourced, using the primers shown in Table 2.5. D50A and E129A were sequenced using GlnSeq 5 and GlnSeq 6. E357A was sequenced using GlnSeq 9 and GlnSeq 10, and E327V and Y397V were verified using GlnSeq 7 and GlnSeq 8.

Table 2.6. Mutations carried out on the *E.coli glnA* gene using the QuikChange System. Mutations to change amino acid residues are shown in bold and restriction sites are underlined.

Mutation	Oligonucleotide Sequence	Restriction Site
D50A	5'-GAAGAAGGCAAAATGTTT**GCA**GGCTC-ATCGATTGGCGGCTGG-3' 5'-CCAGCCGCCAATCGATGAGCC**TGC**AA-ACATTTTGCCTTCTTC-3'	*Cla*I
E129A	5'-CCGTACTGTTCGGGCCC**GCT**CCTGAAT-TCTTCCTGT-3' 5'-ACAGGAAGAATTCAGG**AGC**GGGCCCG-ACAGTACGG-3'	*Apa*I
E327V	5'-GTCTGGTCCCGGGCTAT**GTA**GCATCG-ATAATGCTGG-3' 5'-CCAGCATTATCGATGC**TAC**ATAGCCC-GGGACCAGAC-3'	*Cla*I
E357A	5'-GTCGTATC**GCG**GTACGTTTCCCGGATC-CTGCAGCTAACCG-3' 5'-CGGTTAGCTGCAGGATCCGGGAAACG-TAC**CGC**GATACGAC-3'	*Pst*I

2.3 Results

2.3.1 Cloning of the *E.coli* glutamine synthetase gene

The wild type *glnA* gene of *E.coli* was amplified as a 2.1 kb fragment, encoding a protein of 471 amino acids in length (Figure 2.3).

Figure 2.3. Agarose gel electrophoresis of the PCR reaction to amplify the *E. coli glnA* gene . This is shown as a 2124 bp band on the gel.

The 2124 bp PCR amplified *glnA* gene containing the *Nsi*I flanking restriction sites was ligated into the *Pst*I-digested SDM vector pAlter-1 at an insert:vector ratio of 3:1. DNA was isolated from a number of transformants and subjected to restriction analysis using *Bam*HI and *Eco*RI. According to the known sequence of both the gene and the vector, restriction of a construct (with the *glnA* gene in the correct 5' to 3'

orientation required) with *Bam*HI, should produce fragments of 6012 bp and 1797 bp. A correct construct was identified in this way, and was named pGln12 (Figure 2.4).

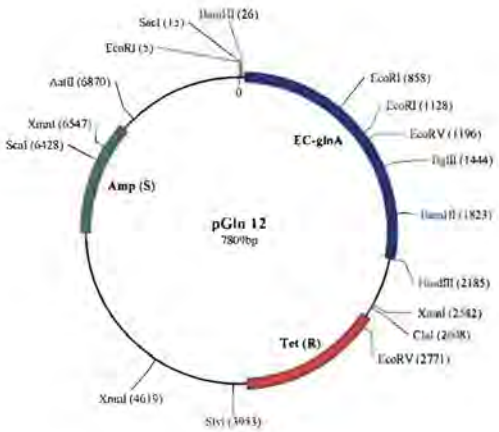

Figure 2.4. Restriction map of pGln12 – wild type *E.coli glnA* cloned into pAlter-1. The construct is tetracycline resistant and ampicillin sensitive.

The restriction analysis of pGln12 with *Bam*HI, resulting in fragment sizes of 6012 and 1797 bp, is shown in Figure 2.5.

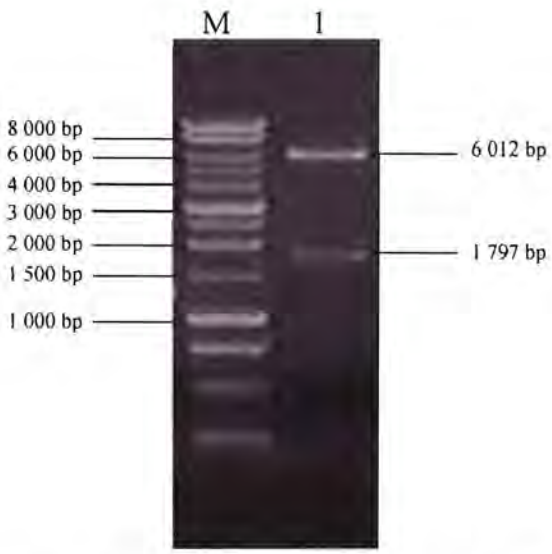

Figure 2.5. Agarose gel electrophoresis showing the *Bam*HI-digested construct pGln12.

To construct the wild type template for the mutagenesis using the QuikChange System, the *glnA* gene was excised from pGln12 as a *Sac*I-*Hind*III fragment, and ligated into similarly digested pBluescript II SK+ at an insert:vector ratio of 3:1. The ligation reaction was transformed into *E.coli* XL1-Blue and plated on LM agar supplemented with 100 μg/ml ampicillin, 80 μg/ml X-Gal and 1mM IPTG. DNA was isolated from a number of white colonies and subjected to restriction analysis with *Sac*I and *Hind*III and *Bam*HI in order to identify a positive subclone. Digestion with *Sac*I and *Hind*III should excise the insert band of 2100 bp from the 2961 bp vector, and digestion with *Bam*HI should produce bands of 3272 bp and 1797 bp (Figure 2.6). A correct construct was identified in this way and named pBSK-ECgln (restriction map shown in Figure 2.7).

Figure 2.6. Agarose gel electrophoresis showing pBSK-ECgln digested with *Bam*HI (Lane 1) and *Sac*I and *Hind*III (Lane 2).

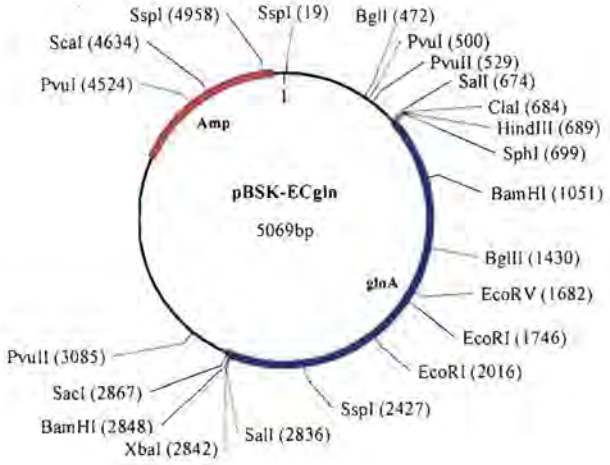

Figure 2.7. Restriction map of pBSK-ECgln.

Sequence analysis was performed on both clones to verify the integrity of the wild type gene before any SDM was carried out (results not shown).

2.3.2 Site Directed Mutagenesis (SDM)

Altered Sites System

The site-directed mutagenesis was carried out as per the protocol, using the oligonucleotides specified in Table 2.4. DNA isolated from the mutants was digested using the enzyme specific for the mutation, and size-fractionated to confirm the presence of the mutation. The presence of the mutation generally resulted in extra fragments as restriction sites were added. In all cases, the wild type construct (pGln12) was digested with the same enzyme as a comparative control. The mutations with their respective introduced restriction sites and expected fragment sizes are outlined in Table 2.7.

Table 2.7. List of mutations introduced into pGln12 with the Altered Sites System, showing the expected restriction fragments and maps resulting from digestion with the appropriate enzyme. The introduced restriction sites are shown in bold on the maps.

Mutation	Introduced restriction site	Restriction Fragments (bp)		Restriction Map
		With Mutation	Without mutation	
Y397V	*Sal*I	5918 1891	7809	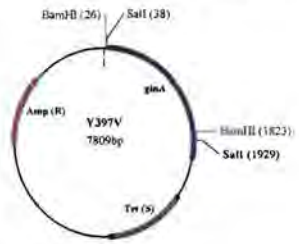
S52A	*Cla*I	6095 1714	7809	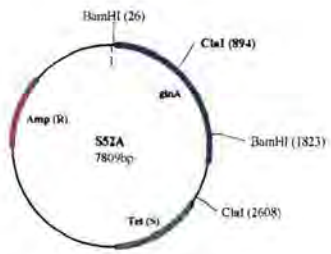
S53A	*Bam*HI	6012 935 862	6012 1797	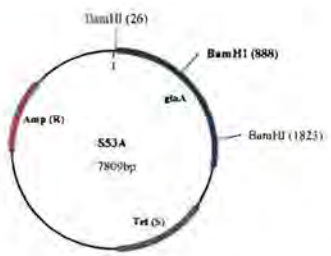
S52A S53A	*Pvu*I	5420 1352 1037	6457 1352	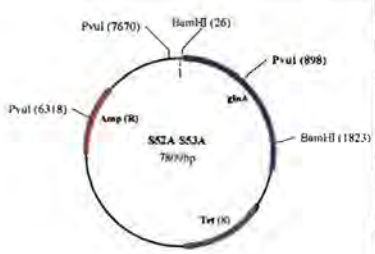

H210V	*Nru*I	4439 1478 1189 703	4439 1892 1478	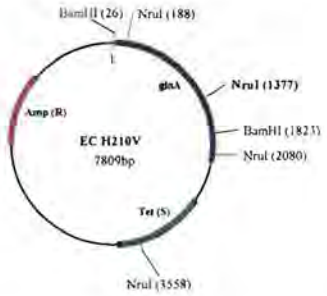
H211V	*Pvu*II	3047 2254 1493 1015	3047 2508 2254	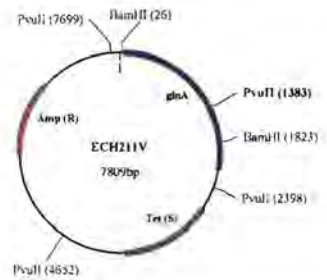
E327V	*Cla*I	6926 883	7809	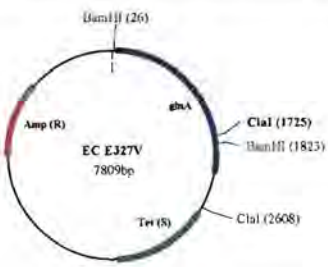

Agarose gel electrophoresis confirmed the presence of the mutations, as the expected DNA fragment sizes (as outlined in Table 2.7) were obtained. The results for each mutant are shown in Figures 2.8 and 2.9.

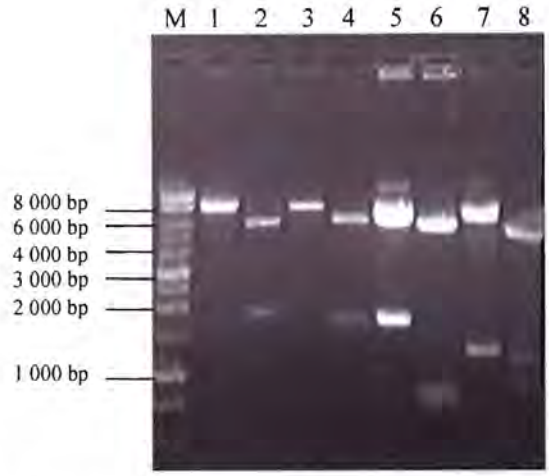

Figure 2.8. Agarose gel electrophoresis of the mutant constructs in comparison to the wild type pGln12 construct, showing the selection of positive mutants. (Lane 1) pGln12 digested with *Sal*I, (2) Y397V digested with *Sal*I, (3) pGln12 digested with *Cla*I, (4) S52A digested with *Cla*I, (5) pGln12 digested with *Bam*HI, (6) S53A digested with *Bam*HI, (7) pGln12 digested with *Pvu*I, (8) S52A S53A digested with *Pvu*I.

Figure 2.9. Agarose gel electrophoresis of mutant constructs in comparison to the wild type pGln12 construct, showing the selection of positive mutants. (Lane 1) pGln12 digested with *Nru*I, (2) H210V digested with *Nru*I, (3) pGln12 digested with *Pvu*II, (4) H211V digested with *Pvu*II, (5) pGln12 digested with *Cla*I, and (6) E327V digested with *Cla*I.

Once these single mutations had been confirmed, the double mutants were produced. In each case the Y397V mutation was added to each of the S52A, S53A, S52A S53A, H210V, H211V and to produce S52A Y397V, S53A Y397V, S52A S53A Y397V, H210V Y397V and H211V Y397V, respectively. The mutations with their respective introduced restriction sites and the expected fragment sizes are outlined in Table 2.8.

Table 2.8. List of mutations introduced into Y397V with the Altered Sites System, showing the expected restriction fragments and maps resulting from digestion with the appropriate enzyme. The introduced restriction sites are shown in bold on the maps

Mutation	Introduced restriction site	Restriction Fragments (bp)		Restriction Map
		With Mutation	Without mutation	
S52A Y397V	*Cla*I	6095 1714	7809	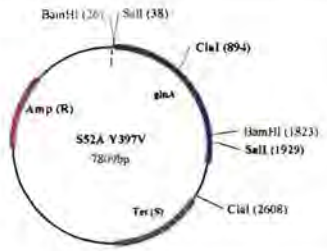
	*Sal*I	5918 1891	7809	
S53A Y397V	*Bam*HI	6012 935 862	6012 1797	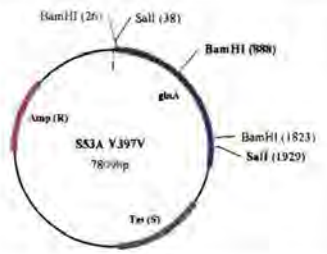
	*Sal*I	5918 1891	7809	
S52A S53A Y397V	*Pvu*I	5420 1352 1037	6457 1352	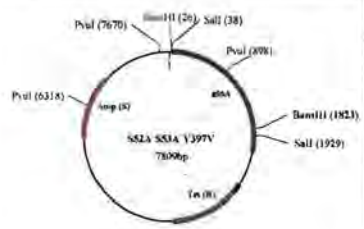
	*Sal*I	5918 1891	7809	

H210V **Y397V**	*Nru*I	4439 1478 1189 703	4439 1892 1478	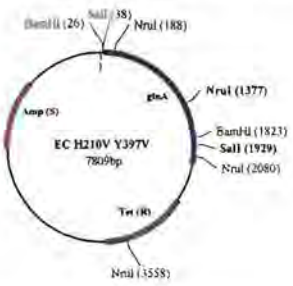
	*Sal*I	5918 1891	7809	
H211V **Y397V**	*Pvu*II	3047 2254 1493 1015	3047 2508 2254	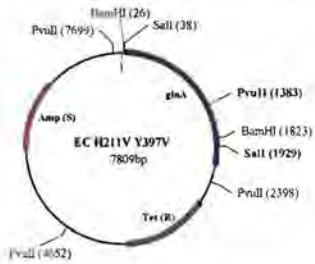
	*Sal*I	5918 1891	7809	

Agarose gel electrophoresis confirmed the presence of the mutations, as the expected DNA fragment sizes (as outlined in Table 2.8) were obtained. The results for each mutant are shown in Figures 2.10 and 2.11.

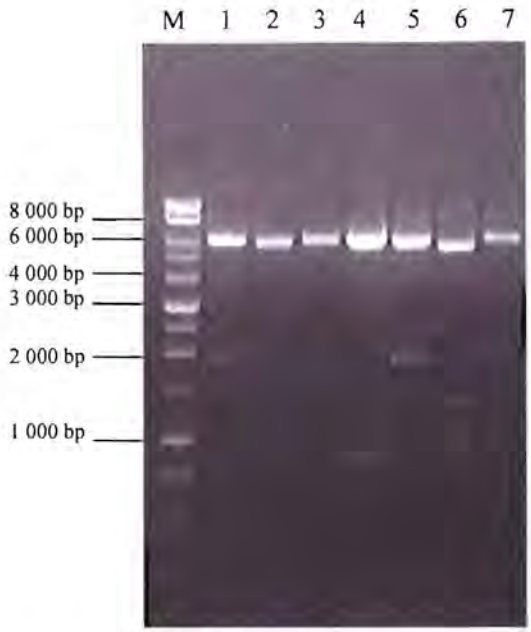

Figure 2.10. Agarose gel electrophoresis of the double mutant constructs, showing the selection of positive mutants. (Lane 1) Y397V digested with *Sal*I, (2) S52A Y397V digested with *Cla*I confirming the presence of the S52A mutation, (3) S52A Y397V digested with *Sal*I confirming the presence of the Y397V mutation, (4) S53A Y397V digested with *Bam*HI confirming the presence of the S53A mutation, (5) S53A Y397V digested with *Sal*I confirming the presence of the Y397V mutation, (6) S52A S53A Y397V digested with *Pvu*I confirming the presence of the S52A S53A mutation, (7) S52A S53A Y397V digested with *Sal*I confirming the presence of the Y397V mutation.

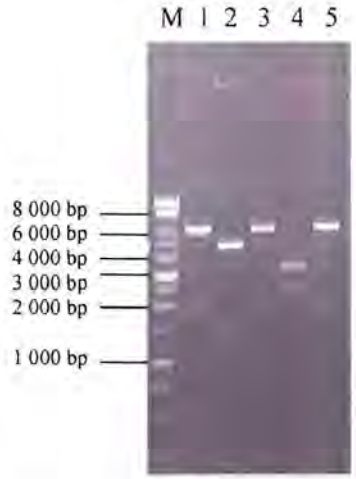

Figure 2.11. Agarose gel electrophoresis of the double mutant constructs, showing the selection of positive mutants. (Lane 1) H210V Y397V digested with *Nru*I confirming the presence of the H210V mutation, (2) H210V Y397V digested with *Sal*I confirming the presence of the Y397V mutation, (3) H211V Y397V digested with *Pvu*II confirming the presence of the H21IV mutation, and (4) H211V Y397V digested with *Sal*I confirming the presence of the Y397V mutation.

Mutant Gene Expression

Mutant genes (from pAlter) were subcloned into pBluescript II SK^+ and transformed into *E.coli* YMC11 , to facilitate protein purification and enzyme studies. The presence of the subcloned genes in the vector was confirmed by PCR screening. Transformant colonies containing the mutant *glnA* genes were detected as a 2170 bp band on an agarose gel. A negative control consisting of the vector transformed into *E.coli* YMC11 was included in the PCR screens, and appeared on the gel as a band the size of the vector multiple cloning site. A positive control of DNA of pBSK-ECgln, also in *E.coli* YMC11, was included. This appeared on the gel as a band the same size as any

positive mutant subclones. An example of an agarose gel showing the results of a PCR screening experiment is given in Figure 2.12.

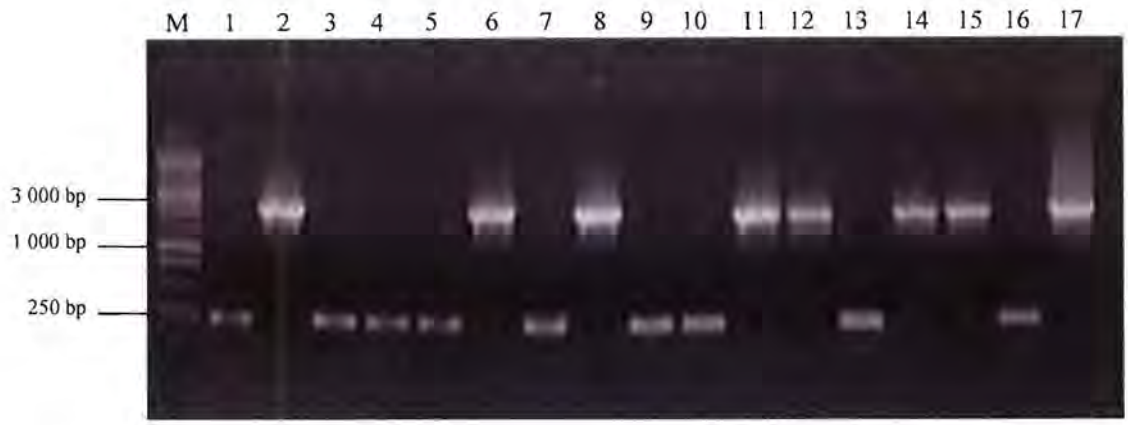

Figure 2.12. Agarose gel electrophoresis showing the results of a PCR screening experiment. The Marker (M) is the 1 kb DNA Ladder. The negative control, showing a band of approximately 250 bp, is in Lane 16. The positive control, showing a band of approximately 2170 bp, is shown in Lane 17. Positive subclones were identified as those in Lanes 2, 6, 8, 11, 12, 14 and 15. Negative subclones were identified as those in Lanes 1, 3, 4, 5, 7, 9, 10 and 13.

The DNA from a single subclone of each mutant identified in this way, was then digested with the restriction enzyme specific for the mutation to confirm the presence of the specific mutation. The correct sizes for each construct are shown in Table 2.9.

Table 2.9. Outline of the expected restriction fragments of the mutant *glnA* subclones

Mutation	Restriction Fragments (bp)		Restriction Map
	Enzyme	Fragment Sizes	
pBSK-Y397V	*Sal*I	2907 1891 271	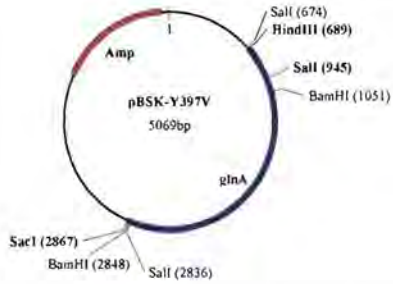
pBSK-S52A	*Cla*I	3771 1298	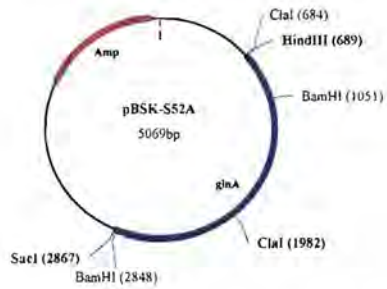
pBSK-S52A Y397V	*Cla*I *Sal*I	3771 1298 2907 1891 271	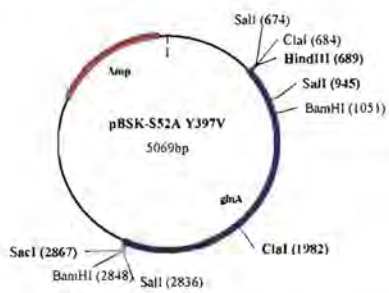
pBSK-S53A	*Bam*HI	3272 935 862	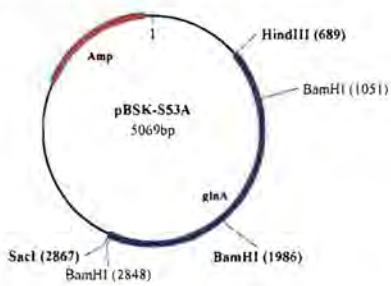

pBSK-S53A Y397V	*Bam*HI *Sal*I	3272 935 862 2907 1891 271	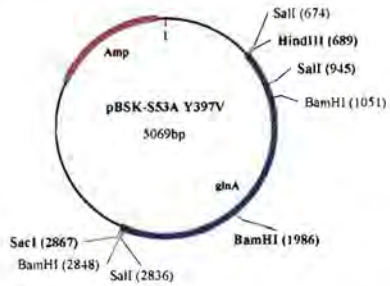
pBSK-S52A S53A	*Pvu*I	2542 1482 1045	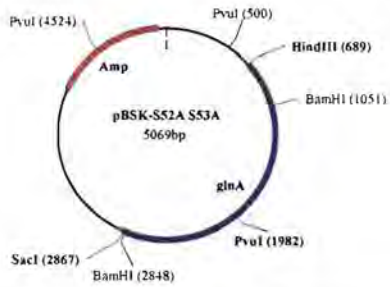
pBSK-S52A S53A Y397V	*Pvu*I *Sal*I	2542 1482 1045 2907 1891 271	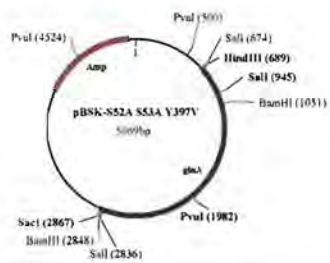
pBSK-H210V	*Nru*I	3177 1189 703	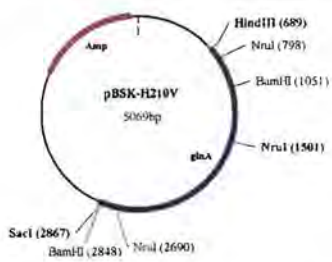
pBSK-H210V Y397V	*Nru*I *Sal*I	3177 1189 703 2907 1891 271	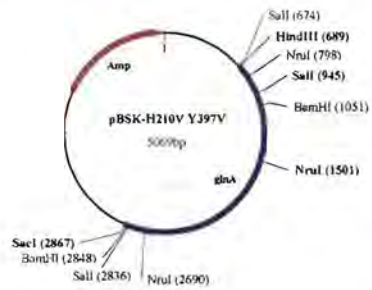

pBSK-H211V	*Pvu*II	2513 1590 966	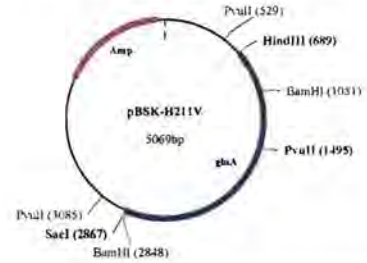
pBSK-H211V Y397V	*Pvu*II *Sal*I	2513 1590 966 2907 1891 271	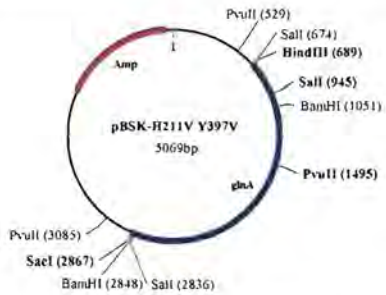
pBSK-E327V	*Cla*I	4602 467	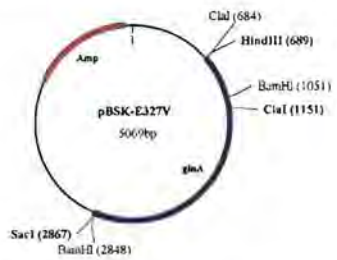

Agarose gel electrophoresis confirmed the presence of the mutations in the subclones, as the expected DNA fragement sizes (as outlined in Table 2.9). The results for each mutant are shown in Figures 2.13 and 2.14.

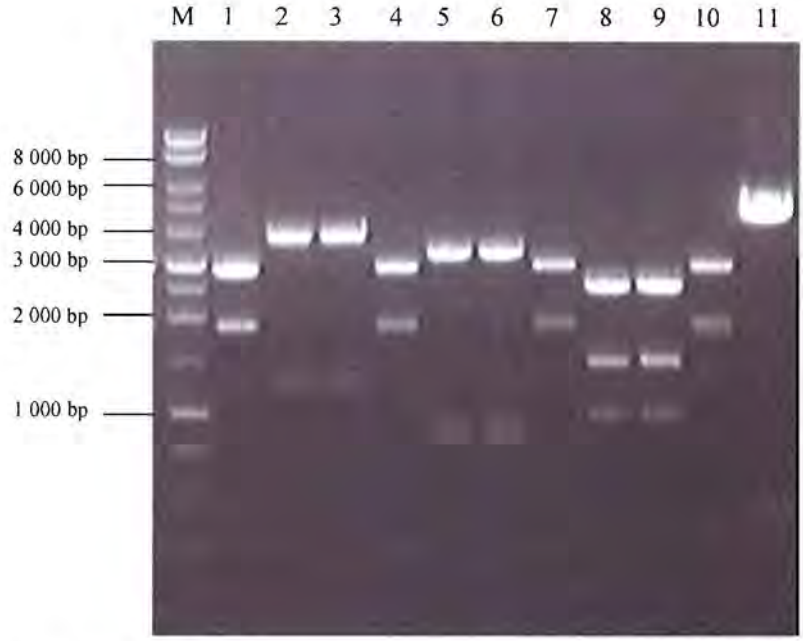

Figure 2.13. Agarose gel electrophoresis of the mutant subclones showing the presence of the mutations. (Lane 1) pBSK-Y397V digested with *Sal*I, (2) pBSK-S52A digested with *Cla*I, (3) pBSK-S52A Y397V digested with *Cla*I, (4) pBSK-S52A Y397V digested with *Sal*I, (5) pBSK-S53A digested with *Bam*HI, (6) pBSK-S53A Y397V digested with *Bam*HI, (7) pBSK-S53A Y397V digested with *Sal*I, (8) pBSK-S52A S53A digested with *Pvu*I, (9) pBSK-S52A S53A Y397V digested with *Pvu*I, (10) pBSK-S52A S53A Y397V digested with *Sal*I, and (11) pBSK-E327V digested with *Cla*I.

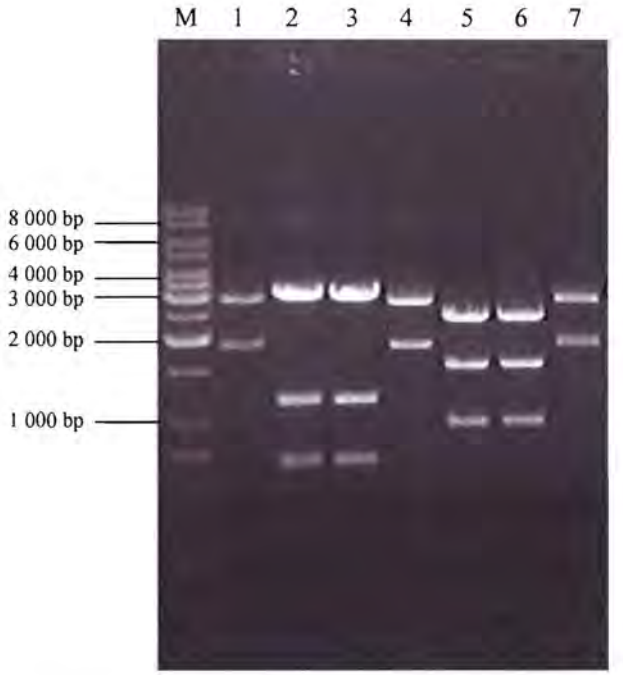

Figure 2.14. Agarose gel electrophoresis of the mutant subclones showing the presence of the mutations. (Lane 1) pBSK-Y397V digested with *Sal*I, (2) pBSK-H201V digested with *Nru*I, (3) pBSK-H201V Y397V digested with *Nru*I, (4) pBSK-H201V Y397V digested with *Sal*I, (5) pBSK-H211V digested with *Pvu*II, (6) pBSK-H211V Y397V digested with *Pvu*I, (7) pBSK-H211V Y397V digested with *Sal*I.

QuikChange Mutagenesis

SDM using the QuikChange System was carried out as per the protocol, using the oligonucleotides specified in Table 2.6.

DNA was isolated from the possible mutants, digested using the enzyme specific for the mutation, and size-fractionated to confirm the presence of the mutation. A control consisting of the parent template was digested with the same enzyme as a comparative control. The mutations with their respective restriction sites and expected fragment sizes are outlined in Table 2.10. pBSK-ECgln was used as the template for the E207T, H271N, D50A, E129A and E357A mutations. The double mutants E207T Y397V and H271N Y397V were produced in pBSK-Y397V, and the triple mutants H269N S52A S53A and H271N S52A S53A were produced by the addition of the H269N and H271N mutations in pBSK-S52A S53A, respectively.

Table 2.10. List of mutations introduced into various templates with the QuikChange System, showing the expected restriction fragments and maps resulting from digestion with the appropriate enzyme. The introduced restriction sites are shown in bold on the maps

Mutation	Introduced restriction site	Restriction Fragments (bp)		Restriction Map
		With Mutation	Without Mutation	
D50A	*Cla*I	3771 1298	5069	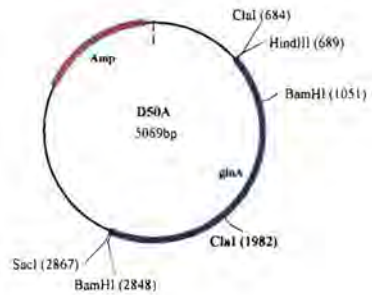
E129A	*Apa*I	3970 1099	5069	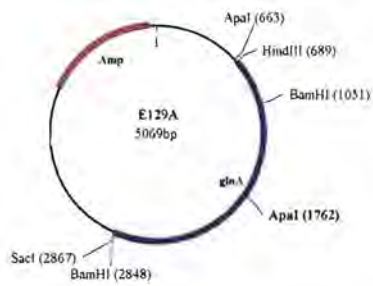
E357A	*Pst*I	5069	uncut	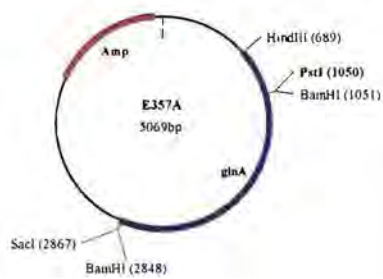

D50A **Y397V**	*Cla*I *Sal*I	3771 1298 2907 1891 271	5069 2907 2162	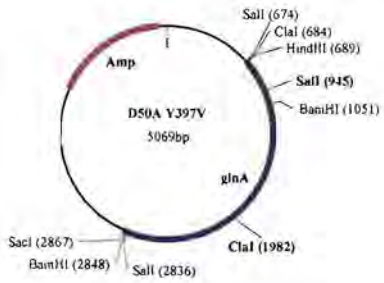
E129A **Y397V**	*Apa*I *Sal*I	3970 1099 2907 1891 271	5069 2907 2162	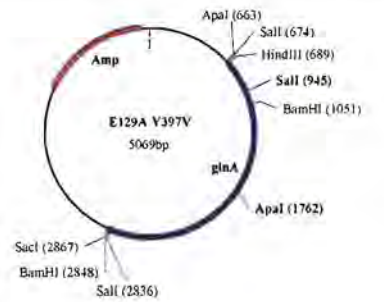
E327V **Y397V**	*Cla*I *Sal*I	4602 467 2907 1891 271	5069 2907 2162	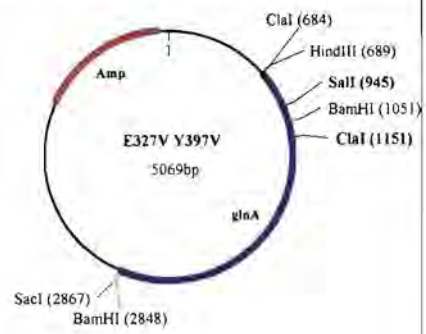
E357A **Y397V**	*Pst*I *Sal*I	5069 2907 1891 271	Uncut 2907 2162	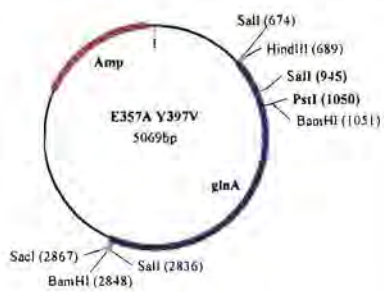

Agarose gel electrophoresis confirmed the presence of the mutations, as the expected DNA fragment sizes (as outlined in Table 2.10) were obtained. The results for each mutant are shown in Figures 2.15 and 2.16.

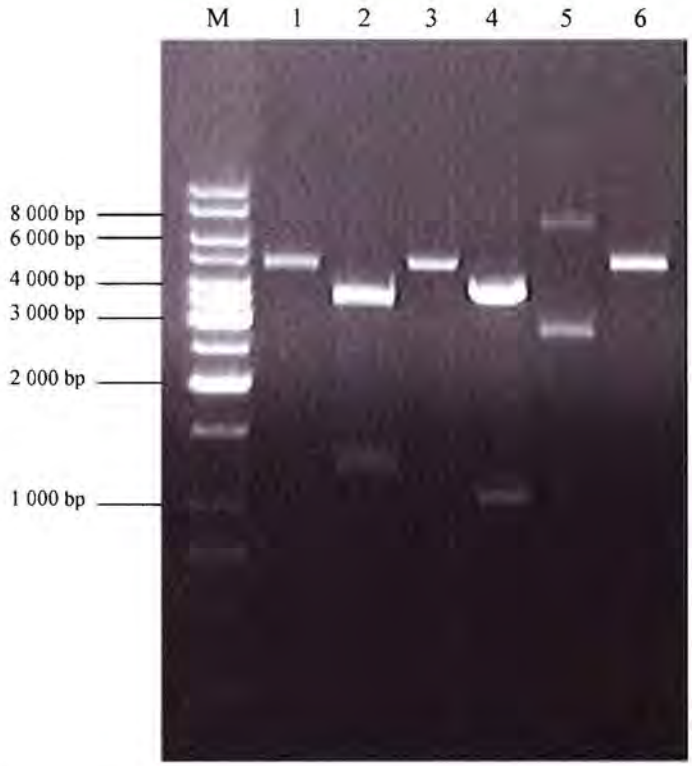

Figure 2.15. Agarose gel electrophoresis of mutant constructs in comparison to the wild type construct, showing the selection of positive mutants. (Lane 1) pBSK-ECgln digested with *Cla*I, (2) D50A digested with *Cla*I, (3) pBSK-ECgln digested with *Apa*I, (4) E129A digested with *Apa*I, (5) pBSK-ECgln digested with *Pst*I, and (6) E357A digested with *Pst*I.

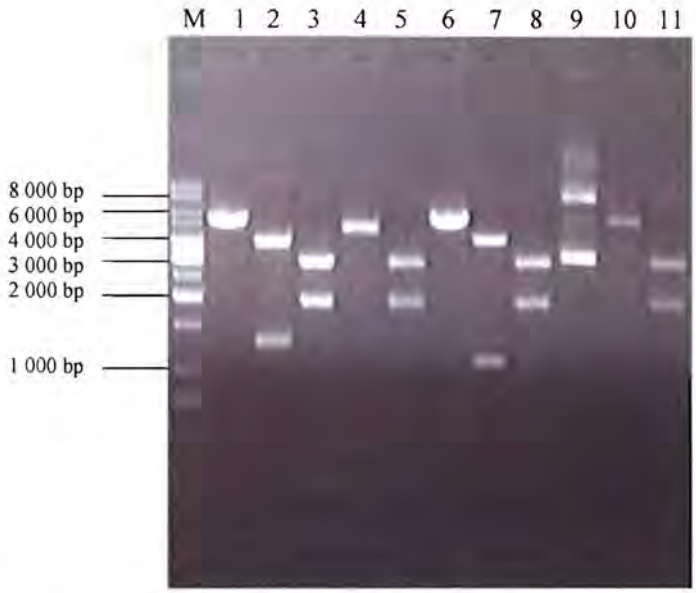

Figure 2.16. Agarose gel electrophoresis of mutant constructs in comparison to the wild type construct, showing the selection of positive mutants. (Lane 1) pBSK-Y397V digested with *Cla*I, (2) D50A Y397V digested with *Cla*I, (3) D50A Y397V digested with *Sal*I, (4) E327V Y397V digested with *Cla*I, (5) E327V Y397V digested with *Sal*I, (6) pBSK-Y397V digested with *Apa*I, (7) E129A Y397V digested with *Apa*I, (8) E129A Y397V digested with *Sal*I, (9) pBSK-Y397V digested with *Pst*I, (10) E357A Y397V digested with *Pst*I, and (11) E357A Y397V digested with *Sal*I.

2.4 Conclusion

Several molecular modelling exercises carried out on the *E.coli* glutamine synthetase gene led to the identification of a number of highly conserved amino acid residues. In order to investigate the role that these residues played in the active site of the glutamine synthetase, it was necessary to change them using site-directed mutagenesis.

All the desired mutations were successfully produced using the selected site-directed mutagenesis systems. Silent mutations encoding restriction sites were included in the oligonucleotides designed for the mutagenesis. This allowed for primary screening without the need to sequence every potential mutant.

The following mutations were produced in the *E.coli* glutamine synthetase gene:

Site of Adenylylation	Y397V
Catalytic Triad	S52A, S52A Y397V
	S53A, S53A Y397V
	S52A S53A, S52A S53A Y397V
	H210V, H210V Y397V
	H211V, H211V Y397V
	D50A, D50A Y397V
	E129A, E129A Y397V
	E327V, E327V Y397V
	E357A, E357A Y397V

Chapter 3

Complementation Studies, Protein Purification and Enzymology

3.1 Introduction

The primary aim of this investigation was to determine if the reaction mechanism employed by glutamine synthetase in the formation of glutamine from the γ-glutamyl phosphate synthesized in the first step of the reaction, occurred via two catalytic triads similar to those employed by the serine proteases.

Mutants were constructed to alter the residues thought to be involved in the putative catalytic triads. These were the serine residues S52 and S53, the histidine residues H210 and H211, as well as D50, E129, E327 and E357.

All the constructed mutants were tested by complementation of the glutamine synthetase auxotrophy in *E.coli* YMC11.

The various recombinant mutant glutamine synthetase enzymes were purified using a combination of streptomycin sulphate precipitation, pH changes and ammonium sulphate precipitation, until a pure enzyme preparation was achieved. An affinity column chromatography method was also developed and used to purify certain of the enzymes.

Two enzyme assays were utilised to assess glutamine synthetase activity. The first assay used, the γ-glutamyl transferase assay, measures the "reverse" reaction as glutamyl transferase activity. In this reverse reaction, hydroxylamine and glutamine react to form γ-glutamylhydroxamate and free ammonia in the presence of ADP, arsenate and manganese or magnesium (Shapiro and Stadtman, 1970). This forms the basis of an assay for the presence of glutamine synthetase activity. At the correct pH, which is derived from determining the isoactivity point of the enzyme, the transferase activities of both the adenylylated and deadenylylated forms of glutamine synthetase are the same. The two forms can, however, be distinguished because at the isoactivity point, fully adenylylated glutamine synthetase is completely inhibited by 60mM Mg^{2+}, whereas the deadenylylated enzyme is unaffected (Bender et al, 1977).

In addition, the rate of conversion of ATP, glutamate and ammonia to glutamine and ADP was assessed using HPLC. This is termed the 'forward' or 'biosynthetic" reaction and is assayed in two different assays; one which measures the ability of glutamine synthetase to convert glutamate to glutamine in the presence of ATP, and the second determines the conversion of ATP to ADP and AMP in the same assay mixture.

3.2 Methods and Materials

3.2.1 General Techniques

All chemicals were of analytical or molecular biology grade and were used without further purification. All chemicals were obtained from Merck or Sigma unless otherwise stated.

$Mn(HCO_3)ATP$ was prepared in-house from Na_2ATP (obtained from Roche) which was dissolved in water to a concentration of approximately 80 mM. The Na^+ ions were then removed from the ATP by passing the solution over a Dowex 50 WX2 strong cation exchange resin. All samples containing the acid-ATP were pooled and reacted with an equivalent molar concentration of $Mn(HCO_3)$. The solution was stirred until all the $MnCO_3$ was dissolved. The pH of the $Mn(HCO_3)$-ATP solution was then adjusted to pH 7.0 with $NaHCO_3$.

SDS Polyacrylamide gel electrophoresis (SDS-PAGE) was carried out according to standard protocols (Laemmli, 1970). Acrylamide was purchased from Sigma as a 40% Acrylamide:bis-acrylamide mixture (19:1 ratio). The broad range protein molecular weight marker from Fermentas was used for all PAGE gels.

3.2.2 Complementation of the glutamine auxotrophy in *E.coli* YMC11

Single colonies of each of the mutant recombinant glutamine synthetase constructs in pBluescript II SK^+ in the *E.coli* glutamine synthetase auxotrophic strain YMC 11 were

plated on M9 Minimal Medium (Sambrook *et al*, 1989), to assess their ability to complement the auxotrophy of *E.coli* YMC11. Glutamine, at a concentration of 250 mg/l, was added to one plate, and a duplicate plate contained no glutamine. Ampicillin was added to both plates at a concentration of 100 µg/ml. *E.coli* YMC11 transformed with non-recombinant pBluescript II SK^+ was used as a negative control. The wild type recombinant construct, pBSK-ECgln was used as the positive control.

The plates were incubated at 37°C and observed over a 48 hour period for the presence or absence of growth.

3.2.3 Purification of the *E.coli* glutamine synthetase

All recombinant constructs used for the isolation of GS were cultured in a modified M9 medium (6 g/l Na_2HPO_4, 3g/l KH_2PO_4, 0.5g/l NaCl) supplemented with 70mM L-glutamate, 5mM L-glutamine and 100 µg/ml ampicillin. All cultures were incubated at 37°C for 48 hours with shaking at 220rpm. Cells were harvested from the culture medium by centrifugation at 16 000 x g at 4°C. The biomass was then either used fresh or stored at -20°C until required.

In addition, the wild type glutamine synthetase (from pBSK-ECgln) was purified in both the adenylylated and deadenylylated forms, from biomass obtained from continuous culture being carried out as part of another investigation. Adenylylated enzyme was produced under conditions of nitrogen excess and carbon limitation, while deadenylylated enzyme was produced under conditions of nitrogen limitation

and carbon excess (Senior, 1975). The cells obtained were harvested by centrifugation at 16 000 x g for 10 minutes at 4°C, and stored at -20°C until required.

The method used for the purification of glutamine synthetase was developed from the method of Shapiro and Stadtman (1970).

The biomass from 1 litre of culture, was resuspended in 10 mls of Resuspending Buffer A or RBA (10mM Imidazole-HCl, 2mM β-mercaptoethanol, 10mM $MnCl_2.4H_20$; pH 7.0). The cells were sonicated for 10 minutes on a 50% duty cycle. This sonicated solution was centrifuged for 10 minutes at 12 000 x g, and the supernatant was retained. Streptomycin sulphate was added (10% of a 10% w/v), and the suspension was stirred at 4°C for 10 minutes. Centrifugation was then carried out at 12 000 x g for 10 minutes and the supernatent was retained. The pH of the supernatant was adjusted to 5.15 with sulphuric acid. This mixture was stirred at 4°C for 15 minutes, and then centrifuged at 20 000 x g for 10 minutes. Again, the supernatant was retained. Saturated ammonium sulphate (30% of volume) was added and the pH was adjusted to 4.6 with sulphuric acid. The suspension was stirred at 4°C for 15 minutes, and then centrifuged at 20 000 x g for 10 minutes. The precipitate obtained was resuspended in 2-5 mls of RBA and the pH adjusted to 5.7 with sulphuric acid. This suspension was stirred overnight at 4°C to allow the glutamine synthetase to resuspend, and then centrifuged at 20 000 x g for 10 minutes. The supernatant was retained and the pH of the suspensions was adjusted to 7.0.

Further purification of the wild type and the Y397V enzymes was achieved through the use of affinity chromatography using an AKTA Explorer (Amersham

Biosciences). Separation was achieved with 5'AMP Sepharose resin with an HR10/10 column which has a length of 10cm and an internal diameter of 10mm. The glutamine synthetase enzyme preparation (approximately 2 mls) was loaded onto the prepared column which was equilibrated with 10mM Imidazole (pH 7.0), 150 mM NaCl and 10 mM $MnCl_2.4H_2O$. The bound glutamine synthetase was eluted off the column with 2.5 mM ADP across a 40 ml linear gradient of 150 to 500 mM NaCl, and 1 ml fractions were collected. The fractions containing pure glutamine synthetase were then pooled and dialysed overnight against RBA.

An aliquot of each protein suspension was electrophoresed on a 7.5 % SDS PAGE gel according to standard protocols (Laemmli, 1970). Protein concentration was determined using the Lowry protein determination method (Lowry et al, 1951), and the concentration was used in determining all enzyme specific activities.

3.2.4 MALDI-TOF Analysis of Purified Proteins

In order to verify that the proteins isolated were definitely glutamine synthetase, each mutant protein was analysed using MALDI-TOF mass spectroscopy.

The desired protein band was excised from a 7.5% SDS PAGE gel (multiple lanes of the same protein were run to obtain sufficient protein). The desired bands were excised from the gel and placed into an Eppendorf tube. Sixty µl of a solution of 75 mM NH_4HCO_3 in 40% ethanol was added to the gel plug and vortexed for 30 minutes. The liquid was removed and discarded. This destaining procedure was repeated until no Coomassie blue remained in the gel plug. The gel plug was then

covered with acetonitrile, and incubated at room temperature for 15 mins, following which all liquid was removed from the tube leaving the gel plug. Sufficient volume of a solution of 5mM dithiothreitol in 50mM ammonium bicarbonate was then added to the tube to cover the gel plug and this was incubated at 60°C for 30 mins. The suspension was then centrifuged at 10 000 x g for 5 mins, and the supernatant was removed and discarded.

Ten µl of a solution of 55 mM Iodoacetamide in 50 mM ammonium bicarbonate was added to the gel plug and incubated at room temperature for 60 mins in the dark. Following incubation, the suspension was centrifuged at 10 000 x g for 5 mins and the supernatant was removed and discarded. The gel plug was covered with 60 µl of acetonitrile, and this suspension was allowed to stand for 10 mins. Following 5 mins of centrifugation at 10 000 x g the supernatant was discarded, and the gel plug was dried in a Speedvac for 10 mins.

Freshly prepared bovine trypsin (5-20 µl) was then added at a concentration of 0.01 µg/ µl in 50 mM NH_4HCO_3. The amount added was dependent on the amount of gel in the Eppendorf tube. This was incubated on ice for 60 mins. After brief centrifugation, the supernatant was removed and 10 µl of 50 mM NH_4HCO_3 was added to the gel plug. This was incubated at 37°C overnight.

The sample was then sonicated for 10 mins in a sonicating bath and the supernatant was recovered after centrifugation at 10 000 x g for 5 mins. Ten µl of a Tri-fluoroacetic acid (TFA)/ acetonitrile solution (50% of 2% TFA and 50% acetonitrile) was added and the sample was sonicated again for 10 mins. After

centrifugation, the supernatant was recovered. Acetonitrile (10 µl) was added and the sample vortexed for 10 mins. The sample was centrifuged at 10 000 x g for 5 mins and the supernatant retained. Equal volumes of the prepared protein sample and a 10mg/ml solution of alpha-cyano hydroxyl cinnamic acid in 01% TFA in acetonitrile were then combined. This is mixed vigorously, and 1 µl of the solution applied to the sample plate. The proteins were then analysed by MALDI-TOF MS.

3.2.5 Determination of Glutamine Synthetase Activity using the Glutamyl Transferase Assay

The γ-glutamyl transferase assay measures the "reverse" reaction as glutamyl transferase activity. This assay was used to routinely to measure the total amount of glutamine synthetase present. Both the adenylylated and deadenylylated forms of the enzyme are active in this assay in the presence of Mn^{2+}. When the same assay is supplemented with 60mM Mg^{2+}, the activity of only the deadenylylated enzyme is determined. The activities of the two forms of the enzyme can therefore be differentiated on the basis of the difference in activity in the presence of Mn^{2+} or Mg^{2+}, at pH 7.15. The assay mixture was adapted from Shapiro and Stadtman (1970). Glutamine synthetase activity is measured in two different assay mixtures; one containing only Mn^{2+} and a second containing both Mn^{2+} and Mg^{2+}. All reagents are prepared in Imidazole Buffer (pH 7.15). Both assays were run in a total volume of 600 µl. The Mn^{2+} assay was set up as shown in Table 3.1.

Table 3.1. Assay Mixture for the Mn^{2+}-based glutamyl transferase assay

Component	Final Concentration in Assay
L-Glutamine	15 mM
NaADP	0.4 mM
Sodium Arsenate	30 mM
$MnCl_2.4H_2O$	0.3 mM
Hydroxylamine	60 mM

The combination (Mn^{2+} and Mg^{2+}) assay was set up as shown in Table 3.2.

Table 3.2. Assay Mixture for the Mn^{2+} and Mg^{2+}-based glutamyl transferase assay

Component	Final Concentration in Assay
L-Glutamine	15 mM
NaADP	0.4 mM
Sodium Arsenate	30 mM
$MnCl_2.4H_2O$	0.3 mM
$MgCl_2.7H_2O$	60 mM
Hydroxylamine	60 mM

A blank reaction was prepared in the same manner as the Mn^{2+} reaction, but replacing the ADP and arsenate solutions with an equivalent volume of water. The assay mix was equilibrated for 5 mins at 37°C, and then initiated by the addition of 50µl of enzyme preparation. The reaction was allowed to proceed for 30 mins, and then terminated by the addition of 900 µl of Stop Mix (1M $FeCl_3.6H_2O$, 0.2M Trichloroacetic acid and 7.1% v/v HCl). The samples were then centrifuged at 13 000rpm for 2 mins in an Eppendorf microfuge to remove any precipitate that may have formed, and the absorbance measured at 540nm. All absorbance readings were entered into a spreadsheet, and the results presented as specific activity in terms of µmoles glutamyl hydroxamate complex/min/mg protein. The degree of adenylylation was calculated from the ratio of the deadenylylated γ-glutamyl transferase activity to the total γ-glutamyl transferase activity (Mn^{2+} reaction), taking the number of subunits into account (Shapiro and Stadtman, 1970).

The effect of pH on the adenylylated WT enzyme, the deadenylylated WT enzyme and the Y397V mutant enzyme was also assessed, using the assay setup described above, but at a range of pH levels. This was carried out as data indicated that the Y397V mutant enzyme behaved similarly to the adenylylated WT enzyme, at specific pH values.

3.2.6 Determination of Glutamine Synthetase Activity by HPLC

This assay was developed to measure the forward reaction of glutamine synthetase. The assay measured the amount of glutamine formed from L-glutamate in the presence of $MnHCO_3$-ATP (the basis of one reaction) and MgATP (the basis of a second reaction), and the amount of ATP, ADP and AMP formed were also measured. The same assay mix solution was run in 2 HPLC methods, one for the glutamate/glutamine assay and one for the ATP/ADP/AMP assay. The assay set-up is shown in Table 3.3.

Table 3.3. Assay Components for the HPLC assay to determine the rate of conversion of glutamate and ATP to glutamine and ADP.

Mn^{2+} Assay		Mg^{2+} Assay	
Component	**Concentration in Assay**	**Component**	**Concentration in Assay**
$MnHCO_3$-ATP	4 mM	Na-ATP	4 mM
L-Glutamate	4 mM	L-Glutamate	4 mM
NH_4HCO_3	4 mM	$(NH_4)_2HPO_4$	2 mM
		$MgCl_2.6H_2O$	4 mM

The Mn^{2+} assay was carried out at a pH of 6.3, and the Mg^{2+} assay at a pH of 7.3. All enzyme preparations were added to the assay mixture in a volume of 50 µl. The addition of the enzyme started the reaction, which was then allowed to proceed for

1 hour. The reaction was stopped by the addition of 6 µl of a 50% solution of trichloroacetic acid. Each assay was then aliquoted into 4 HPLC vials (150 µl per vial), two of which were assayed for glutamate and glutamine, and for ADP and ATP, using a Phenomenex Luna 5µ C18 Column on an Agilent 100 HPLC instrument. All assays were run in triplicate.

As it is believed that two putative catalytic triads, similar to those in the serine proteases, are involved in the reaction mechanism of glutamine synthetase, certain of the mutants were also assayed by HPLC in the presence of the serine protease inhibitors, AEBSF and PMSF, in order to assess the effect that these inhibitors had on the enzyme. The enzymes assessed were the adenylylated WT enzyme, the deadenylylated WT enzyme, and the mutant enzymes S52A, S52A Y397V, S53A, S53A Y397V, S52A S53A and S52A S53A Y397V. The enzymes were pre-incubated for 60 minutes in the presence of 1mM PMSF or 1mM AEBSF. Both PMSF and AEBSF were used, as both compounds bind irreversibly by covalent bonding to serine residues. A control reaction was set up for each enzyme, which contained no inhibitor. Each enzyme was then added to assays set up as described above. The assay was allowed to proceed for 60 minutes, then stopped by the addition of 6 ml of 50% TCA, after which they were analysed by HPLC. All assays were run in triplicate.

3.3 Results

3.3.1 Complementation Studies

The mutant glutamine synthetase gene constructs were grown on M9 minimal medium agar in the presence and absence of glutamine, and assessed for their ability to complement the *glnA* mutation of *E.coli* YMC11. After 48 hours of incubation at 37°C, it was observed that while the negative control (pBluescript II SK^+ in YMC11) was unable to grow in the absence of glutamine, and often grew poorly on medium supplemented with glutamine, the positive control (pBSK-ECgln) was capable of complementing the auxotrophy in YMC11. A problem that was often experienced was that 250 mg/l of glutamine appears to be insufficient to support the growth of the YMC11 strain, and therefore the vector alone in YMC11 struggled to grow. The presence of a functional multicopy glutamine synthetase gene, as in the postive control, ECgln, appears to overcome this problem. pBSK-Y397V, the recombinant deadenylylated construct, was also capable of complementing the auxotrophy of YMC11. Both the WT enzyme and the Y397V enzyme are therefore functional. This is shown in Figure 3.1.

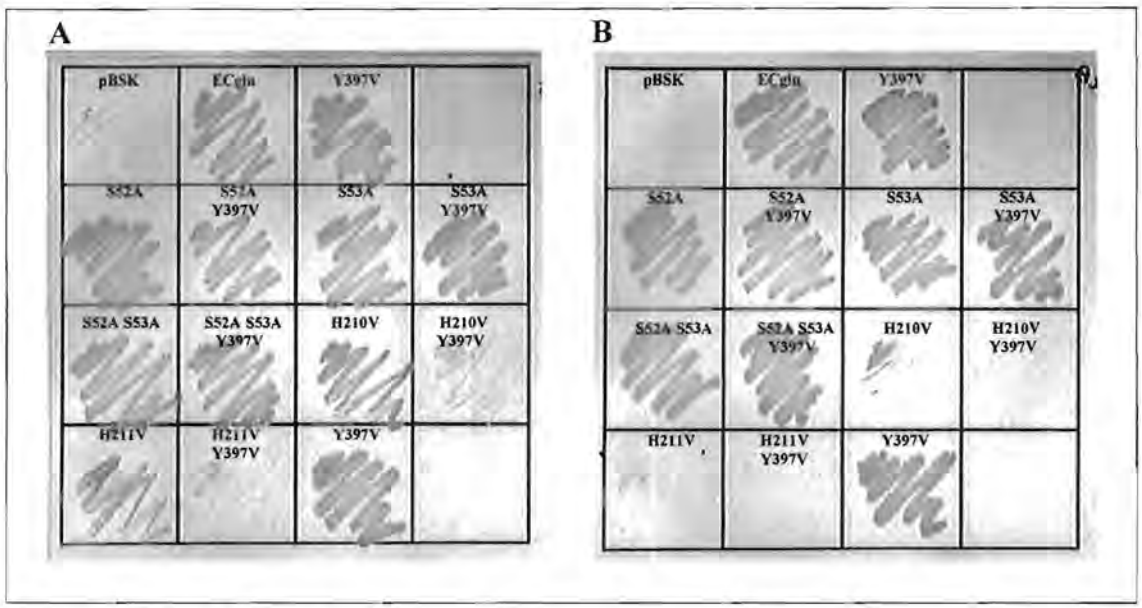

Figure 3.1. Minimal media plates containing 100 μg/ml ampicillin, showing complementation of the auxotrophy of *E.coli* YMC11 by the various mutants. *E.coli* YMC11 containing the vector only (pBSK) was streaked as a negative control and *E.coli* YMC11 containing the WT construct (pBSK-ECgln) was streaked as the positive control. Plate A was supplemented with 250 mg/l of glutamine, and Plate B contained no glutamine.

The S52A and S53A mutants as well as the double mutants, S52A Y397V and S53A Y397V, were all capable of complementing the auxotrophy of *E.coli* YMC 11, thus indicating functionality. The same was found to be true for the double serine mutant, S52A S53A, and its counterpart, S52A S53A Y397V. The two histidine mutants, H210V and H211V, grew well on the minimal plate supplemented with glutamine, but grew very badly on the plate containing no glutamine, thus indicating enzymes with little functionality. The double histidine mutants, H210V Y397V and H211V Y397V, on the other hand, grew very badly even on the plate supplemented with glutamine, and not at all on the plates containing no glutamine. It was therefore assumed that

these two enzymes had virtually no functionality and that these mutations created auxotrophy with the result that they have an absolute requirement for glutamine.

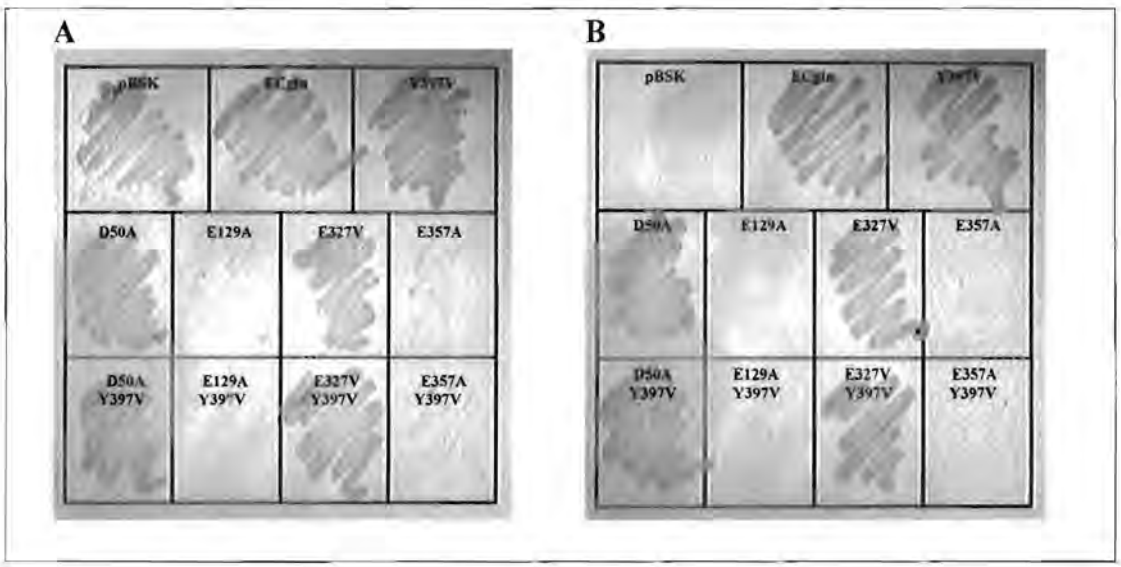

Figure 3.2. Minimal media plates containing 100 μg/ml ampicillin, showing complementation of the auxotrophy of *E.coli* YMC11 by the various mutants. *E.coli* YMC11 containing the vector only (pBSK) was streaked as a negative control and *E.coli* YMC11 containing the WT construct (pBSK-ECgln) was streaked as the positive control. Plate A was supplemented with 250 mg/l of glutamine, and Plate B contained no glutamine.

Mutants D50A and D50A Y397V exhibited good growth on both plates, and are both, therefore, obviously functional (Figure 3.2). Both E129A and E357A, however, were not capable of complementing the auxotrophy of YMC11, and both exhibited very poor growth even on the plate supplemented with glutamine. The same applied to the double mutants, E129A Y397V and E357A Y397V. E327V and E327V Y397V exhibited good growth on both plates, and both, therefore, have functional glutamine synthetase enzymes.

3.3.2 Purification of the *E.coli* GS

For the purification of the mutant proteins, each mutant was grown in a modified M9 minimal medium supplemented with glutamate as the sole nitrogen source. A small amount of glutamine was added to facilitate cell growth, as the YMC11 strain is a glutamine auxotroph.

All cultures were grown for 48 hours at 37°C, and then checked for contamination. Recombinant plasmid integrity was checked by isolating the plasmid DNA, subjecting it to restriction analysis, followed by agarose gel electrophoresis (results not shown).

It was found that some of the double mutants, namely H210V Y397V, H211V Y397V and E357A Y397V required the addition of 10 mM glutamine to the minimal medium in order to get sufficient biomass to enable enzyme purification, as the growth was so poor.

Glutamine synthetase enzyme was successfully purified to at least 90% homogeneity from all the mutants. The SDS-PAGE gels demonstrating this are shown in Figures 3.3 to 3.5. In each instance, between 300 and 700 ng of protein was loaded per lane.

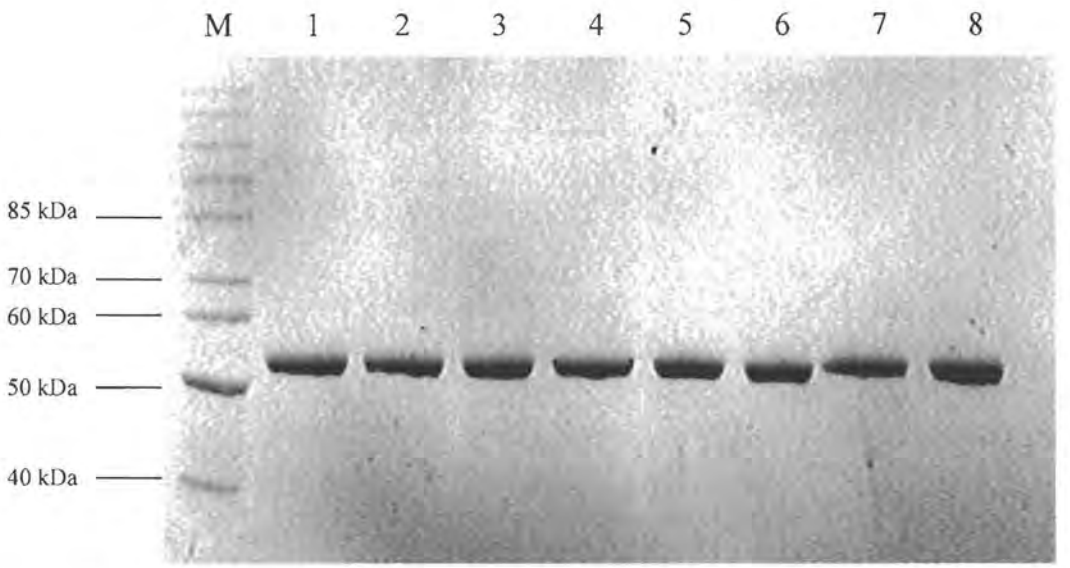

Figure 3.3. SDS-PAGE gel showing purified glutamine synthetase enzyme from various mutants. (Lane 1) WT glutamine synthetase (ECgln) (grown in M9), (2) Adenylylated WT glutamine synthetase (N excess, C limited continuous culture), (3) Deadenylylated WT glutamine synthetase (N limited, C excess continuous culture) (4) Y397V, (5) S52A, (6) S52A Y397V, (7) S53A, (8) S53A Y397V.

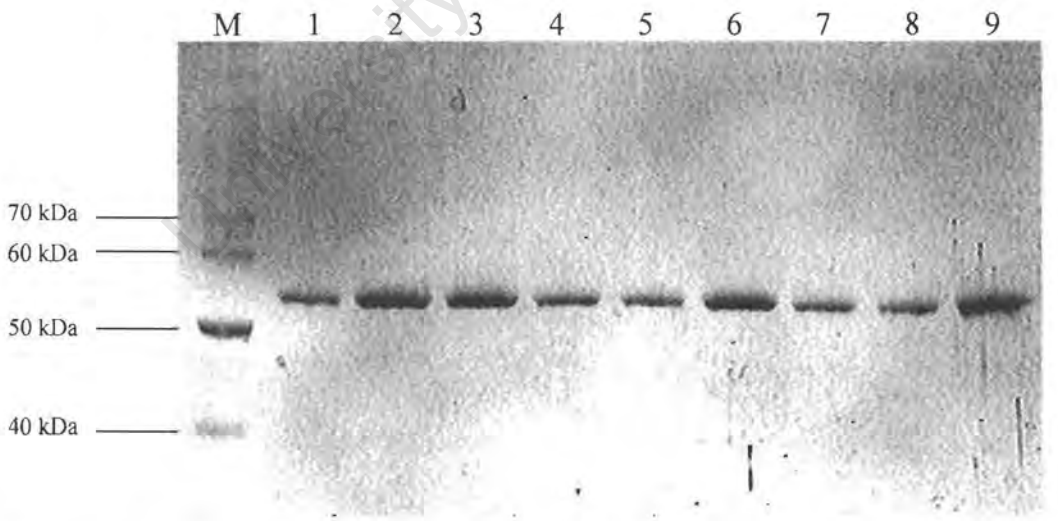

Figure 3.4. SDS-PAGE gel showing purified glutamine synthetase enzyme from various mutants. (Lane 1) S52A S53A, (2) S52A S53A Y397V, (3) H210V, (4) H210V Y397V, (5) H211V, (6) H211V Y397V, (7) D50A, (8) D50A Y397V and (9) E129A.

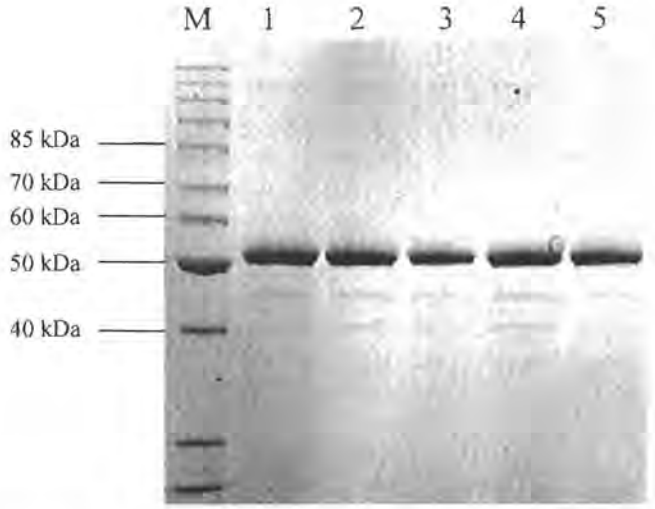

Figure 3.5. SDS-PAGE gel showing purified glutamine synthetase enzyme from various mutants. (Lane 1) E129A Y397V, (2) E327V, (3) E327V Y397V, (4) E357A, and (5) E357A Y397V.

In all instances, the presence of purified glutamine synthetase was demonstrated as the presence of a single band at approximately 55 kDa.

3.3.3 Verification of Purified Glutamine Synthetase

As some mutant enzymes had effectively no activity, all the purified mutant glutamine synthetase enzymes were subjected to MALDI-TOF analysis to verify that the enzymes were indeed glutamine synthetase. Each enzyme was run on a 7.5% SDS-PAGE gel and the bands expected to be glutamine synthetase were cut out and the protein was purified as described. At least 3 μg of protein was loaded in each instance. An example of this type of gel is shown in Figure 3.6.

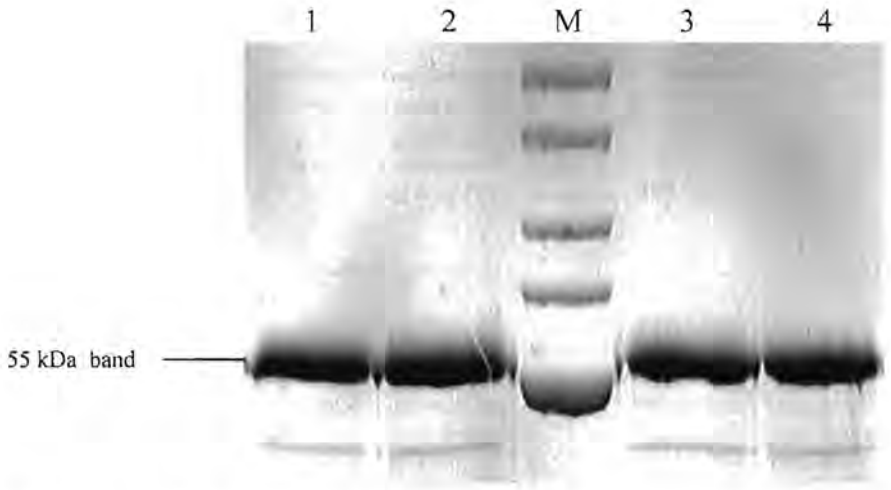

Figure 3.6. 7.5% SDS-PAGE gel for MALDI-TOF Analysis. The protein bands at 55kDa were excised from the gel and purified. (Lane 1) Y397V, (2) S52A, (3) S53A and (4) H210V.

Purified protein samples were pipetted onto a sample plate, and subjected to analysis by MALDI-TOF mass spectroscopy. A typical result obtained from the analysis is shown in Figure 3.7.

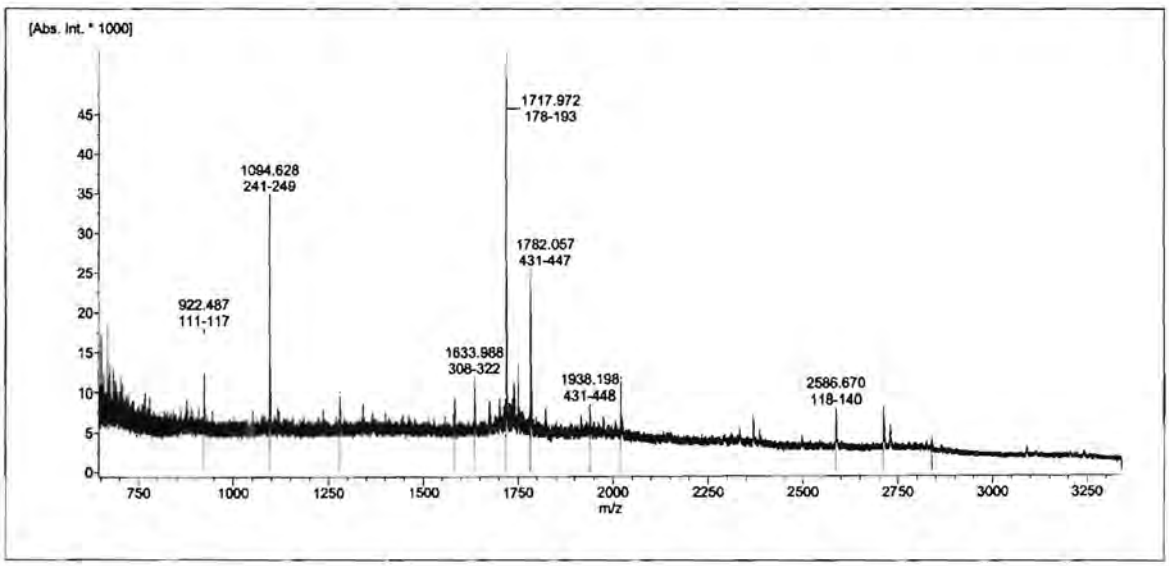

Figure 3.7. Example of a MALDI-TOF analysis result, establishing the identitiy of the S52A mutant protein as glutamine synthetase.

The proteins were then identified by entering the values obtained into the database at http://us.expasy.org/tools/peptident. All the isolated proteins were identified as glutamine synthetase in this manner.

3.3.4 Glutamyl Transferase Assays

Each mutant was assessed for activity using the γ-glutamyl transferase assay. This determines the presence of a ferric-hydroxamate complex in a colourimetric assay in which the absorbance is read at 540nm. The assay determines total enzyme activity in a reaction containing Mn^{2+}. In addition, the degree of adenylylation of the glutamine synthetase enzyme being screened is determined in a reaction containing both Mn^{2+} and Mg^{2+}, as the adenylylated form of the enzyme is inhibited in the presence of Mg^{2+} (Shapiro and Stadtman, 1970; Bender et al, 1977). The degree of adenylylation of the glutamine synthetase enzyme is reported as a percentage in Table 3.4.

The results of the assays are shown in Table 3.4, with the enzyme activities shown in μmoles per minute per mg of protein.

The WT enzyme grown in the same way as the mutants in a modified M9 medium (WT in Table 3.4), is largely in the adenylylated form as most of the activity is inhibited approximately 4-fold from 91 to 20 μmoles/min/mg protein, in the presence of Mg^{2+}, giving a percentage of adenylylation of 78%. A similar level of adenylylation is seen in the WT strain grown under continuous culture conditions of N excess and C limitation, where the glutamine synthetase would be predominantly

adenylylated (WT (AD) in Table 3.4). The WT enzyme, grown in N limitation and C excess continuous culture, should be in the deadenylylated form (WT (DD) in Table 3.4) and this is reflected in the assay results. The specific activities for this particular strain are almost identical in the assay run in the presence of Mn^{2+} only (55.8), as in the presence of Mn^{2+} and Mg^{2+} (56.1), giving, as would be expected, a percentage of adenylylation of 0.

Table 3.4. Glutamyl transferase assay results of the *E.coli* WT and constructed mutants. The WT enzyme refers to the strain grown in the modified M9 medium, and the WT (AD) and WT (DD) refers to the adenylylated and deadenylylated enzymes, respectively, produced in continuous culture. The values presented represent the average of at least three assays where the variation in activity was less than 10%.

Enzyme	Total Enzyme Activity : 4.5mM $MnCl_2$ (µmoles/min/mg protein)	Activity of deadenylylated Enzyme : 4.5 mM $MnCl_2$ + 60 mM $MgCl_2$ (µmoles/min/mg protein)	Percentage of Adenylylaton
WT	91.5	20.2	78
WT (AD)	84.9	21.1	75
WT (DD)	55.8	56.1	0
Y397V	64.5	5.1	92
Catalytic Triad			
S52A	35.5	8.9	75
S52A Y397V	78.6	14.0	82
S53A	47.8	19.1	60
S53A Y397V	86.2	30.5	65
S52A S53A	7.2	2.8	61
S52A S53A Y397V	29.9	7.5	75
H210V	2.8	0.0	100
H210V Y397V	0.0	0.0	-
H211V	0.0	0.0	-
H211V Y397V	0.0	0.0	-
D50A	1.28	0.60	53
D50A Y397V	1.78	0.20	89
E129A	2.38	0.60	75
E129A Y397V	12.06	2.05	83
E327V	0.7	0.0	100
E327V Y397V	1.73	0.32	82
E357A	3.3	3.5	0
E357A Y397V	0.03	0.05	0

The mutant enzyme, Y397V, was expected to be in the deadenylylated form, as the Tyr397 has been substituted with a valine residue. The mutant showed a very high total activity of 64.5 μmoles/min/mg protein, but does not appear to be deadenylylated, but more adenylylated, as the activity in the presence of Mn^{2+} and Mg^{2+} (5.1) is much lower than that detected in the presence of Mn^{2+} only (64.5), resulting in a percentage of adenylylation of 92%. This could be due to the fact that the adenyltransferase is incapable of adenylylating or deadenylylating the valine residue, resulting in a glutamine synthetase enzyme that is improperly folded. It is postulated that, the adenylylation and deadenylylation events carried out by the adenyltransferase entail the specific folding of the glutamine synthetase loop, by the adenyltransferase, into either one of two conformations required for each state of the enzyme, with the steric effect of the adenine groups facilitating the folding of the enzyme into the correct conformation. The Y397V mutant enzyme may, therefore have a loop conformation similar to the adenylylated form of the enzyme, as the adenyltransferase would not have folded the Y397 loop into the "correct" conformation required for deadenylylation. The adenylylated form of this enzyme, therefore, tends towards being the default structure.

A pH profile of γ-glutamyl transferase activity, comparing the WT (AD), WT (DD) and the Y397V mutant enzyme, indicated that the Y397V enzyme does, in fact, behave similarly to the adenylylated enzyme, except at the isoactivity point (Figure 3.8). The isoactivity point is defined as the pH at which equal amounts of glutamine synthetase activity are obtained, irrespective of the state of adenylylation of the enzyme.

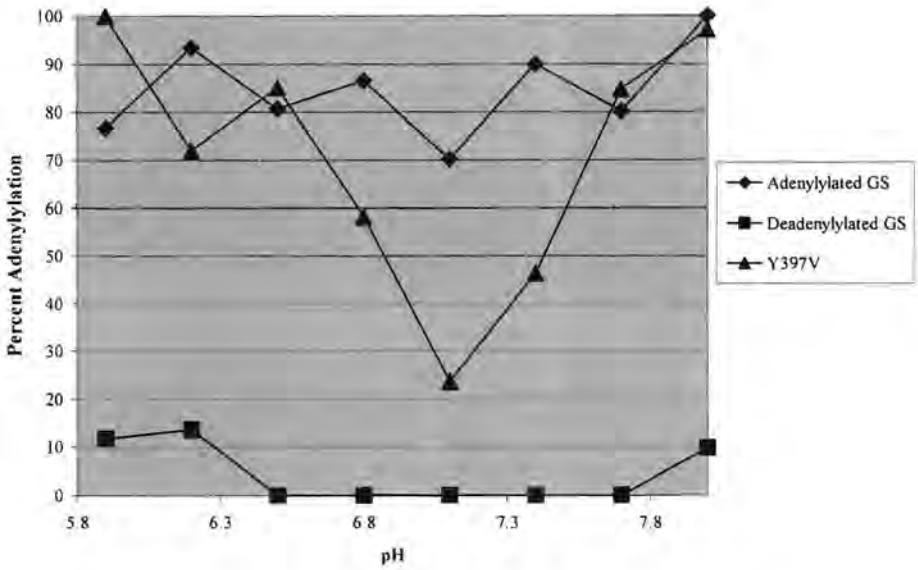

Figure 3.8. pH profile of γ-glutamyl transferase activity of the WT (AD), WT (DD) and Y397V enzymes, showing that the Y397V mutant enzyme behaves similarly to the adenylylated enzyme.

The two serine residues, 52 and 53, were altered singly in two mutant strains and both of these mutations resulted in a lowering of the total γ-glutamyl transferase activity, to 35.5 and 47.8 μmoles/min/mg of protein, respectively, indicating that these residues play a role in the catalytic activity of the enzyme. Altering the serine residues each separately, together with the Y397V mutation, to produce S52A Y397V and S53A Y397V, resulted in an increase in the Mn^{2+} activity over that seen in the two individual serine mutants, to levels comparable with the WT enzyme (78.6 and 86.2 μmoles/min/mg protein). The percentage of adenylylation in S52A and S52A Y397V is similar to that obtained for the WT (all in the region of 75-80%). Altering S53 results in a lowering of the percentage of adenylylation to 60-65% in both mutants (S53A and S53A Y397V), possibly indicating that S53 is an important residue for deadenylylated form of the enzyme. Altering both the serine residues simultaneously, to produce the double mutant S52A S53A, resulted in a large reduction in γ-glutamyl

transferase activity to 7.2 μmoles/minmg protein. When the triple mutant, S52A S53A Y397V was assayed, some γ-glutamyl transferase activity was restored (29.9 μmoles/min/mg protein), but this activity was still less than that obtained in the WT strains. This would seem to confirm that these serine residues play an important role in the active site of the glutamine synthetase enzyme. The implications of this data is discussed when outlining the HPLC based assay data.

The two histidine residues identified as potentially forming part of a catalytic triad, proved to be crucial to the catalytic activity of the enzyme. H210V exhibited a very small amount of Mn^{2+}-dependent γ–glutamyl transferase activity (2.8 μmoles/min/mg protein), which decreased to nothing in the double mutant H210V Y397V. Neither mutant of H211V exhibited any activity at all. H210V was fully adenylylated (percentage of adenylylation of 100%). When the ability to adenylylate or deadenylylate this enzyme was removed in the double mutant H210V Y397V, no activity was obtained.

The four residues identified as potentially being the acid residue of the catalytic triad ie D50A, E129A, E327V and E357A, all showed varying amounts of activity. D50A and D50A Y397V showed a small amount of total γ–glutamyl transferase activity (1.28 and 1.78 μmoles/min/mg protein, respectively, but show different degrees of adenylylation (53% and 89% respectively). E129A showed a small amount of activity (2.38 μmoles/min/mg protein), which increases to 12.06 μoles/min/mg protein in the double mutant E129A Y397V. None of the mutants E327V, E327V Y397V, E357A and E357A Y397V exhibit much γ-glutamyl transferase activity, the highest amount being 3.3 μmoles/min/mg protein shown by E357A. Both E357A mutants showed 0%

adenylylation, although this is off a very low activity base. As observed in the literature, these four residues are important for catalytic activity as the introduction of the mutations resulted in a reduction in activity in all instances (Liaw et al, 1993, Liaw and Eisenberg, 1994a, Alibhai and Villafranca, 1994).

Generally, in all the double mutants created, the degree of adenylylation appeared to increase over that obtained for the single mutants. The Y397V mutation, therefore, appears to affect all the catalytic sites in a similar way.

3.3.5 HPLC Assays

In addition to the γ-glutamyl transferase assays, assays were also developed to measure the rate of conversion of ATP and glutamate to ADP and glutamine by HPLC. These were set up as single assays but were analysed separately for glutamate and glutamine and ATP and ADP. The results are shown in Table 3.5. The conversion rates for glutamate to glutamine, in both the presence of Mn^{2+} and Mg^{2+} by glutamine synthetase is referred to as the glutamine-based specific activity (presented in μmoles/min/mg protein), as the concentration of glutamine formed is used to calculate the specific activity. The conversion rates for ATP to ADP, in both the presence of Mn^{2+} and Mg^{2+} by glutamine synthetase is referred to as the ADP-based specific activity (presented in μmoles/min/mg protein), as the concentration of ADP formed is used to calculate the specific activity. The percentage of conversion was also calculated as the ratio of the glutamine-based specific activity to the ADP-based specific activity, and this value is interpreted as the ability of the enzyme to complete

Table 3.5. Assay results showing the rate of conversion of glutamate and ATP to glutamine and ADP as determined using HPLC. The WT enzyme refers to the strain grown in the modified M9 medium, and the WT (AD) and WT (DD) refer to the adenylylated and deadenylylated enzymes produced in continuous culture. The values presented represent the average of three different assays, in which the difference in the values was less than 5%.

Enzyme	Glutamine-Based Specific activity : Mn^{2+} Assay (μmoles/min/mg protein)	ADP-Based Specific activity : Mn^{2+} Assay (μmoles/min /mg protein)	Percentage Conversion Mn^{2+} Assay	Glutamine-Based Specific activity : Mg^{2+} Assay (μmoles/min/mg protein)	ADP-Based Specific activity : Mg^{2+} Assay (μmoles/min /mg protein)	Percentage Conversion Mg^{2+} Assay	AMP-Based Specific activity : Mn^{2+} Assay (μmoles/min /mg protein)
WT	4.31	4.37	98	4.26	4.21	100	-
WT (AD)	3.76	3.65	100	3.02	3.12	97	-
WT (DD)	4.98	4.62	100	14.54	13.92	100	-
Y397V	2.81	4.95	57	0.12	0.23	50	-
Catalytic Triad							
S52A	2.08	2.30	91	2.41	2.85	85	-
S52A Y397V	5.37	6.24	86	5.31	7.68	69	-
S53A	5.80	6.36	91	4.88	6.96	70	-
S53A Y397V	15.45	21.32	73	10.66	15.42	69	-
S52A S53A	2.29	2.59	88	0.91	1.27	72	0.39
S52A S53A Y397V	3.01	4.54	66	0.11	0.30	36	0.36
H210V	0.15	0.14	100	0.03	0.06	62	0.05
H210V Y297V	0.01	0.00	100	0.00	0.01	49	0.01
H211V	0.02	0.02	100	0.05	0.06	87	0.08
H211V Y397V	0.09	0.09	93	0.02	0.05	40	0.05
D50A	0.62	0.92	67	0.29	0.85	34	-
D50A Y397V	2.82	4.90	58	1.98	4.19	47	-
E129A	0.00	0.00	-	0.00	0.04	0	-
E129A Y397V	0.00	0.00	-	1.42	2.03	70	-
E327V	0.32	0.42	78	0.00	0.03	0	-
E327V Y397V	0.46	0.53	86	1.64	1.71	100	-
E357A	0.36	0.21	100	0.00	0.00	-	-
E357A Y397V	0.04	0.06	62	0.04	0.01	100	-
							-

both steps of the reaction, ie glutamate to glutamine and ATP to ADP, at an equivalent level of efficiency. In some instances, when screening the various mutants, it was discovered that some had the ability to convert ATP all the way to AMP. The amount of AMP produced was then also converted to a specific activity, referred to as the AMP-based specific activity which was also reported in μmoles/min/mg protein.

The WT enzyme grown in the minimal medium shows similar Mn^{2+} glutamine- and ADP-based specific activities (4.31 μmoles/min/mg protein and 4.37 μmoles/min/mg protein, respectively) and a conversion rate of 98%. The levels of activity produced in the Mg^{2+} assays are of a similar level – 4.26 μmoles/min/mg protein glutamine-based specific activity and 4.21 μmoles/min/mg protein ADP-based specific activity, with a conversion rate of 100%.

The WT enzyme produced under conditions of nitrogen excess and carbon limitation, to be adenylylated (WT(AD) in Table 3.5), shows very similar levels of activity in both the Mn^{2+} and Mg^{2+} assays and has a conversion rate of 100%. The WT enzyme produced under conditions of nitrogen limitation and carbon excess to be deadenylylated (WT(DD) in Table 3.5) was much more active in the Mg^{2+} assays (14.54 μmoles/min/mg protein in the glutamine assay and 13.92 μmoles/min/mg protein in the ADP assay) than in the Mn^{2+} assays (4.98 μmoles/min/mg protein in the glutamine assay and 4.62 μmoles/min/mg protein in the ADP assay). Both the Mn^{2+} and Mg^{2+} assays showed a percentage of conversion of approximately 100%, indicating that both steps of the assay were carried out at an equivalent level of efficiency. As the deadenylylated enzyme should exhibit more Mg^{2+} activity than the adenylylated enzyme, this result was to be expected.

The Y397V enzyme is more active in the Mn^{2+} assays than in the Mg^{2+} assays, with conversion rates of only 50%. This low conversion efficiency is possibly due to the incorrect folding of the Tyr397 flexible loop producing an active site containing unbound water. This water can then act as the nucleophile, reacting with the highly unstable glutamyl phosphate intermediate converting it back to glutamate and PO_4, creating the inefficiency. In addition, as postulated in Section 3.3.4, the adenylylation of the enzyme by the adenyltransferase entails the adenylylation of the Tyr397 flexible loop, and the specific conformation of this loop is induced by the steric effects of the adenine groups, facilitating the folding of the enzyme into the correct conformation.

S52A and S52A Y397V are both active but S52A showed reduced glutamine synthetase activity compared to the WT enzymes screened. S52A produced similar activity levels in both the glutamine- and ADP-based Mn^{2+} and Mg^{2+} assays (in the region of 2.0 to 2.8 μmoles/min/mg protein), with a percentage of conversion of 91% for the Mn^{2+} assays and 85% for the Mg^{2+} assays. S52A Y397V, on the other hand was more active than S52A producing a glutamine-based Mn^{2+} specific activity of 5.37 μmoles/min/mg protein and an ADP-based Mn^{2+} specific activity of 6.24 μmoles/min/mg protein. This was equivalent to a conversion rate of 91%. The Mg^{2+} assays gave a glutamine-based Mg^{2+} specific activity of 5.31 μmoles/min/mg protein and an ADP-based Mg^{2+} specific activity of 7.68 μmoles/min/mg protein, representing a percentage conversion of 69%.

S53A produced activity levels slightly higher than those produced in the WT strains – 5.80 μmoles/min/mg protein for the Mn^{2+} glutamine-based assay, 6.36

μmoles/min/mg protein for the Mn^{2+} ADP-based assay, 4.88 μmoles/min/mg protein for the Mg^{2+} glutamine-based assay and 6.96 μmoles/min/mg protein for the Mg^{2+} ADP-based assay. These represented conversion rates of 91% and 70 %, respectively. The activity levels found for S53A Y397V were significantly higher than those found in the WT strains. The Mn^{2+} activities increased to 15.45 for the glutamine-based assay and 21.32 μmoles/min/mg protein for the ADP-based assay. The Mg^{2+} activities were 10.66 μmoles/min/mg protein for the glutamine-based assay and 15.42 μmoles/min/mg protein for the ADP-based assay.

S52A S53A was not as active as the two S53A mutants. It produced Mn^{2+} activities of 2.29 μmoles/min/mg protein for the glutamine assay and 2.59 μmoles/min/mg protein for the ADP assay, with a percentage of conversion of 88%. The enzyme did, however, exhibit the ability to convert ATP right through to AMP in the presence of Mn^{2+}, with a specific activity of 0.39 μmoles/min/mg protein being obtained for the conversion of ADP to AMP. An example of the chromatogram obtained for this mutant is shown in Figure 3.9. S52A S53A did exhibit much lower Mg^{2+} activity levels – 0.91 μmoles/min/mg protein for the glutamine assay and 1.27 μmoles/min/mg protein for the ADP assay. This lower activity may be occurring in the active site attributed to the adenylylated form of the enzyme. The enzymes capable of converting ATP to AMP were able to synthesize glutamine from ADP (data not shown).

When the S52A S53A mutation was combined with the Y397V mutation, the Mn^{2+} activity levels increased compared to the S52A S53A mutant (to 3.01 μmoles/min/mg protein for the glutamine assay and 4.54 μmoles/min/mg protein for the ADP assay.

The Mg^{2+} glutamine- and ADP-based specific activities for this triple mutant, however, decreased quite significantly to 0.11 and 0.30 μmoles/min/mg protein.

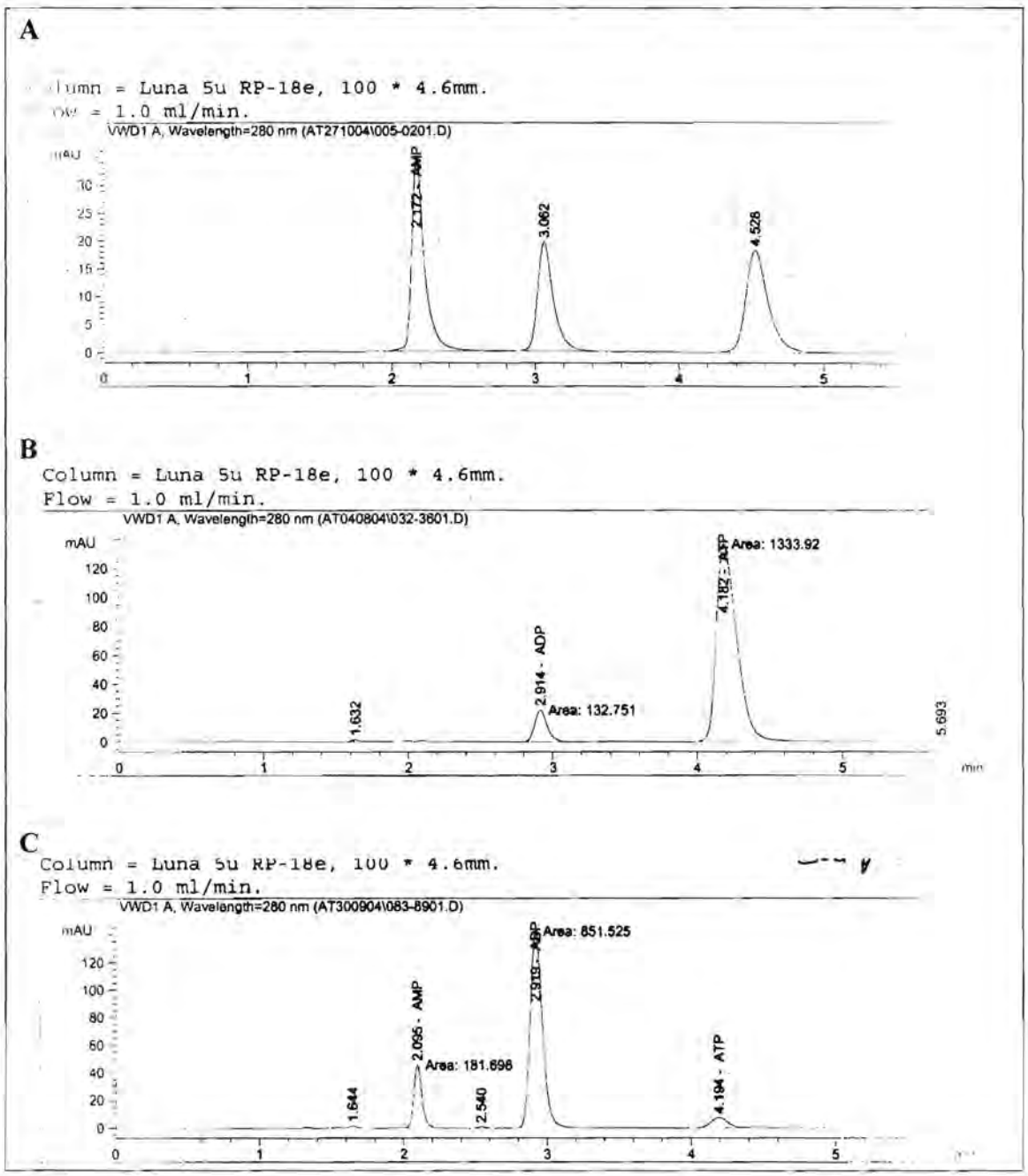

Figure 3.9. HPLC Chromatograms of the ATP/ADP assay showing : (A) Standards showing ATP, ADP and AMP, (B) no production of AMP in the WT assay, and (C) the production of the AMP in the S52A S53A reaction.

Again, this enzyme exhibited the ability to produce AMP in the assay, showing a specific activity of 0.36 μmoles/min/mg protein. These results showed that the two serine residues are very important for the catalytic activity of the enzyme. Again, as in the case of the Y397V enzyme, the conversion efficiency of the triple mutant is compromised (66%), with the activity primarily appearing to occur in the "adenylylated" active site.

As outlined in Section 3.3.4, it is proposed that on deadenylylation of the glutamine synthetase, the adenyltransferase folds the loop into a specific conformation and, on adenylylation, it is the steric effect of the adenyl groups that creates the conformational change. In the case of the mutants containing the Y397V mutation, no specific folding of the Tyr397 loop occurs. As a result, no steric interactions can occur, with the 'default' position of the enzyme being similar to the adenylylated form of the enzyme. If this theory is correct, all the double mutants produced with the Y397V mutation would also be affected, with the 'default' position of all these enzymes being similar to the adenylylated form of the enzyme. It is also important to note, that all mutant enzymes capable of producing AMP had significantly reduced Mg^{2+}-based specific activities.

The two histidine residues believed to form part of the catalytic triad, showed, in general, very low levels of activity. Activity levels of 0.15 μmoles/min/mg protein for the Mn^{2+} glutamine-based assay and 0.14 μmoles/min/mg protein for the Mn^{2+} ADP-based assay were detected for the H210V mutant. The levels of activity produced by this mutant in the Mg^{2+} assay were very low (0.03 μmoles/min/mg protein for the glutamine-based assay and 0.06 μmoles/min/mg protein for the ADP-based assay).

The double mutant H210V Y397V showed very little activity in any assay – 0.01 μmoles/min/mg protein in the Mn^{2+} glutamine-based assay, 0.0 μmoles/min/mg protein in the Mn^{2+} ADP-based assay, 0.0 μmoles/min/mg protein in the Mg^{2+} glutamine-based assay and 0.01 μmoles/min/mg protein in the Mg^{2+} ADP-based assay. Neither H211V nor H211V Y397V exhibited much activity in any assay, indicating their importance in the active site of glutamine synthetase. All four mutants have specific activities in all the assays of less than 0.1 μmoles/min/mg protein. It was interesting to note, however, that all four of these mutants could convert ATP all the way to AMP, although a lower level of AMP was produced than for the double serine mutants.

Of the residues identified as the potential acid residue in the putative catalytic triad, *viz* D50A E129A, E327V and E357A, all showed reduced levels of activity, and varying rates of conversion. D50A showed reduced activity compared to the WT clones. This mutation, when combined with the Y397V mutation, resulted in an increase in activity in all the assays, compared to D50A. The Mn^{2+} glutamine-based assay specific activity and the Mn^{2+} ADP-based assay specific activity increased from 0.62 μmoles/min/mg protein and 0.92 μmoles/min/mg protein, respectively, in D50A to 2.82 μmoles/min/mg protein and 4.90 μmoles/min/mg protein, respectively, in D50A Y397V. The Mg^{2+} activities showed a similar trend, increasing from 0.29 μmoles/min/mg protein and 0.85 μmoles/min/mg protein, respectively, in D50A to 1.98 μmoles/min/mg protein and 4.19 μmoles/min/mg protein, respectively, in D50A Y397V. The conversion rates in both mutants were low, indicating that the enzyme was not fully functional. E129A exhibited no activity in any assay. Some activity became detectable in the double mutant, E129A Y397V. E327V showed low specific

activities in the Mn^{2+} assay (0.32 μmoles/min/mg protein in the glutamine-based assay and 0.42 μmoles/min/mg protein in the ADP-based assay, but these levels dropped in the Mg^{2+} assay. E327V Y397V, on the other hand, had similar Mn^{2+} glutamine-based and ADP-based specific activities to those obtained in E327V, but the Mg^{2+} activities were significantly higher than the Mg^{2+} activities of E327V. This could be an indication that this residue is important in the adenylylated form of the enzyme. E357A produced specific activities in the Mn^{2+} assay of 0.36 μmoles/min/mg protein glutamine-based activity and 0.21 μmoles/min/mg protein ADP-based activity. No activity was detected in either Mg^{2+} assay. When E357A was combined with Y397V, the double mutant showed lower Mn^{2+} activities than E357A, but Mg^{2+} activity was restored (0.04 μmoles/min/mg protein glutamine-based activity and 0.01 μmoles/min/mg protein ADP-based activity).

The results of the serine protease inhibitor experiment are shown in Table 3.6.

The values are presented as a percentage in the reduction of activity between the result obtained in the absence of inhibitor and the result obtained in the presence of inhibitor. The percentage of conversion, reflecting the conversion efficiency of the enzymes is also shown. Negative % reduction values obtained indicate an increase in activity in the presence of the inhibitor, above the level obtained in the control. This was especially evident in the ATP hydrolysis reactions, indicating that the first step of the reaction occurs at an increased rate in the presence of the inhibitor. A percentage of reduction of ± 15% was taken as a reflection of the error in the assay, and it was, therefore, assumed that the protease inhibitor was having little or no effect.

Table 3.6. HPLC data obtained in the experiments using the serine protease inhibitors, PMSF and AEBSF. Data is presented as a percentage reduction in specific activity between the control reaction run in the absence of the inhibitor and the reaction run in the presence of the inhibitor.

		Mn			Mg		
Enzyme		% Reduction in ADP-based Specific Activity	% Reduction in Glutamine-based Specific Activity	% Conversion	% Reduction in ADP-based Specific Activity	% Reduction in Glutamine-based Specific Activity	% Conversion
WT (AD)	**No Inhibitor**			101			116
	PMSF	15.63	49.20	61	-48.13	46.33	42
	AEBSF	26.76	14.86	118	34.60	24.59	134
WT (DD)	**No Inhibitor**			92			76
	PMSF	3.53	17.69	78	6.07	16.55	67
	AEBSF	4.73	2.23	94	14.98	8.43	82
Y397V	**No Inhibitor**			91			108
	PMSF	17.58	44.47	61	4.88	31.39	78
	AEBSF	20.13	4.98	108	43.37	10.83	107
S52A	**No Inhibitor**			92			84
	PMSF	13.41	39.84	64	19.51	43.54	59
	AEBSF	-30.66	-15.27	81	31.77	10.61	109
S52A Y397V	**No Inhibitor**			80			100
	PMSF	15.50	29.12	67	-73.28	77.41	49
	AEBSF	16.65	11.57	85	100.00	-1.95	-
S53A	**No Inhibitor**			115			51
	PMSF	-46.95	22.73	61	17.31	-6.90	66
	AEBSF	15.43	15.19	115	39.50	1.70	83
S53A Y397V	**No Inhibitor**			82			105
	PMSF	-39.67	-6.07	63	ND	ND	-
	AEBSF	-14.80	-5.16	75	100.00	55.60	-
S52A S53A	**No Inhibitor**			89			82
	PMSF	13.56	16.92	85	23.74	23.24	82
	AEBSF	16.20	7.69	98	41.91	17.82	115
S52A S53A Y397V	**No Inhibitor**			72			-
	PMSF	4.83	18.20	62	DI	DI	-
	AEBSF	5.20	1.65	75	DI	DI	-

ND = Not Done

DI = Data Inaccurate; Extremely low activity levels obtained, making interpretation of the results inaccurate

PMSF was found to particularly inhibit the adenylylated WT, deadenylylated WT, Y397V, S52A and the S52A Y397V glutamine-based specific activity. Less effect was observed in the other mutants examined. Less inhibition was also observed with PMSF in the ADP-based assays. AEBSF appeared to cause inhibition of the ADP-based enzyme activity the adenylylated WT enzyme, as well as the mutants Y397V,

S52A, S52A Y397V, S53A, S53A Y397V and S52A S53A. The extent of the inhibition profile appeared to be quite variable though. Where AEBSF did not cause a significant reduction in the glutamine-based specific activity, it's presence in the active site did appear to increase the ADP-based specific activity. PMSF did not significantly inhibit the activity of S52A S53A or S52A S53A Y397V. This was to be expected, as both serines have been removed from the active site. The mechanism of action of AEBSF, therefore, appears to be different from that of PMSF, as it did inhibit both these mutant enzymes. This apparent difference in mechanism of action may be as a result of the steric effect of the different shape of the two molecules.

Both PMSF and AEBSF were found to bind to the active site while still allowing ATP hydrolysis to occur. This may be interpreted as competitive binding of the serine protease inhibitor to the glutamate site, while still allowing ATP hydrolysis to occur. It is important to note that in all cases, while inhibition was found to occur, there was a concomitant reduction in the conversion efficiency.

3.4 Conclusion

The primary aim of this investigation was to determine if the following hypothesis could be validated - that the reaction mechanism employed by glutamine synthetase in the formation of glutamine from the γ-glutamyl phosphate synthesized in the first step of the reaction, occurred with two catalytic triads similar to those employed by the serine proteases.

All the constructed mutants were tested by complementation of the glutamine synthetase auxotrophy in *E.coli* YMC11. Mutants were routinely tested by assaying for γ-glutamyl transferase activity, using a 'reverse' reaction, and by determining the rate of conversion of glutamate and ATP to glutamine and ADP, by HPLC. All the mutants were compared to a WT enzyme, which had been cultivated in the same minimal medium used for all the mutants, as well as WT enzymes which had been produced in continuous culture to be either adenylylated or deadenylylated.

A summary table of the results obtained for the mutants is presented in Table 3.7.

Table 3.7. Comparison table of data from the complementation studies, γ-glutamyl transferase assay results and HPLC assay results from the mutants generated to elucidate the catalytic triad of glutamine synthetase.

	Complementation Results	Glutamyl Transferase Assay Results			HPLC Assay Results						
Enzyme	Complementation of the glutamine synthetase auxotrophy of YMC11	Glutamyl Transferase Assay : Total Enzyme Activity (Mn^{2+}) (μmoles/min/mg protein)	Glutamyl Transferase Assay : Deadenylylated Enzyme Activity (Mn^{2+} & Mg^{2+}) (μmoles/min/mg protein)	Percentage of adenylylation	Glutamine-Based Specific activity : Mn^{2+} Assay (μmoles/min/mg protein)	ADP-Based Specific activity : Mn^{2+} Assay (μmoles/min/mg protein)	Percentage Conversion Mn^{2+} Assay	Glutamine-Based Specific activity : Mg^{2+} Assay (μmoles/min/mg protein)	ADP-Based Specific activity : Mg^{2+} Assay (μmoles/min/mg protein)	Percentage Conversion Mg^{2+} Assay	AMP-Based Specific activity : Mn^{2+} Assay (μmoles/min/mg protein)
WT	+++	91.5	20.2	78	4.31	4.37	98	4.26	4.21	100	-
WT (AD)	Not Done	84.9	21.1	75	3.76	3.65	100	3.02	3.12	97	-
WT (DD)	Not Done	55.8	56.1	0	4.98	4.62	100	14.54	13.92	100	-
Y397V	+++	64.5	5.1	92	2.81	4.95	57	0.12	0.23	50	-
Catalytic Triad											
S52A	+++	35.5	8.9	75	2.08	2.30	91	2.41	2.85	85	-
S52A Y397V	+++	78.6	14.0	82	5.37	6.24	86	5.31	7.68	69	-
S53A	+++	47.8	19.1	60	5.80	6.36	91	4.88	6.96	70	-
S53A Y397V	+++	86.2	30.5	65	15.45	21.32	73	10.66	15.42	69	-
S52A S53A	+++	7.2	2.8	61	2.29	2.59	88	0.91	1.27	72	0.39
S52A S53A Y397V	+++	29.9	7.5	75	3.01	4.54	66	0.11	0.30	36	0.36
H210V	++	2.8	0.0	100	0.15	0.14	100	0.03	0.06	62	0.05
H210V Y397V	-	0.0	0.0	-	0.01	0.00	100	0.00	0.01	49	0.01
H211V	-	0.0	0.0	-	0.02	0.02	100	0.05	0.06	87	0.08
H211V Y397V	-	0.0	0.0	-	0.09	0.09	93	0.02	0.05	40	0.05
D50A	+++	1.28	0.60	53	0.62	0.92	67	0.29	0.85	34	-
D50A Y397V	+++	1.78	0.20	89	2.82	4.90	58	1.98	4.19	47	-
E129A	-	2.38	0.60	75	0.02	0.00	-	0.00	0.04	0	-
E129A Y397V	-	12.06	2.05	83	0.85	0.00	-	1.42	2.03	70	-
E327V	+++	0.7	0.0	100	0.32	0.42	78	0.00	0.03	0	-
E327V Y397V	+++	1.73	0.32	82	0.46	0.53	86	1.64	1.71	100	-
E357A	-	3.3	3.5	0	0.36	0.21	100	0.00	0.00	-	-
E357A Y397V	-	0.03	0.05	0	0.04	0.06	62	0.04	0.01	100	-

The 'deadenylylated' mutant Y397V was the first mutant constructed and then examined. It was expected that this mutant would produce enzyme that exhibited deadenylylated activity, but this was proved not to be the case. It is postulated that this mutant does not exhibit true deadenylylated activity as a result of the inability of the adenyltransferase to adenylylate or deadenylylate the valine residue, resulting in a glutamine synthetase enzyme that is improperly folded. The adenylylation and deadenylylation events carried out by the adenyltransferase entail the specific folding of the Tyr397 loop, by the adenyltransferase, into either one of two conformations required for each state of the glutamine synthetase enzyme. It is also postulated, that the deadenylylation of the enzyme by the adenyltransferase entails the folding of the loop into a specific conformation, and with the adenylylation of the enzyme, it is the steric effects of the adenine groups that facilitate the folding of the enzyme into the correct conformation. The Y397V mutant enzyme may, therefore have a loop conformation similar to the adenylylated form of the enzyme, as the adenyltransferase could not recognise and fold the Y397 loop into the "correct" conformation required for deadenylylation.

The two serine residues, 52 and 53, were altered singly in two mutant strains (S52A and S53A), as well as in conjunction with the Y397V mutation (S52A Y397V and S53A Y397V). All four of these mutants complemented the auxotrophy of YMC 11, and all had γ-glutamyl transferase activity. The two single mutations resulted in a lowering of the total γ-glutamyl transferase activity, compared to that seen in the WT strains, indicating that these residues do play a role in the catalytic activity. Altering the serine residues each separately, together with the Y397V mutation, to produce S52A Y397V and S53A Y397V, resulted in an increase in the Mn^{2+} activity over that

seen in the two individual serine mutants, to levels comparable with the WT enzyme. S52A showed reduced glutamine synthetase activity, compared to the WT enzymes, in both the Mn^{2+} and Mg^{2+} HPLC assays, and this activity increased in the double mutant, S52A Y397V. S53A Y397V was much more active in the Mn^{2+}-based forward reaction, showing a three-fold increase over any of the other mutant or WT enzymes screened. In the HPLC based assay, the activity obtained from the S53A Y397V enzyme was similar to that of the deadenylylated WT enzyme indicating that S52 has adenylylated functionality. This enzyme, S53A Y397V, is however, equally efficient in functioning using either Mn^{2+} or Mg^{2+}, indicating that S52 functions under conditions of adenylylation. Similar data was found for the S52A Y397V mutant. It is feasible that, as these serine residues lie adjacent to one another, that both are capable of functioning in both the adenylylated or deadenylylated forms of the glutamine synthetase, and the specificity for the reactions is housed in the histidine and acid residues.

Both serine residues were then altered simultaneously, to produce a double mutant, S52A S53A, which resulted in an enzyme that had reduced γ-glutamyl transferase activity and reduced activity levels in the Mn^{2+} and Mg^{2+} HPLC assays. It was discovered that the enzyme also had the ability to convert ATP all the way to AMP, producing two equivalents of glutamine per ATP (Table 3.5). A triple mutant was produced, which combined the S52A, S53A and Y397V mutations, which then resulted in a significant increase in the enzyme activity levels, compared to the WT strains, and this mutant also had the ability to convert ATP all the way to AMP. The conversion efficiency of this enzyme was also severely compromised. If, as suspected, these serine residues play a catalytic role similar to the serine residues

making up the catalytic triad in the serine proteases, one would expect that the double serine mutation (S52A S53A) would create a non-functional enzyme. As this was obviously not the case, it was speculated that another reaction mechanism is possibly available to this enzyme. It is proposed that the γ-glutamyl phosphate, in the absence of both serine residues, may undergo nucleophilic attack by NH_3 in the absence of the catalytic triad, forming glutamine, however inefficiently. In these strains, ADP may also phosphorylate the glutamate to γ-glutamyl phosphate, allowing the subsequent synthesis of glutamine in an ADP-based reaction. The role of the catalytic triads is, therefore, to regulate the reaction rates and, not just to facilitate that the reactions occur. This regulation of the reaction rate forms part of the control of the carbon and nitrogen flux within the cell.

The two histidine residues identified as potentially forming part of a catalytic triad, proved to be crucial to the catalytic activity of the enzyme. Four mutants were generated to alter these residues - H210V, H210V Y397V, H211V and H211V Y397V. H210V was the only mutant capable of growth on the minimal plates with no supplementation of glutamine, and the only mutant to exhibit a very small amount of Mn^{2+}-dependent γ-glutamyl transferase activity. H210V Y397V, H211V and H211V Y397V were not capable of complementing the auxotrophy of YMC11, and, in fact, H210V Y397V and H211V Y397V, even struggled to grow in the presence of glutamine. All three exhibited no γ-glutamyl transferase activity at all. All four mutants had low activity levels in all the HPLC assays (~0.1 μmoles/min/mg protein), and as seen in the double serine mutants, had the ability to convert ATP all the way through to AMP, albeit at lower levels than the double serine mutants.

Four residues were identified as potentially being able to fill the role of the acid residue of the proposed catalytic triad. These were D50, E129, E327 and E357. Asp50 has been identified in the binding of NH_4^+, and may also play a role in catalysing the deprotonation of NH_4^+ to form NH_3. Glu327 reportedly participates in lowering the free energy of the transition state involved in the formation of the positively charged tetrahedryl adduct resulting in the condensation of γ-glutamyl phosphate and ammonia (Alibhai and Villafranca, 1994). All four of these residues have also previously been identified as important for the catalytic activity of glutamine synthetase (Liaw and Eisenberg, 1994a). This would explain the reduction in activities obtained with all these mutants. Eight mutants were produced to attempt to determine which of the four residues was involved. These were, D50A, D50A Y397V, E129A, E129A Y397V, E327V, E327V Y397V, E357A and E357A Y397V. Identifying the residues associated with each catalytic triad is however complex. Both mutants of D50A and E327V were capable of complementing the auxotrophy of YMC11, in contrast to E129A and E357A, which could not. D50A Y397V showed more γ-glutamyl transferase activity and a higher percentage of adenylylation than D50A, whereas D50A Y397V had more Mn^{2+} and Mg^{2+} glutamine-based and ADP-based HPLC activity than the single mutant. The percentage of conversion in this mutant was low, however. The γ-glutamyl transferase activity of E129A Y397V was significantly higher than that in E129A, and, in general, this applied to the levels of activity determined in the HPLC assays. The γ-glutamyl transferase assay results for these two mutants indicate that the E129 residue is more important for the adenylylated form of the enzyme as the activity increases in the double mutant. As the E129A mutant did not complement the auxotroph, it is believed that this residue makes up the first acid residue and is found in the adenylylated catalytic triad.

Virtually no γ-glutamyl transferase activity was detected in E327V, but the level of γ-glutamyl transferase activity increased when this mutation was introduced into the Y397V mutant. The Mg^{2+} glutamine-based and ADP-based specific activities were lower than the Mn^{2+} specific activities for E327V, where they decreased to almost 0. The Mg^{2+} activities in the double mutant, however, showed a significant increase in the double mutant, E327V Y397V. The introduction of the valine residue in place of the glutamate residue in this mutant had an effect on the enzyme, but enabled it to retain sufficient functionality to enable both mutants to complement the auxtrophy of YMC11. E357A had moderate γ-glutamyl transferase activity, which decreased to nothing in the double mutant E357A Y397V. More activity was also seen in the HPLC assays of E357A, than in the assays from E357A Y397V. As the E357A mutant did not complement the auxotroph, it is believed that this residue makes up the second acid residue and is found in the deadenylylated catalytic triad.

Taking these results into account, the model was again examined to attempt to put the interpretations into context. The model had been reduced to 4 subunits, designated A, B, G and H (Figure 1.7) for explanation purposes, and to demonstrate the interaction of the subunits in the putative catalytic triad-based reaction mechanism. It is proposed that on adenylylation of Tyr397 on subunit A, interaction occurs with Trp57 of subunit B, which is held in a flexible loop containing Ser52 and Ser53. This loop contains the sequence GITMFDGSSIGGWKG, with the glycine residues allowing the flexibility in the loop. It is this interaction by adenylylation of the adjacent subunit that allows for the selection of the serine residue that makes up the proposed catalytic triad. On adenylylation, the Tyr397 of subunit H also reacts with Trp57 of subunit B.

From this study, and following examination of the inter-atomic distances of the model, it is proposed that the amino acids that make up the respective catalytic triads are Ser52, His211 and Glu129 for the adenylylated form of the enzyme and Ser53, His210 and Glu357 for the deadenylylated form of the enzyme. It is proposed that on adenylylation of Tyr397 from subunit A, Trp57 on subunit B interacts with the aromatic rings of the adenyl group of both AMP residues from subunit A and subunit H. Trp 57 is on the serine containing flexible loop of subunit B. This allows the serine loop to swivel, thereby bringing Ser52 into closer proximity to Glu129 on subunit A. If Tyr397 on subunit H is also adenylylated, it interacts with the adenyl ring on the Tyr397 of subunit A, bringing Glu129 on subunit A into closer proximity within the active site. This resulting change in configuration between the active site residues that exist between subunits A and B, as well as the adenylylation of the Tyr397 on subunit A, then allows for sufficient change in the internal structure of the active site allowing His211 to move into position and complete the catalytic triad made up of Ser52', His211 and Glu129.

The data reported in this study, therefore supports the theory that the glutamine synthetase from *E.coli* uses two catalytic triads as a possible mechanism to switch between the adenylylated and deadenylylated forms of the enzyme, thereby affecting its specificity for MgATP or Mn_2ATP and NH_4^+ or NH_3. Using the data obtained from the SDM analysis, the putative catalytic triads are believed to be comprised of the following residues :

Adenylylated glutamine synthetase:	Ser52'	(Subunit B)
	His211	(Subunit A)
	Glu129	(Subunit A)
Deadenylylated glutamine synthetase:	Ser53'	(Subunit B)
	His210	(Subunit A)
	Glu357	(Subunit A)

Chapter 4

Conclusion

Structural and molecular dynamics analysis of the glutamine synthetase indicates that a possible mechanism by which the adenylylation/deadenylylation of the enzyme affects the enzyme specificity for either MgATP or Mn_2ATP and NH_4^+ or NH_3, is by switching between two putative catalytic triads. The solution chemistry of the NH_4^+/NH_3 also dictates the regulation of GS (Senior, 1975). At low ammonium salt concentrations, the NH_4^+ dissociates to $NH_3 + H^+$ (Kenyon, 1992). The NH_3 is a strong nucleophile and capable of carrying out the nucleophilic attack on the proposed γ-glutamyl acyl enzyme intermediate, however at high concentrations NH_4^+ is not a nucleophile and therefore requires deprotonation. By definition, if the catalytic triads play a role in the catalysis, the reaction must pass through a γ-glutamyl acyl enzyme intermediate.

Site-directed mutagenesis of a number of residues identified as playing a role in these catalytic triads, led to the following observations. Both Ser52 and Ser53 were important for the catalytic activity of the enzyme. It was determined that Ser52 appeared to have adenylylated functionality and Ser53 deadenylylated functionality. It is possible, however, that as these serine residues lie adjacent to one another, both are capable of functioning in the adenylylated and deadenylylated forms of the enzyme. When both serine residues were removed, resulting in decreased glutamine synthetase activity, the importance of these residues in the active site, was reinforced. Evaluating these serine mutant enzymes in the presence of the serine protease inhibitors, AEBSF and PMSF, led to the conclusion that Ser52 and Ser53, did, indeed, appear to form part of a catalytic triad, as the activity of the enzymes

was inhibited in the presence of the inhibitors. The double serine mutant was not significantly inhibited by either PMSF or AEBSF. Both AEBSF and PMSF appeared to cause an increase in the rate of hydrolysis of the ATP with a concomitant reduction in the formation of glutamine and the conversion efficiency. This may be interpreted as competitive binding of the serine protease inhibitor to the glutamate site, while still allowing ATP hydrolysis to occur. It is important to note that in all cases, while inhibition was found to occur, there was a concomitant reduction in the conversion efficiency. His210 and His211 were found to be equally important to the functionality of the enzyme, and the results, in consultation with the model, led to the conclusion that His210 had deadenylylated activity and His211 had adenylylated activity. All the potential acid residues, when removed, had an effect on activity, but this was to be expected as all had previously been identified in the literature as important in the active site of the glutamine synthetase from *E.coli* (Liaw and Eisenberg, 1994a). Again, consultation of the model led to the conclusion that the two acid residues that filled the function of the acid residue in each catalytic triad, were Glu129 for the adenylylated form of the enzyme, and Glu357 for the deadenylylated form of the enzyme.

The two putative catalytic triads are found at the interface between two subunits of glutamine synthetase. By way of example, using the active site that exists between subunits A and B of glutamine synthetase (Figure 1.7), and using the data obtained from the SDM analysis, the putative catalytic triads are believed to be comprised of the following residues :

Adenylylated GS: Ser52 (Subunit B)
His211 (Subunit A)
Glu129 (Subunit A)

Deadenylylated GS: Ser53 (Subunit B)

His210 (Subunit A)

Glu357 (Subunit A)

The deadenylylated GS is produced under conditions of nitrogen limitation (Senior, 1975), and, therefore, at low NH_3 concentrations, the enzyme is deadenylylated, switching to the catalytic triad containing residue Ser53' (Subunit B), and at high NH_3 concentrations, the enzyme is adenylylated switching to the catalytic triad containing the residue Ser52' (Subunit B). The catalytic site using Ser52' will also have to deprotonate the NH_4^+ to create the nucleophile. It has been proposed that the deprotonation of the NH_4^+ may occur via Asp50 (Liaw and Eisenberg, 1994a). This deprotonation of the NH_4^+ could, however, also occur via a carbonium ion once the acyl enzyme intermediate has been formed. This depends on the reaction mechanism employed. The two proposed reaction mechanisms, whereby the nucleophilic attack by ammonia of a γ-glutamyl-acyl enzyme intermediate is facilitated by a catalytic triad mechanism, is discussed later. The acyl enzyme intermediate has been postulated before in work carried out on glutamine synthetase isolated from sheep brain, where ^{14}C-glutamate binding to glutamine synthetase in the absence of NH_3 was demonstrated (Krishnaswamy et al, 1962).

The reaction kinetics of the nucleophilic attack by the ammonia show two sets of kinetic constants for the ammonia (Meek and Villafranca, 1980). We have postulated, that either the γ-oxygen of Ser52' or Ser53' forms a covalent bond to the glutamate, via nucleophilic attack on the carbonyl carbon of the ester bond of the carboxylic-phosphoric acid anhydride of the glutamyl phosphate formed in the first step of the reaction (Figures 4.1 and 4.2).

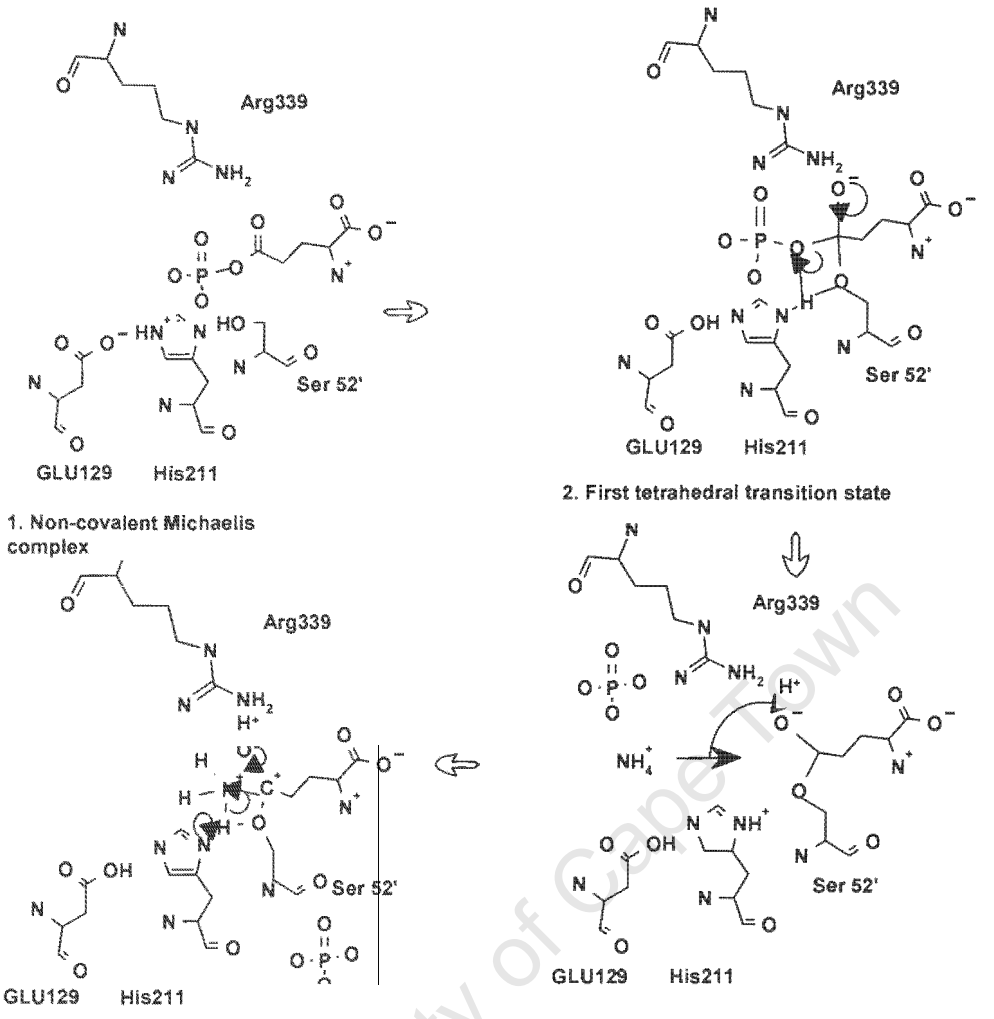

Figure 4.1. Postulated reaction mechanism of the adenylylated glutamine synthetase, at high concentrations of ammonia, requiring the deprotonation of the NH_4^+.

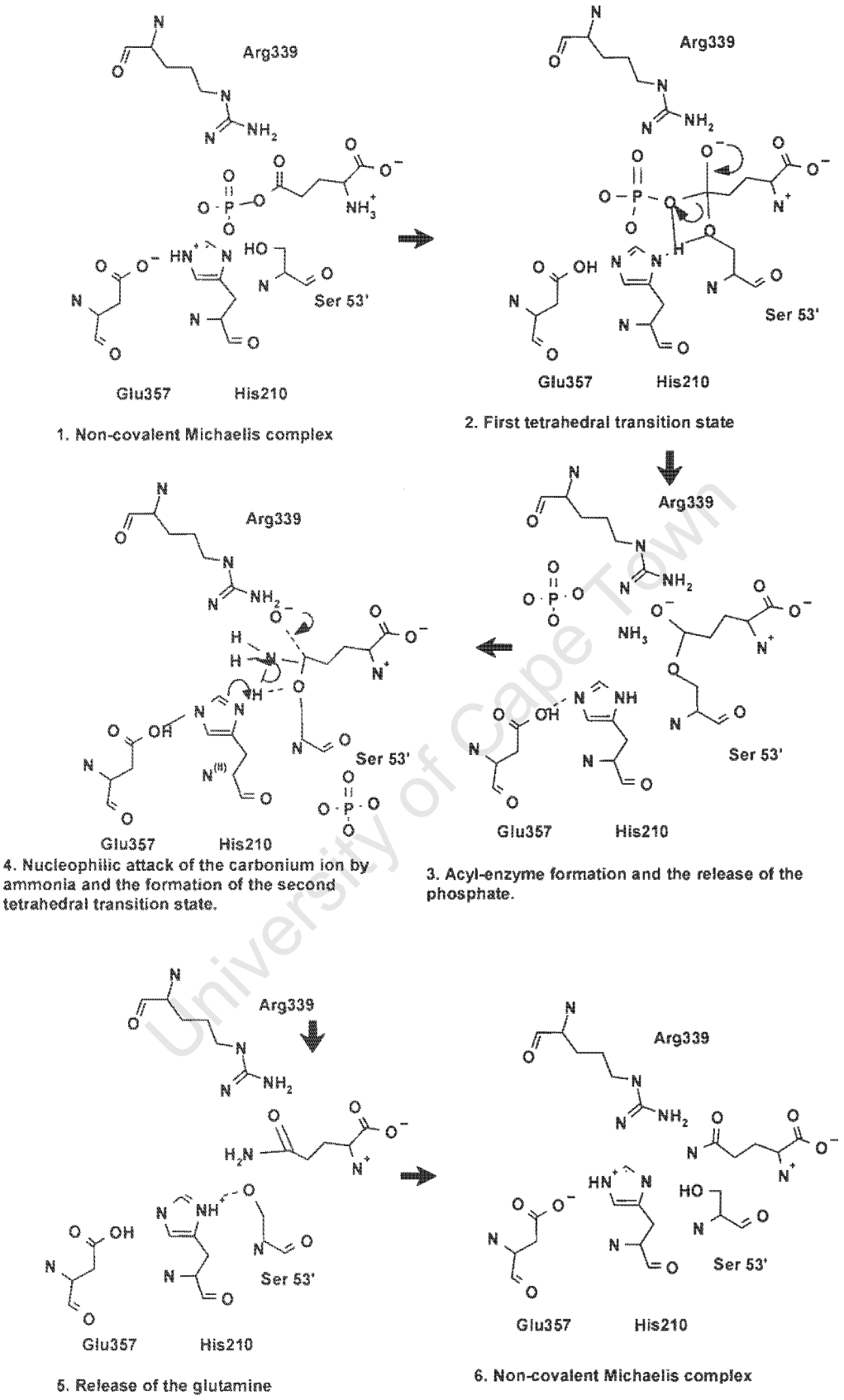

Figure 4.2. Postulated reaction mechanism of deadenylylated glutamine synthetase at low concentrations of ammonia.

His210 and His211 act as general base catalysts by removing the proton from the respective Ser O^{γ}. This N^{ε}-bound proton forms hydrogen bonds to the Ser O^{γ} and to the substrate phosphate oxygen. The resulting tetrahedral oxyanion intermediate is possibly stabilised by Arg339. In the next step, the N^{ε}-proton from His210 and His211 is transferred to the bridging oxygen substrate, releasing the acid phosphate, with the concomitant formation of an acyl enzyme intermediate. It is after the formation of the first acyl enzyme intermediate at either Ser52' or Ser53', that there appears to be a fundamental difference in the reaction mechanisms of the nucleophilic attack by ammonia and the subsequent deacylation of the enzyme and the formation of glutamine. It is believed that the "choice" of the serine is mediated by the adenylylation state of the active site and the use of either Mg^{2+} or Mn^{2+} in the transfer of phosphate from ATP to glutamate. This transfer of phosphate to the glutamate may occur via phosphoryl transfer mediated by His269, which has been identified as a ligand of the n2 metal ion (Abell et al, 1995).

The adenylylated Tyr397 of subunit H is opposite a Trp57' on subunit B, which is in the serine flexible loop. It is believed that on adenylylation, an interaction is created between the aromatic side chains of the adenylylated Tyr397 and the Trp57', as well as the interaction between the adenyl residues between Tyr397 (Subunit H) and Tyr397 (Subunit A), which cause the enzyme to "switch" the catalytic triad (Figures 4.3 and 4.4). No crystal structure exists for the adenylylated glutamine synthetase.

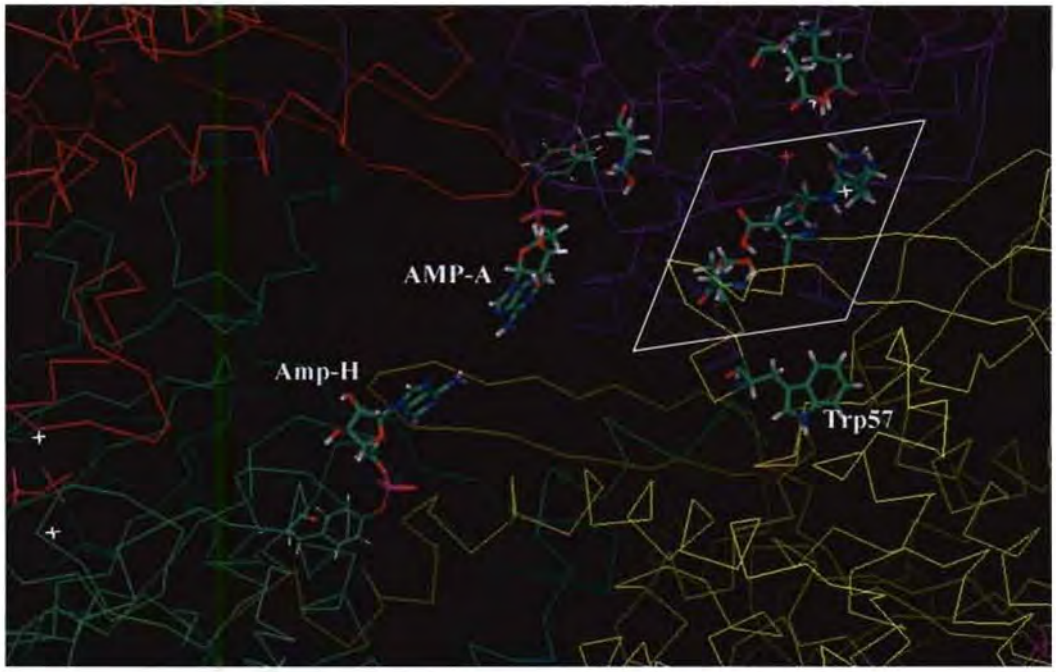

Figure 4.3. Adenylylated glutamine synthetase subunits A and H showing the proximity to Trp57 and the serine loop (boxed).

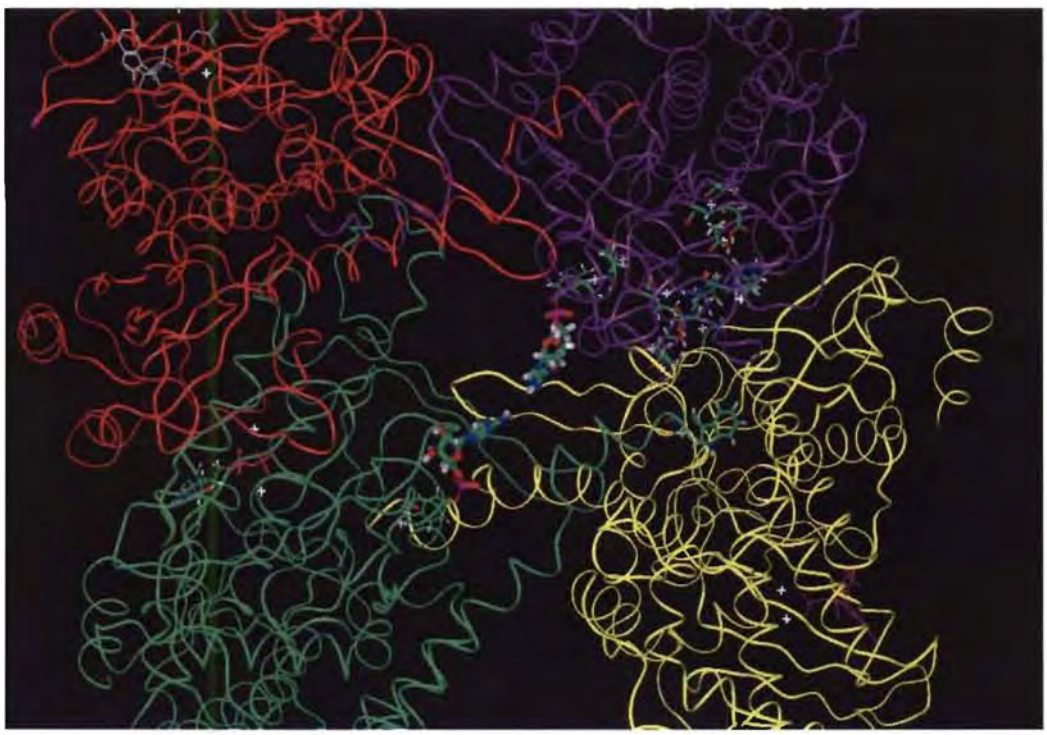

Figure 4.4. Adenylylated glutamine synthetase subunits A and H showing the interaction between the subunits.

Another factor that may play a role in the switching mechanism is Mn_2ATP has a different structure to MgATP as the ATP folds around the Mn^{2+} ions in a binary complex with the closest approach of the adenine ring being made by N_7 (Kingdon et al, 1967a; Kingdon and Stadtman, 1967b). The Mn_2ATP and the MgATP may cause different oxygens of the Glu δ carbonyl group to be phosphorylated. In aqueous solution these would normally be equivalent. However, within the active site, as the acyl intermediate, the Glu $O^{\varepsilon 1}$ and Glu $O^{\varepsilon 2}$ are assymmetric in nature maintaining their stereo chemistry. This asymmetry may be important in deciding the nature of nucleophilic attack. It is therefore conceivable that either S_N1 or S_N2 nucleophilic attack may occur as a result of the orientation created by the phosphorylation of either Glu $O^{\varepsilon 1}$ or Glu $O^{\varepsilon 2}$.

Thus, a possible model mechanism for the adenylylated form of the enzyme, that is formed in the cells grown under conditions of nitrogen excess and carbon limitation, using the Ser52'/His211/Glu129 catalytic triad is outlined in Figure 4.1 (Kenyon, personal communication). The γ-carboxyl group on the glutamate acyl intermediate may play a role in the deprotonation of the NH_4^+. In work carried out by Liaw and Eisbenberg (1994a), Asp50' was identified as the residue that may play a role in the deprotonation of the NH_4^+. The first tetrahedral transition state occurs during the dephosphorylation of the γ-glutamyl phosphate. This proton, in activating this zwitter-ionic form of the carboxyl group, increases its susceptibility to nucleophilic attack. The overall activity of the adenylylated enzyme, in the presence of Mn_2ATP, was found to be generally lower than the deadenylylated enzyme. The high activation energy in the adenylylated enzyme, however, may be linked to the enzyme having to deprotonate the NH_4^+ to $NH_3 + H^+$ at the high NH_4^+ concentrations, to create the nucleophile.

A possible model mechanism for the deadenylylated form of the enzyme, that is formed in the cells grown under conditions of nitrogen limitation and carbon excess, using the Ser53'/His210/E357 catalytic triad is outlined in Figure 4.2 (Kenyon, personal communication). After the formation of the first tetrahedral transition state, and after the N^{ε} proton of His210 has been transferred to the substrate, thereby releasing the acid phosphate, the acyl enzyme intermediate is formed. This acyl enzyme complex may be stabilised by the Arg339 in an oxyanion hole. The nucleophilic attack by the ammonia then occurs. As the deadenylylated form of the enzyme is produced by the cells under nitrogen limited conditions, it is believed that the NH_4^+ is fully dissociated to $NH_3 + H^+$, with NH_3 being brought into the active site and not NH_4^+.

It has been shown that an aqueous solution of $(NH_4)_2SO_4$ dissociates into $2NH_4^+$ and SO_4^{--}. However, in dilute solutions, as the concentration tends towards infinite dilution, it is believed that the $2NH_4^+$ further dissociates to $2NH_3$ and $2H^+$ (Kenyon, 1992). Therefore, a possible third mechanism involved in facilitating the nucleophilic attack of the acyl enzyme, by the ammonia, may occur. This is a "gas phase" or "solvent free" reaction. The rates of bimolecular nucleophilic substitution reactions involving anions and polar molecules vary over 20 orders of magnitude in changing from the gas phase to polar media (solvent) (Olmstead and Brauman, 1977; Pellerite and Brauman, 1980; Shaik and Pross, 1982, Chandrasekhar et al, 1984, Chandrasekhar et al, 1985). This is believed to be due to the increase in the activation energy by hydration as a result of the reduction in the strength of the hydrogen bonds. The ion-dipole attraction is nullified by the energy required to desolvate the ion (nucleophile). The transition state, which has a dispersed charge distribution as a result of the hydration forms weaker hydrogen bonds to the solvent. This results in a unimodal energy profile with a large, narrow central energy barrier that is significantly greater than in the gas

phase. It is therefore postulated, that at very low ammonia concentrations the active site is "closed", thereby reducing or eliminating the solvent accessible area in the active site, allowing a gas phase type reaction to occur. This would possibly occur when the enzyme is deadenylylated and functioning in the Mg^{2+} form. It would also account for the very low K_m which the enzyme has for ammonia at low substrate concentrations (Meek and Villafranca, 1980). The adverse effect of H_2O was evident in the enzyme reactions of the mutant enzymesY397V, S52A S53A Y397V, H210V Y397V and H211V Y397V as the conversion efficiency of ATP hydrolysed to glutamine formed was as low as 36 %.

The data presented in this study supports the hypothesis that the reaction mechanism employed by glutamine synthetase in the formation of glutamine from the γ-glutamyl phosphate synthesized in the first step of the reaction, occurred with two catalytic triads similar to those employed by the serine proteases. These catalytic triads are believed to be comprised of Ser52', His211 and Glu129 for the adenylylated form of the enzyme, and Ser53', His210 and Glu357 for the deadenylylated form of the enzyme. It will be necessary to crystallize the adenylylated WT, the deadenylylated WT and the mutant Y397V glutamine synthetase, grown in continuous culture to ensure that the effect of the adenyltransferase is guaranteed, in order to conclusively prove this postulated reaction mechanism.

References

Abell, L M, J Schineller, P J Keck and J Villafranca (1995). Effect of metal-ligand mutations on phosphoryl transfer reactions catalysed by *Escherichia coli* glutamine synthetase. Biochemistry 34: 16695-16702.

Alibhai M and J J Villafranca (1994). Kinetic and mutagenic studies of the role of the active site residues Asp-50 and Glu-327 of *Escherichia coli* glutamine synthetase. Biochemistry 33 : 682-686.

Almassy R J, C A Janson, R Hamlin, N-H Xuong and D Eisenberg (1986). Novel subunit-subunit interactions in the structure of glutamine synthetase. Nature 323 : 304-309

Atkins WM (1994). Supramolecular self-assembly of *Escherichia coli* glutamine synthetase: Effects of Pressure and adenylylation state on dodecamer stacking. Biochemistry 33 : 14965-14973.

Backman K, Y-M Chen and B Magasanik (1981). Physical and genetic characterization of the *glnA-glnG* region of the *Escherichia coli* chromosome. Proceedings of the National Academy of Sciences 78 : 3743-3747.

Bender R A, K A Janssen, A D Resnick, M Blumberg, F Foor and B Magasanik (1977). Biochemical parameters of glutamine synthetase from *Klebsiella aerogenes.* Journal of Bacteriology 129 : 1001-1009.

Brown J R, Y Masuchi, F T Robb and W F Doolittle (1994). Evolutionary relationships of bacterial and archaeal glutamine synthetase genes. Journal of Molecular Evolution 38 : 566-576.

Burkovski A (2003). Ammonium assimilation and nitrogen control in *Corynebacterium glutamicum* and its relatives : an example for new regulatory mechanisms in actinomycetes. FEMS Microbiology Reviews 27 : 617-628.

Chandrasekhar J, D C Spellmeyer and W L Jorgensen (1984). Energy component analysis for dilute aqueous solutions of Li^+, Na^+, F^- and Cl^- ions. Journal of the American Chemical Society 106 : 903-910.

Chandrasekhar J, S F Smith and W L Jorgensen (1985). Theoretical examination of the S_N2 reaction involving chloride ion and methyl chloride in the gas phase and aqueous solution. Journal of the American Chemical Society 107 : 154-163.

Chen Y-M, K Backman and B Magasanik (1982). Characterisation of a gene, *glnL*, the product of which is involved in the regulation of nitrogen utilization in *Escherichia coli*. Journal of Bacteriology 150 : 214-220.

Denton M D and A Ginsburg (1970). Some characteristics of the binding of substrates to glutamine synthetase from *Escherichia coli*. Biochemistry 9 : 617-631.

Eisenberg D, H S Gill, G M U Pfluegl and S H Rotstein (2000). Structure-function relationships of glutamine synthetases. Biochemica et Biophysica Acta 1477 : 122-145.

Fisher S H (1999). Regulation of nitrogen metabolism in *Bacillus subtilis* : *vive la différence*! Molecular Microbiology 32 : 223-232.

Gill H S and D Eisenberg (2001). The crystal structure of phosphinothricin in the active site of glutamine synthetase illuminates the mechanism of enzymatic inhibition. Biochemistry 7 : 1903-1912

Harth G, D L Clemens and M A Horwitz (1994). Glutamine synthetase of *Mycobacterium tuberculosis* : Extracellular release and characterization of its enzymatic activity. Proceedings of the National Academy of Sciences 91 : 9342-9346.

Harth G and M A Horwitz (1997). Expression and efficient export of enzymatically active *Mycobacterium tuberculosis* glutamine synthetase in *Mycobacterium smegmatis* and evidence that the information for export is contained within the protein. Journal of Biological Chemistry 272 : 22728-22735.

Harth G, P C Zamecnik, J-Y Tang, D Tabatadze and M A Horwitz (1999). Treatment of *Mycobacterium tuberculosis* with antisense oligonucleotides to glutamine synthetase mRNA inhibits glutamine synthetase activity, formation of the poly-L-glutamate/glutamine cell wall structure and bacterial replicon. Proceedings of the National Academy of Sciences 97 : 418-423.

Hunt J B and A Ginsburg (1972). Some kinetics of the interaction of divalent cations with glutamine synthetase from *Escherichia coli*. Metal ion induced conformational changes. Biochemistry 11 : 3723-3735.

Hunt J B, P Z Smyrniotis, A Ginsburg and E R Stadtman (1975). Metal ion requirement by glutamine synthetase of *Escherichia coli* in catalysis of γ-glutamyl transfer. Archives of Biochemistry and Biophysics 166 : 102-124.

Hunt J B and A Ginsburg A (1980). Mn^{2+} and substrate interactions with glutamine synthetase from *Escherichia coli*. Journal of Biological Chemistry 255 : 590-594.

Kenyon C (1992). Dissociation of $(NH_4)_2SO_4$ and its implication in fermentation culture media and the availability of NH_4^+ for bacterial metabolism. AECI Confidential Report : RN1396/C

Kingdon H S, B M Shapiro and E R Stadtman (1967a). Regulation of glutamine synthetase VIII. ATP:glutamine synthetase adenylyltransferase, an enzyme that catalyzes alterations in the regulatory properties of glutamine synthetase. Proceedings of the National Academy of Sciences 58 : 1703-1710.

Kingdon H S and E R Stadtman (1967b). Regulation of glutamine synthetase X. Effect of growth conditions on the susceptibility of *Escherichia coli* glutamine synthetase to feedback inhibition. Journal of Bacteriology 94 : 949-957.

Krishnaswamy P R, V Pamiljans and A Meister (1962). Studies on the mechanism of glutamine synthesis: Evidence for the formation of enzyme-bound activated glutamic acid Journal of Biological Chemistry 237 : 2932 - 2940 .

Laemmli U K (1970). Cleavage of structural proteins during the assembly of the head of bacteriophage T4. Nature 227 : 680-685.

Liaw S-H, C Pan and D Eisenberg (1993a). Feedback inhibition of fully unadenylylated glutamine synthetase from *Salmonella typhimurium* by glycine, alanine and serine. Proceedings of the National Academy of Sciences 90 : 4996-5000.

Liaw S-H, J J Villafranca and D Eisenberg (1993b). A model for oxidative modification of glutamine synthetase, based on crystal structures of mutant H269N and the oxidised enzyme. Biochemistry 33 : 7999-8003.

Liaw S-H and D Eisenberg (1994a). Structural model for the reaction mechanism of glutamine synthetase, based on five crystal structures of enzyme-substrate complexes. Biochemistry 33 : 675-681.

Liaw S-H, G Jun and D Eisenberg (1994b). Interactions of nucleotides with unadenylylated glutamine synthetase from *Salmonella typhimurium*. Biochemistry 33 : 11184-11188.

Liaw S-H, I Kuo and D Eisenberg (1995). Discovery of the ammonium substrate site on glutamine synthetase, a third cation binding site. Protein Science 4 : 2358-2365.

Logusch E W, D M Walker, J F McDonald and J E Franz (1990). Inhibition of *Escherichia coli* glutamine synthetase by α- and γ-substituted phosphinothricins. Biochemistry 29 : 366-372.

Lowry O H, N J Rosebrough, A L Farr and R J Randall (1951). Protein measurement with the Folin Phenol reagent. Journal of Biological Chemistry 193 : 265-275.

Magasanik B (1982). Genetic control of nitrogen assimilation in bacteria. Annual Reviews in Genetics 16 : 135-168.

Meek T D and J J Villafranca (1980). Kinetic mechanism of *Escherichia coli* glutamine synthetase. Biochemistry 19 : 5513-5519

Meek T D, K A Johnson and J J Villafranca (1982). *Escherichia coli* glutamine synthetase. Determination of rate-limiting steps by rapid-quench and isotope partitioning experiments. Biochemistry 21 : 2158-2167.

Mehta R, J T Pearson, S Mahajan, A Nath, M J Hickey, D R Sherman and W M Atkins (2004). Adenylylation and catalytic properties of *Mycobacterium tuberculosis* glutamine synthetase expressed in *Escherichia coli* versus mycobacteria. Journal of Biological Chemistry 279 : 22477-22482.

Merrick M and R A Edwards (1995). Nitrogen control in bacteria. Microbiology Reviews 59 : 604-622.

Ninfa A J, and M R Atkinson (2000). P_{II} signal transduction proteins. Trends in Microbiology 8 : 172-179.

Nosworthy N J and A Ginsburg (1997). Thermal unfolding of dodecameric glutamine synthetase: Inhibition of aggregation by urea. Protein Science 6 : 2617-2623.

Olmstead W N and J I Brauman (1977). Gas-phase nucleophilic displacement reactions. Journal of the American Chemical Society 99 : 4219-4228.

Pellerite M J and J I Brauman (1980). Intrinsic barriers in nucleophilic displacements. Journal of the American Chemical Society 102 : 5993-5999.

Pesole G, M P Bozzetti, C Lanave, G Preparata and C Saccone (1991). Glutamine synthetase gene evolution : A good molecular clock. Proceedings of the National Academy of Sciences, USA 88 : 522-526.

Reitzer L J and B Magasanik (1996). Ammonia assimilation and the biosynthesis of glutamine, glutamate, aspartate, L-alanine and D-alanine; p. 391-407. In: *Escherichia coli* and *Salmonella typhimurium*, 2nd edition. FC Neidhardt and R Curtiss (EDS); ASM Press, Washington DC.

Schreier H J and C A Rostkowski (1995). *Bacillus subtilis glnR* mutants defective in regulation. Gene 161 : 51-56.

Senior P J (1975). Regulation of nitrogen metabolism in *Escherichia coli* and *Klebsiella aerogenes* : Studies with the continuous culture. Journal of Bacteriology 123 : 407-418.

Shaik S S and A Pross (1982). S_N2 reactivity of CH_3X Derivatives. A valence bond approach. Journal of the American Chemical Society 104 : 2708-2719.

Shapiro B M and E R Stadtman (1967). Regulation of glutamine synthetase IX. Reactivity of the sulfhydryl groups of the enzyme from *Escherichia coli*. Journal of Biological Chemistry 242 : 5069-5079.

Shapiro B M and E R Stadtman (1968). Effects of specific divalent cations on some physical and chemical properties of glutamine synthetase from *Escherichia coli*. Taut and relaxed enzyme forms. Biochemistry 7 : 2153-2167.

Shapiro B M and Stadtman E R (1970). The regulation of glutamine synthesis in microorganisms. Annual Reviews in Microbiology 24 : 501-524.

Stadtman E R, A Ginsburg, J E Ciardi, J Yeh, S B Hennig and B M Shapiro (1970). Multiple molecular forms of glutamine synthetase produced by enzyme catalyzed adenylylation and deadenylylation reactions. Advances in Enzyme Regulation 8 : 99-118.

Tullius M V, G Harth and MA Horwitz (2003). Glutamine synthetase *glnA1* is essential for growth of *Mycobacterium tuberculosis* in human THP-1 macrophages and guinea pigs. Infection and Immunity 71 : 3927-3936.

Whitley E J and A Ginsburg (1980). A novel reaction catalysed by unadenylylated glutamine synthetase from *Escherichia coli*. Journal of Biological Chemistry 255 : 10663-10670.

Woolfolk C A, B Shapiro and E R Stadtman (1966). Regulation of glutamine synthetase I. Purification and properties of glutamine synthetase from *Escherichia coli*. Archives of Biochemistry and Biophysics 116 : 177-192.

Yamashita M M, R J Almassy, C A Janson, D Cascio and D Eisenberg (1989). Refined atomic model of glutamine synthetase at 3.5 Å Resolution. Journal of Biological Chemistry 264 : 17681-17690.

Yanchunas J, M J Dabrowski, P Schurke and W M Atkins (1994). Supramolecular self-assembly of *Escherichia coli* glutamine synthetase : Characterisation of dodecamar stacking and high order association. Biochemistry 33 : 14949-14956.